Holocene glacial history of Svalbard: Status, perspectives and challenges

Wesley R. Farnsworth[a,b,c,]*, Lis Allaart[b], Ólafur Ingólfsson[d], Helena Alexanderson[b,e], Matthias Forwick[b], Riko Noormets[a], Michael Retelle[a,f], Anders Schomacker[b]

[a] *Department of Arctic Geology, The University Centre in Svalbard (UNIS), Longyearbyen N-9171, Norway*
[b] *Department of Geosciences, UiT The Arctic University of Norway, Tromsø N-9037, Norway*
[c] *NordVulk, Nordic Volcanological Center, University of Iceland, Askja, Sturlugata 7, Reykjavík IS-101, Iceland*
[d] *Institute of Earth Sciences, University of Iceland, Askja, Sturlugata 7, Reykjavík IS-101, Iceland*
[e] *Department of Geology, Lund University, Sölvegatan 12, Lund S-223 62, Sweden*
[f] *Department of Geology, Bates College, Lewiston, Maine 04240, USA*

ARTICLE INFO

ABSTRACT

We synthesize the current understanding of glacier activity on Svalbard from the end of the Late Pleistocene (12,000 yrs. before present) to the end of the Little Ice Age (*c.* 1920 AD). Our glacier history is derived from the SVALHOLA database, the first compilation of Holocene geochronology for Svalbard and the surrounding waters, including over 1,800 radiocarbon, terrestrial cosmogenic nuclide and optically stimulated luminescence ages. Data have been categorized by geological setting, uniformly (re-)calibrated, quality assessed and ultimately used to constrain glacier fluctuations (deglaciation, ice free conditions, glacier re-advances and ice marginal positions). We advance existing knowledge by mapping the extent and distribution of ice-cover during the Holocene glacial maximum and the glacial minimum, as well as present retreat rates (and percentages) within Early Holocene fjord-systems. Throughout the Holocene, Svalbard glaciers have responded to a varying combination of climatic, environmental and dynamic driving factors which influence both the extent and behavior of ice margins. We discuss the complexities of glacier systems and their dynamics in response to changes in climate. This review provides a holistic state of the art of Holocene glaciers on Svalbard, suitable for orienting future works which address gaps in our current knowledge.

1. Introduction

1.1. Background

Syntheses of accumulated field and geochronology data are prerequisite for placing new observations in context and for re-assessing existing interpretations (e.g., Hughes et al., 2016). Empirical constraints are critical for developing and calibrating models that simulate palaeoclimate as well as past glacier dynamics and processes (Patton et al., 2017). Within this context, we synthesize published literature of Holocene glacier history from the Svalbard archipelago and its surrounding waters. We introduce a database of empirical data specific to the Svalbard region as well as summarize prominent glacier fluctuations through the last 12 ka BP (kiloyears before present; Fig. 1).

The onset of the Holocene (at 11.7 ka BP) marks a rapid transition from the end of the Pleistoceneand the Younger Dryas (YD, 12.9 – 11.7 ka BP) to subsequent warmer interglacial conditions (Dansgaard et al., 1993; Wanner et al., 2008; Cohen et al., 2018). The global climate

during the Holocene has traditionally been regarded as relatively stable, compared to the preceding Late Pleistocene (Dansgaard et al., 1993; Steffensen et al., 2008; Rockström et al., 2009), but this paradigm of a stable Holocene climate is being increasingly challenged (O'Brien et al., 1995; Bond et al., 2001; Mayewski et al., 2004; Wanner et al., 2011). Reviews of Holocene glaciers have been synthesized globally (e.g. Solomina et al., 2015) as well as compiled for numerous Arctic and Alpine regions including the European Alps, Iceland, Arctic Canada and Greenland (Gudmundsson, 1997; Bradley et al., 2003; Ivy-Ochs et al., 2009; Geirsdóttir et al., 2009; Kelly & Lowell 2009; Briner et al., 2016).

The North Atlantic Holocene climate varied considerably, with fluctuations between warm and cold as well as humid and dry conditions on the multidecadal to multicentennial timescale having a direct effect on glacier-systems (Mayewski et al., 2004; Wanner et al., 2011). 'Arctic amplification' refers to the sensitivity of the Arctic to these climatic fluctuations and, specifically, how the Arctic is significantly affected by minor shifts in temperature and precipitation compared to lower latitudes (Masso-Delmotte *et al.* 2013). By studying the rate and

* Corresponding author at: NordVulk, Nordic Volcanological Center, University of Iceland, Askja, Sturlugata 7, Reykjavík IS-101, Iceland.
E-mail address: wesleyf@hi.is (W.R. Farnsworth).

Fig. 1. Location maps with A) inset map of the polar North Atlantic region with the Svalbard archipelago framed in black box. B) Overview map of Svalbard identifying key islands and regions. The warm West Spitsbergen Current (WSC) flows northward along Svalbard's western margin while the cool East Spitsbergen Current (ESC) surrounds the southern tip of Spitsbergen from the east. Figure maps modified from IBCAO (Jakobsson et al., 2012) and TopoSvalbard © Norwegian Polar Institute 2020 respectively.

magnitude of past cryosphere changes we are able to better understand current dynamics, as well as more effectively predict antecedent climate scenarios (McKay and Kaufman, 2014).

The Holocene is divided into three stages; Early, Middle and Late Holocene, which correspond to the Greenlandian, Northgrippian and Meghalayan stages, respectively (Walker et al., 2012; Cohen et al., 2018). The timing of these stages is partitioned as follows: from 11.7 – 8.2 ka BP, 8.2 – 4.2 ka BP and 4.2 ka BP to present. In this paper, the Late Holocene stage is futhermore, broken into three periods, Neoglacial (4.2 ka BP – 1920 AD), Little Ice Age (LIA; 1250 – 1920 AD), and Post-LIA (1920 AD – present).

We reconstruct Svalbard glacier history by synthesizing geochronological data presented in scientific publications detailing Holocene sedimentary archives (marine, terrestrial and lacustrine) and landforms. Our synthesis leads us up to the earliest historical ice front observations from Svalbard, and places this accumulated Holocene data and observations in context with the ever-developing understanding of ice dynamics and the Arctic climate system. We strive to not only distinguish spatial trends in ice expansion and decay of Svalbard glaciers and ice caps through the Holocene. Furthermore, we discuss how reconstructed phases of ice-marginal change relate to palaeo-environmental conditions, e.g. climate, relative sea level, internal glacial processes or some combination. Understanding Arctic Holocene history can provide insight as to how future changes may influence glaciers, sea level and environmental conditions.

Svalbard has a long and rich history of scientific observations. The first field observations of Svalbard coincide with the earliest undisputed discovery of "Spitsbergen" by Willem Barentsz in 1596 (Claesz, 1598; Hacquebord, 1995; Arlov, 2005). Although early settlers were initially drawn north to the coasts of Svalbard for hunting, whaling and trapping, in the first half of the 1800s by the mid-1800s scientific expeditions began accumulating detailed observations of the landscape, climate and ice-cover around the archipelago (Lottin et al., 1842; Bertrand, 1852). Through the second half of 19th century, numerous international scientific expeditions visited Svalbard eventually culminating in the first International Polar Year in 1882-1883 (Ekholm, 1887; Fig. 2). During the last *c.* 150 years, the Svalbard archipelago has become a natural laboratory for observing glacial landforms, processes and dynamics as well as the terrain which ice masses have shaped

through the Quaternary (Holmström, 1865; Ingólfsson, 2011; Ingólfsson and Landvik, 2013). The bulk of this work has focused on constraining the Weichselian growth and break-up of the marine-based Svalbard-Barents Sea Ice Sheet (SBSIS; Blake, 1962; Boulton, 1979; Österholm, 1990; Landvik et al., 1998; Mangerud et al., 1998; Gjermundsen et al., 2013; Hormes et al., 2013; Ingólfsson and Landvik, 2013; Hughes et al., 2016). These reviews predominantly focus on Last Glacial Maximum (LGM) ice configuration, timing and disintegration, often excluding Holocene data. However, several studies of postglacial sea level and subsequent isostatic uplift have been used to better understand LGM ice cover and previous centers of mass. These works have indirectly summarized chronological shoreline development through the Holocene (e.g. Salvigsen, 1981; Forman, 1990; Forman et al., 2004; Bondevik et al., 1995; Forman et al., 2004; Sessford et al., 2015; Schomacker et al., 2019).

Holocene studies have long targeted unknowns of the glacier and climate history of Svalbard by mapping (terrestrial and marine) glacier landforms and deposits as well as investigations of lacustrine sediments from threshold lakes. Our synthesis addresses the following outstanding research questions: (1) When were Svalbard glaciers at their Holocene maximum and minimum ice extent and how extensive were they during these periods? (2) When were Svalbard's glaciers retreating / advancing, and what were the key drivers controlling Holocene glacier activity? (3) To what extent has ice dynamics and surge-type behavior influenced Holocene glacier fluctuations on Svalbard?

1.2. Setting and climate

Located along the dominant corridor of atmospheric moisture, between the Atlantic and the Arctic Basin, Svalbard spans from 74° to 81° N (Fig. 1; Drange et al., 2005). At present, glaciers and ice caps cover roughly 57 % of the archipelago (Nuth et al., 2013). The region has a sensitive climate due to its position at the northern extent of the North Atlantic Drift (West Spitsbergen Current; Fig. 1A) and the southern border of the Arctic sea-ice front (Aagaard et al., 1987; Rogers et al., 2005). Svalbard is categorized as having a dry High Arctic climate with periglacial conditions, extreme winter temperatures and continuous permafrost (French, 2007; Christiansen et al., 2010).

Despite its high latitude, Svalbard currently experiences a relatively
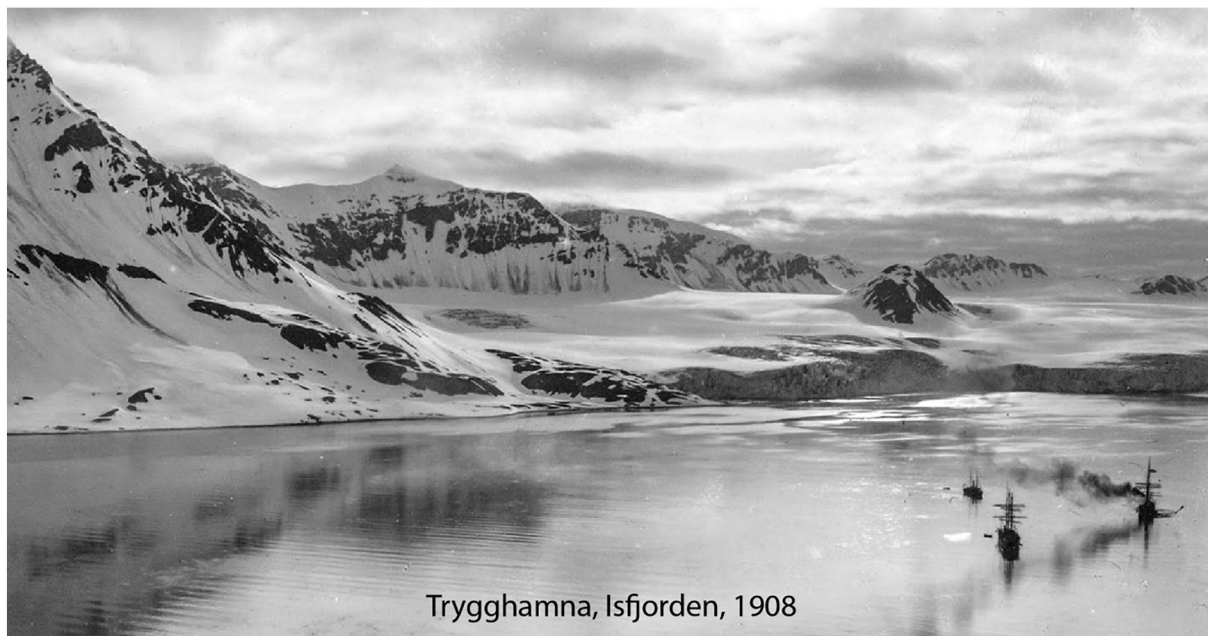
Trygghamna, Isfjorden, 1908

Fig. 2. Modified photograph taken of Trygghamna in 1908 by Oscar Halldin. Glaciers Protektorbreen and Harrietbreen with ice-margins calving into the bay beyond Swedish expedition ships. Photograph restoration and editing by Erik S. Holmlund. Expeditions described by De Geer (1908).

mild climate where the warm West Spitsbergen Current flows along the western coast of Spitsbergen and influences weather and sea ice conditions (Fig. 1; Førland et al., 1997). Regional climate is influenced by the interactions between the Icelandic Low and Siberian High pressure systems and as a result high temperatures are driven north over Svalbard by the main North Atlantic cyclone track (Hanssen-Bauer et al., 1990). Svalbard precipitation is closely coupled to the mode of the North Atlantic Oscillation (NAO; Dickson et al., 2000) and falls predominantly in solid form (Eckerstorfer and Christiansen, 2011). Today, the interactions of these air masses along the western margin of the archipelago commonly drive winter conditions with warmer and wetter climate than normally expected at such latitudes (Førland et al., 1997; Eckerstorfer and Christiansen, 2011).

1.3. Sedimentary archives, landforms and geological reconstructions

Holocene reconstructions of glaciers represent a mosaic of data developed through a suite of sedimentary archives and landforms present in both marine and terrestrial environments. The different stratigraphic archives used to reconstruct glacier and climate history include terrestrial geological sections, marine sediment cores and threshold-lake sediment records (Fig. 3). Geophysical data such as ground penetrating radar or sub-bottom profiler records can be paired with sediment cores and terrestrial stratigraphy to extrapolate across larger areas. Additionally, the relative (and absolute) age of landforms and their cross-cutting relationships identified in submarine and subaerial data (marine bathymetry and aerial imagery) are used to reconstruct past glacier extent, dynamics and other environmental conditions like relative sea level (Fig. 3). Moraines formed on land or at the margin of a tidewater glacier have been identified and correspond to glacier readvances (or still-stands). Raised marine sediments fingerprint postglacial coastlines around Svalbard, in some cases containing datable drift material (i.e. mollusc shells, whalebones and driftwood). Ice-core

stratigraphy is discussed based on 10 studies from 12 ice cores taken on Svalbard, however it is not the focus of this review given the relatively short and young cryostratigraphic record (less than 1 ka BP; Isaksson et al., 2003, 2005; Grinsted et al., 2009; Divine et al., 2011).

2. Methods

2.1. Compilation of ages

Age determinations from Svalbard and the surrounding waters that provide chronological constraints on glacier cover and marginal fluctuations or insight into climatic conditions over the last 12.0 ka were compiled into the SVALHOLA database (Table S1). Compiled ages and their meta-data were extracted from scientific publications, books, doctoral theses, geological reports, and maps (Table 1). Dates obtained from compilations are cited as well as the original source. To assure quality and consistency, ages from M.Sc. theses were excluded unless subsequently referenced in a peer-reviewed publication. The SVALHOLA database compiles previously published ages of radiocarbon (^{14}C, ^{14}C AMS, ^{14}C Conv.), luminescence (optically and infrared stimulated, OSL and IRSL) and terrestrial cosmogenic nuclide (TCN^{10}Be, TCN^{26}Al, TCN^{36}Cl). Thermoluminescence is nowadays considered less suitable for sediment dating and is not included in the database (Fuchs and Owen, 2008; Wintle, 2008). The database omits ^{210}Pb chronologies as the review does not focuses the post-LIA period.

The database has a census date of the 1st May, 2020 (which will be updated to the date of publication). All ages presented in the text are referred to in kiloyears (ka) unless otherwise stated. All radiocarbon ages have been calibrated and are referred to in ka before present (ka BP; present = 1950 AD), whereas the luminescence and cosmogenic nuclide ages are referred to in ka.
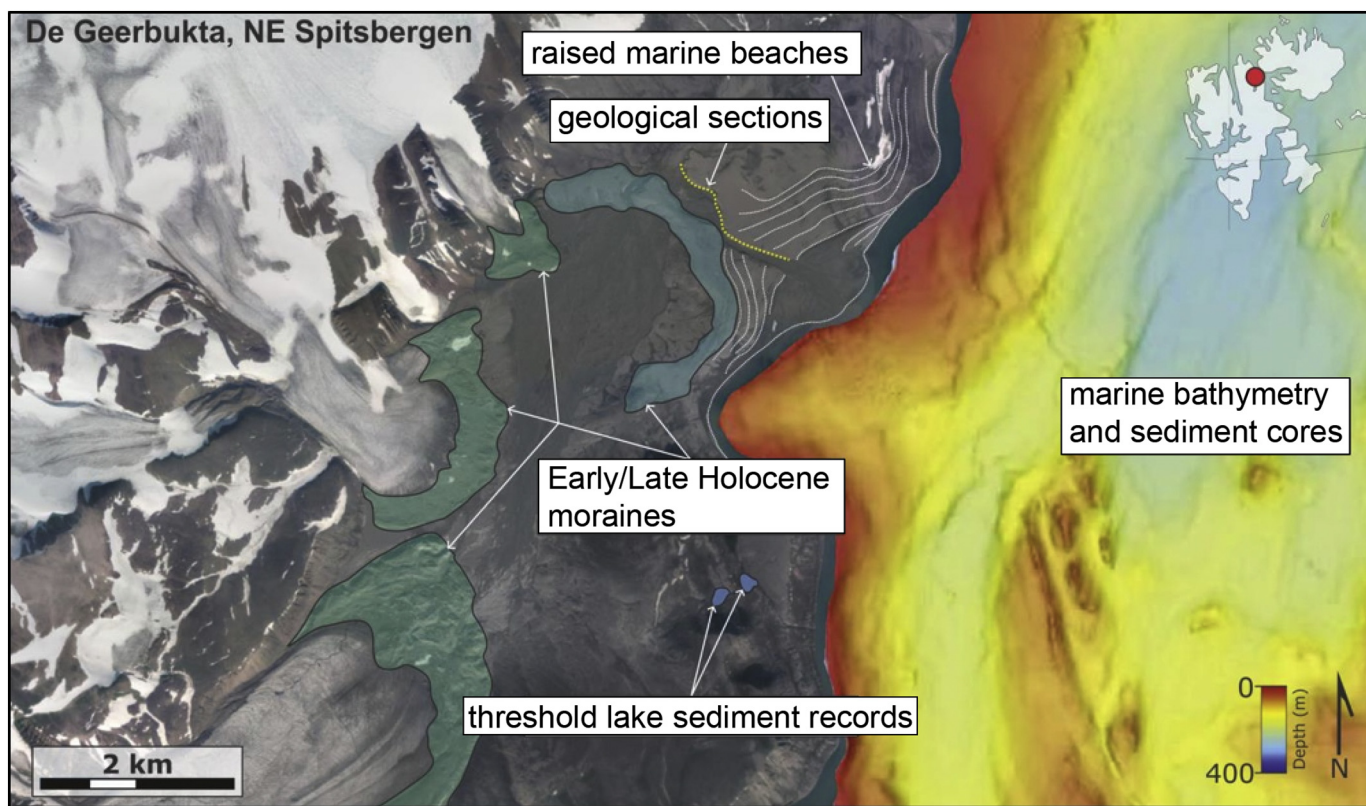

Fig. 3. Holocene landforms and sedimentary archives have been used to provide insight into the glacier history of Svalbard, here with examples from De Geerbukta, NE Spitsbergen. Aerial images from TopoSvalbard © Norwegian Polar Institute 2020 and fjord bathymetry modified from Streuff et al. (2017).

Table 1

Presented metadata recorded for each date included in the database (Table S1). Metadata from the database form the core of the criteria for quality assessment and palaeoglaciological classifications of each date as defined by the DATED1 database (Modified from Hughes et al., 2016).

SVALHOLA ID	• Unique database identification number
Location	• Country/sea, region, site name, SVALHOLA site number
	• Latitude and longitude in decimal degrees: ˚N, ˚E (WGS84)
	• Comment on precision of location if not reported from original source
Sample properties	• Site type: marine core, lake core, section, surface
	• Elevation (m a.s.l.)
	• Sample depth (m), if applicable
Dated material	• Sample field number and/or Laboratory ID number
	• Class of dated material: TPM (terrestrial plant macrofossils, including wood), organic (peat, insects, detritus, bulk, mixed, aquatic macrofossils), bone (whalebone, tusks), shell (molluscs and mollusc fragments), foraminifera (single species and mixed), tephra, sand, boulder, bedrock
	• Detailed description of dated material: free text
	• Organic material type: terrestrial (T), marine (M)
Stratigraphic context	• Detailed notes on stratigraphic setting: free text
	• Glacial context class: advance, margin, deglacial, ice free, exposure time (cumulative)
Dating method	• Radiocarbon (^{14}C, ^{14}C AMS, ^{14}C Conv.), optically stimulated luminescence (OSL), infrared stimulated luminescence (IRSL), terrestrial cosmogenic nuclide (TCN ^{10}Be, TCN ^{26}Al, TCN ^{36}Cl).
	• Thermo-luminescence (TL), electron spin resonance (ESR), U series and ^{210}Pb dates have been omitted.
Quality control	• Reliability of the age: 1 = likely reliable; 2 = probably reliable; 3 = likely unreliable (see Table 2 for criteria)
Ages	• Uncalibrated radiocarbon age / error (as reported, without marine correction or reservoir effect)
	• TCN age and error (as reported in source)
	• OSL age and error (as reported in source)
	• Calibrated/calendar age and error (reported to 2σ). Radiocarbon ages calibrated to INTCAL13 or MARINE13 (Reimer et al., 2013) as appropriate (on basis of type of organic material: T/M). ^{10}Be and ^{26}Al TCN ages recalculated using 'Arctic' production rate (Young et al., 2013) and Lal/Stone scaling (Lal, 1991; Stone, 2000). Necessary information to recalculate ^{10}Be and ^{26}Al TCN ages using different production rates additionally collated and recorded in Table S3
	• Age label; median age is rounded to nearest 10th as refered to in text.
	• Comments on calibration (e.g. beyond calibration curve limit)
Comments	• Any additional pertinent comments (e.g. reliability of date)
Citation information	• Source reference (author, year)
	• Compilation reference (author, year)
	• Database reference (e.g., Hormes et al., 2013; Mangerud and Svendsen, 2017)

2.2. Calculation and re-calculation of ages

2.2.1. Radiocarbon ages

To present and evaluate the SVALHOLA dataset consistently, all radiocarbon dates were recalibrated with INTCAL13 and MARINE13 calibration curves using the Calib Rev. 7.0.4 program (Reimer et al., 2013). Calibrated age ranges are presented as both 1σ (68% probability range) and 2σ (95% probability range) in the database. We use the centre of the age distribution ± half of the total 2σ range to represent the calibrated uncertainty for each age in our review. Given the past variations in correction and calibration for the geochronological methods, we extend the database to include ages with calibrated 2σ ranges where the upper 2σ falls above 12.0 cal. ka BP, but the full 2σ range indicating that the age potentially is younger than 12.0 ka BP. The ages presented in text and figures are calibrated center ages in kiloyears before present (ka BP) unless otherwise clarified.

A marine reservoir age has been implemented for all marine samples by selecting 'MARINE13' and using a regional "Delta R" (ΔR) value of 70 ± 30 (Table 1, S1; Mangerud et al., 2006; Mangerud and Svendsen, 2017). Our chosen ΔR of 70 ± 30 is specific for the Svalbard region (Mangerud et al., 2006; Mangerud and Svendsen, 2017) and deviates from the DATED1 compilation, which for simplicity utilized a ΔR value of 0 for all marine samples from their reconstruction of the last Eurasian ice sheets (Hughes et al., 2016). Both radiocarbon ages and calibrated ages are presented in the SVALHOLA database (Table S1).

2.2.2. Terrestrial cosmogenic exposure ages

A cosmogenic exposure age represents the cumulative time the sampled material has been exposed to cosmic radiation and need not always correspond to an actual age of an event. However, for the dates included in the SVALHOLA database – samples are almost exclusively erratic boulder ages that target moraines and relate to an ice marginal position. Within the Holocene, we assume that an exposure age represents one continuous exposure history.

Terrestrial cosmogenic exposure ages were (re-)calculated using the

CRONUS-EARTH online calculator v3 (Balco et al., 2008; https://hess.ess.washington.edu) with the Arctic production rate calibration datasets (Young et al., 2013). An 'Lm' scaling (Lal 1991; Stone 2000) has been used in the age label-column accordance with Young et al. (2018). As argued by Hughes et al. (2016) and Young et al. (2018), no corrections have been made for post exposure uplift, erosion, or snow cover. Cosmogenic ages are given in ka prior to the year of sampling. We have chosen not to recalculate the ages to ka before present (BP) and thus there may be roughly a 50-year offset from the radiocarbon ages.

2.2.3. Luminescence ages

Luminescence dating determines the last time a quartz or feldspar grain was exposed to sunlight, which is usually taken to be the time of deposition of the sampled sediment (Wintle, 2008). A luminescence age is given in ka prior to the year of sampling (Alexanderson and Murray, 2012a). Additionally, we have chosen not to recalculated the ages to ka before present (BP) and thus there may be roughly a 50-year offset from the radiocarbon ages. In the SVALHOLA database, ages are listed as presented in original publications (Table S2). For quality assessment criteria of OSL and IRSL ages, see Table 2.

2.3. Consistency and quality assessment of dates

The SVALHOLA database consists of accumulated geochronological information acquired over the last 50 years. Dating techniques have developed over this period and the standard of what is considered "reliable" has risen (Ivy-Ochs and Briner, 2014; Hughes et al., 2016). We utilize the structure of the quality assessment criteria introduced in the DATED1 database (Table 2) to characterize the reliability of each age in the SVALHOLA database (Hughes et al., 2016). We have rated all ages depending on the dating technique on a 3-point system (quality 1-3) to rule-out potentially misleading ages. According to Hughes et al. (2016) a quality mark of; 1 = all criteria is met (likely reliable), 2 = some of the criteria are met but not all (probably reliable), 3 = no

Table 2

Age quality control criteria (based on Duller, 2006, 2008; Thrasher et al., 2009; Wohlfarth, 2009; Heyman et al., 2011; Alexanderson and Murray, 2012b; England et al., 2013; Reimer et al., 2013). Ages within SVALHOLA are given a quality control (QC) rating based on the criteria specific to the dating method used. QC = 1, all criteria are satisfied; QC = 2, most of the criteria are satisfied; QC = 3 no (or few) criteria are satisfied (standard modified from Hughes et al., 2016).

Dating technique	Quality control criteria
Radiocarbon ^{14}C Conv (Conventional), ^{14}C AMS	• Known and uncontaminated sample material; sediment-feeding marine mollusc (e.g. *Portlandia arctica*) receives the lowest rating • Organic content > 5% LOI • Sample composition: Conv - bulk samples not acceptable; AMS - bulk sample acceptable • Within calibration range of INTCAL13/MARINE13 • Uncalibrated ^{14}C age determination provided with errors to enable recalibration using the latest calibration curves • Multiple and/or stratigraphically consistent ages
Terrestrial cosmogenic nuclide TCN ^{10}Be, ^{26}Al, ^{36}Cl	• Multiple (ideally three or more, but at least two) samples from the same feature/site • Ages are internally consistent and clustered (reduced Chi-square value ~1) • Observed spread in ages is similar to expected measurement uncertainty • Geomorphological setting is accounted for: erosion, submergence, uplift • Data necessary to recalculate ages (^{10}Be, ^{26}Al) using different production rates (Balco *et al.* 2008) • No indication of isotopic inheritance, or if present expected/stated
Luminescence OSL, IRSL	• Quartz-derived ages have a higher rating than feldspar-derived ages • Single-grain or small aliquot • Homogenous sample; preferably aeolian or littoral, fluvial, glacifluvial sediments that are likely to have received sufficient exposure • Sample setting considered and accounted for; e.g. water-content history • Dose rate information and equivalent dose including errors described in source • Multiple and/or stratigraphically consistent ages
All dating methods	• Sample considered *in situ*, i.e. no post-depositional disturbance or reworking • Specified error margins • Precise ages: errors < 10% of age • Details of geological and stratigraphical setting given • Considered by original authors to be reliable

criteria are met (likely unreliable). Dates suggested to be likely unreliable by original authors or other subsequent databases or compilations are rated quality 3. Dates of quality 1 and 2 standard have been used to reconstruct glacial history while ages deemed quality 3 are presented in Table S1, but have been excluded from the developed reconstruction. We deviate from the DATED1 standard in one key aspect; radiocarbon ages from sediment-feeding marine molluscs (i.e. *Portlandia arctica*) are considered likely unreliable. We strictly rate them as quality 3, thus excluding them from the reconstruction due to the high probability of an exaggerated age (England et al., 2013; Hughes et al., 2016).

2.4. Palaeoglaciological interpretation and climatic association of dates

2.4.1. Ice free

We have simplified the palaeoglaciological/climatological significance for a portion of the ages compiled in the SVALHOLA database founded upon metadata from the publications or the author's suggestions presented in the different studies. We assume all ages indicate ice-free or non-glaciated conditions unless otherwise stated. In some cases, additional classifications are placed on the ages. We do not classify the palaeoglaciological/climatological significance of individual ages taken from marine or lacustrine cores, but address their chronologies as a whole in both the results and discussion.

2.4.2. Re-advance

Ages of dateable material (e.g. vegetation, shell or bone with ^{14}C or sand with luminescence) that has been reworked or overridden by an advancing glacier are classified as maximum constraining ages for a glacier re-advance (Baranowski and Karlén, 1976; Ronnert and Landvik, 1993; Kristensen et al., 2009). In a study where numerous samples have been dated to constrain one glacier re-advance, all ages are classified as a "re-advance" in the SVALHOLA database, but only the best constraining age (i.e. the youngest) is presented in the figures (Humlum et al., 2005; Table S1). While older ages may inform about when the glacier was smaller than present (Punning et al., 1976; Kristensen et al., 2009; Lyså et al., 2018; Larsen et al., 2018), each re-

advance age presented in figures reflects a specific event for a specific glacier margin. Few Holocene glacier advances have been constrained in time by both maximum and minimum limiting ages (Lønne, 2005; Farnsworth et al., 2018). Based on consideration by original authors, ages classified as a "re-advance" are interpreted to correspond to a glacier fluctuation at or shortly following the mid-point of the youngest age (within the error margin).

2.4.3. Deglacial

We classify ages as "deglacial" where the site possesses stratigraphic information suggesting ice-free conditions shortly following cover by an ice sheet or a glacier. Such dates include basal organic material from lake cores, the lowermost shells or foraminifera in marine cores from fjords and raised glacial marine sediments from fjord-heads (Landvik et al., 1987; Mangerud et al., 1992; Svendsen and Mangerud, 1997; Hald et al., 2004; Alsos et al., 2015; Bartels et al., 2018; Farnsworth et al., 2018; Larsen et al., 2018). Additionally, the classification is used for radiocarbon ages of dateable material that has been sampled up-ice of modern ice margins (Blake, 1989; Oerlemans et al., 2011) suggesting reduced ice-cover. Unlike previous reviews (Landvik et al., 1998; Ingólfsson and Landvik, 2013; Hormes et al., 2013; Hughes et al., 2016; Hogan et al., 2017) we choose not to focus on the deglaciation in this paper but rather ice extent during the transition from Late Pleistocene to Early Holocene.

2.4.4. Margin

An age is classified as "margin" if the dated material is associated with an ice-marginal position. In the SVALHOLA database this is mainly erratic boulder ages, but could also be radiocarbon or luminescence ages relating to e.g. an ice-contact delta. Unlike ages associated with a re-advance, where the youngest age is considered the best constraint, exposure ages corresponding to an ice margin are presented in cumulative probability or in a histogram.

2.4.5. Environmental associations

We assign associated environmental conditions to two types of samples: thermophilous marine molluscs and terrestrial plants that

have been entombed by (passive) ice (Mangerud and Svendsen, 2017 and others therein; Miller et al., 2017). We associate warm regional waters to thermophilous marine molluscs e.g. *Arctica islandica, Mytilus edulis, Modiolus modiolus* and *Zirfaea crispata*. These species of molluscs have been sampled around Svalbard and radiocarbon date to different periods in the Holocene. The occurrence of these shallow marine molluscs, which are "effectively" absent from Svalbard fjords during the 20th century, suggests warmer than present conditions and are indicators of the (marine) Holocene Thermal Maximum on Svalbard (Feyling-Hanssen, 1955; Salvigsen et al., 1992; Hjort et al., 1995; Salvigsen, 2002; Hansen et al., 2011; Farnsworth et al., 2017; Mangerud and Svendsen, 2017).

We classify radiocarbon ages of terrestrial plants that have been entombed by (passive) ice as indicators of ice-cover expansion (ICE; Miller et al., 2017). Contrary to ages associated to a "re-advance", these samples do not correspond to unique/specific glacier systems. Large populations of these ages sampled over a vertical range have been associated with regional snow-line lowering, however a sole age does not indicate a conclusive driving factor of ice-cover expansion (summer temperature, winter precipitation, wind direction or some combination).

3. Results

3.1. The SVALHOLA database

The SVALHOLA database contains 1837 individual dates from over 722 discrete locations compiled from nearly 300 published sources (Fig. 4, Table S1-3). The spatial distribution is uneven and ages are predominantly from the western coast and fjords of Spitsbergen. Within the database, the lacustrine archive has the lowest density of ages (~10 %) followed by marine cores (~29 %). Samples dated from terrestrial archives make up the remaining population (~61 %). Over 90% of the dates in the SVALHOLA database are from radiocarbon analysis and roughly 50% of those samples are from marine organisms. In the database, there is a total of 104 ages from luminescence dating (~6 %) while there is a total of 46 ages (~3 %) from TCN dating.

Holocene radiocarbon ages from Svalbard are skewed toward the earlier half of the Holocene (Fig. 5). Roughly 60% of the SVALHOLA database date prior to 6.0 ka BP with nearly half of those ages falling between 11.5 – 9.5 ka BP (Fig. 5). Roughly 20% of the radiocarbon ages within the SVALHOLA database date to within the last 2 ka BP. Although the Middle Holocene has comparatively fewer dates per 500-year period, there is a relatively consistent distribution of ages, with a gentle decline 9 – 2 ka BP (Fig. 5). There is a lower percentage of "likely reliable" (quality 1) radiocarbon ages versus less reliable ages in the Early Holocene.

There is a less consistent distribution of TCN and luminescence ages throughout the Holocene (Fig. 6). Until recently, few studies have relied on TCN and/or luminescence dating as the main geochronological method for constraining Holocene archives or landforms (Reusche et al., 2014; Philipps et al., 2017; Gilbert et al., 2018). In most cases studies utilizing these methods focused on longer time scales or used the techniques to constrain the deglaciation (Mangerud and Svendsen, 1992; Mangerud et al., 1998; Forman, 1999; Kaakinen et al., 2009; Hormes et al., 2011; Alexanderson et al., 2013; Landvik et al., 2013; Young et al., 2018).

There are a greater percentage of likely unreliable (quality 3) ages in both the TCN and luminescence populations compared to the radiocarbon ages. This is predominantly related to age precision and error ranges exceeding 10% of the age, especially for the younger half of the sample distribution. While the bulk of the luminescence ages fall within the Mid Holocene there is an inverse distribution of TCN ages, with the majority dating to the Late Holocene and the second largest population in the Early Holocene (Fig. 6).

3.2. Holocene Glacier Activity

Our results are compilations of records and ages that (in-)directly enhance our understanding of Holocene glaciers on Svalbard. Here we present a series of age-transects that reflect the Early Holocene deglaciation (rates and percentages) within Svalbard fjords. Additionally, we map the spatial and temporal distribution of glacier re-advances that punctuated this phase of deglaciation during the Early Holocene. By compiling glaciolacustrine and fjord records from Svalbard, we are able to reconstruct Mid Holocene glacier (in-)activity and identify where bodies of ice likely persisted. Furthermore, compilations of glacial lake and fjord records detail Late Holocene glacier expansion, complementing our mapped distribution of glacial landforms constrained to Late Holocene glacier fluctuations.

3.2.1. Retreat within Early Holocene fjord systems

By 12.0 ka BP the mouths of Svalbard fjords had already begun to deglaciate (Hormes et al., 2013; Hughes et al., 2016). Here we highlight six fjord system transects, marking the oldest Holocene ages (found in the SVALHOLA database), from fjord-mouth to fjord-head, to indirectly track the ice marginal retreat during the Early Holocene (Fig. 7). The oldest ages found at the heads of fjord systems range between 11.5 – 9.1 ka BP and averages 10.5 ka BP for all fjord systems. Spatial comparisons of the ages suggest retreat rates within fjord systems ranged from roughly 10 km per 1 ka (St. Jonsfjorden) to as great as 12 km per 0.1 ka (Wijdefjorden). Normalized fjord lengths by percent suggest Svalbard fjords had become half-way deglaciated by 11.6 ± 0.2 ka BP and 75% ice-free by 11.3 ± 0.4 ka BP (Fig. 7). Generally, greater rates of Early Holocene retreat are found in longer fjord systems.

3.2.2. Early Holocene retreat punctuated by glacier re-advances

As Svalbard fjord systems became ice-free during the Early Holocene, tributary ice margins (from cirques, valleys and outlet glaciers) exhibited re-advances (Fig. 8). Reworked dateable material from the Early Holocene has been identified within and sampled from glacial deposits across Svalbard. Most often, this material is shell fragments re-sedimented in glacial (marine) diamictons suggesting glacier overriding and in some cases glaciotectonism (e.g. Salvigsen et al., 1990; Lønne, 2005; Farnsworth et al., 2018). The highest frequency of Early Holocene glacier re-advances (11 of 20 events) occurred between 11 – 10 ka BP (Fig. 8). While re-advances associated with younger ages are located at the heads of fjord systems, older Early Holocene re-advances are identified near the outer extent and mouths of the fjords (Farnsworth et al., 2018; Larsen et al., 2018). The youngest Early Holocene glacier re-advances are found at the head of Wijdefjorden (9.1 ± 0.19 ka BP; Marks and Wysokinski, 1986) and Tempelfjorden (9.1 ± 0.14 ka BP; Forwick et al., 2010; Table S1).

3.2.3. Middle Holocene ice-free lake catchments and reduced glacier influence within fjord systems

Svalbard's glacial lacustrine sedimentary archives have been investigated in order to further reconstruct Holocene glacier activity (e.g., Bøyum & Kjensmo 1980; Svendsen and Mangerud, 1997; Røthe et al., 2015). Glacial lacustrine sedimentary archives provide a unique window into Svalbard's Middle Holocene glaciers during a time when glacier moraine records are absent. A compilation of glacial lake records extending through the Holocene suggests catchments received little or low minerogenic input which has been interpreted as reduced or ice-free catchments (Fig. 9). Lake records suggest lake catchments deglaciated between 10 – 7 ka BP and remained ice-free through the Middle Holocene. As of yet, no (investigated) glacier lake record on Svalbard suggests active glaciers within the catchment through the Middle Holocene.

Glacial reconstructions from lake cores are only as robust as the sediment core chronologies. The distribution of ages within the SVALHOLA database exhibits Svalbard lake records are some of the highest
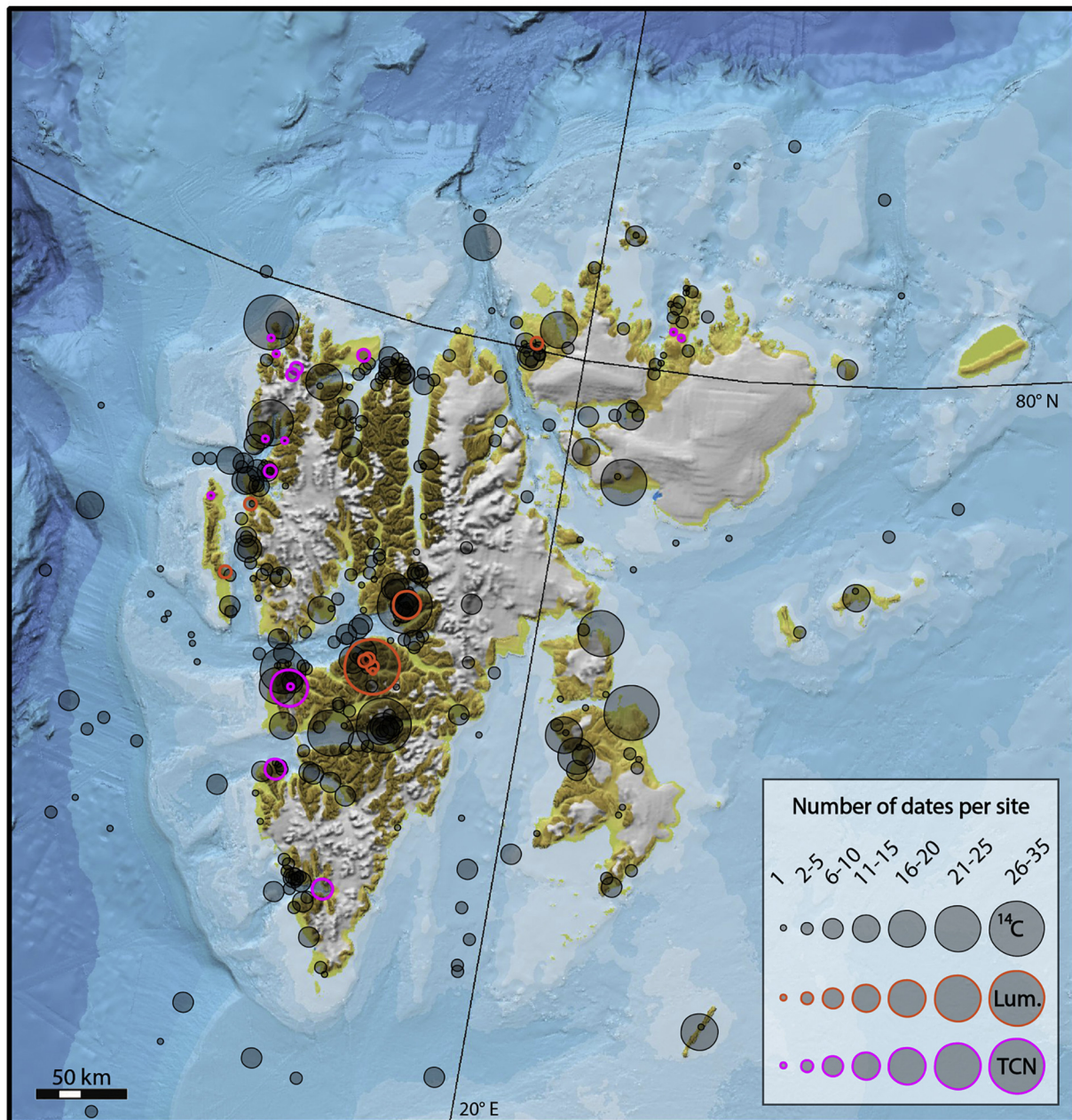
Fig. 4. Spatial distribution of ages compiled in the SVALHOLA database. Colored circles are proportional to the number of dates of each method per site. Note the low density of chronological data from eastern Svalbard and the east coast of Spitsbergen. The bulk of the ages are radiocarbon dates from low elevation coastal regions and from shallow waters to the west of Spitsbergen. Dates were compiled from references presented in Table S1-S3 and at the end of this manuscript (full references are included in the supporting information; Data S1).

concentrations of radiocarbon ages per point-location. However, the resolution of lake core chronology ranges widely as a result of core length and availability of datable material (Fig. 9). In lake sediment cores, a mixture of material has been used to constrain chronologies (Fig. 8). Early investigations using lakes to reconstruct palaeo-environmental conditions relied on radiocarbon dating bulk sediment (e.g. Hyvärinen, 1970), while modern studies target terrestrial plant macrofossils (de Wet et al., 2018) and occasional mollusc shells sampled just below the lacustrine-marine boundary in isolation basins (Svendsen and Mangerud, 1997; Schomacker et al., 2019). Recent studies have used crypto-tephra to constrain lake chronologies where terrestrial macrofossils are sparse (Fig. 8; D'Andrea et al., 2012; van der Bilt et al., 2017). Based on a collection of Svalbard's glacial lake records, composite lake cores average 2.4 m in length and are well dated,

averaging 4.6 ages per meter (Fig. 9).

Marine sedimentary archives have also been investigated in Svalbard fjords to enhance Holocene glacier reconstructions (Fig. 10). While some marine records suggest glaciers retreated back to terrestrial margins during the Early Holocene and coasts remained ice-free through the Middle Holocene, other records suggest continuous (although reduced) input of outsized particles of ice rafted debris (IRD). Studies have suggested that location dependence can greatly influence whether IRD is glacier derived or originating from sea ice plucking beach sediments (Forwick et al., 2010; Joo et al., 2019).

Similar to lake cores, marine core chronology ranges widely as a result of core length and availability of datable material (Fig. 10). Holocene reconstructions from marine sediments often use mollusk shells or foraminifera for radiocarbon dating and constraining core
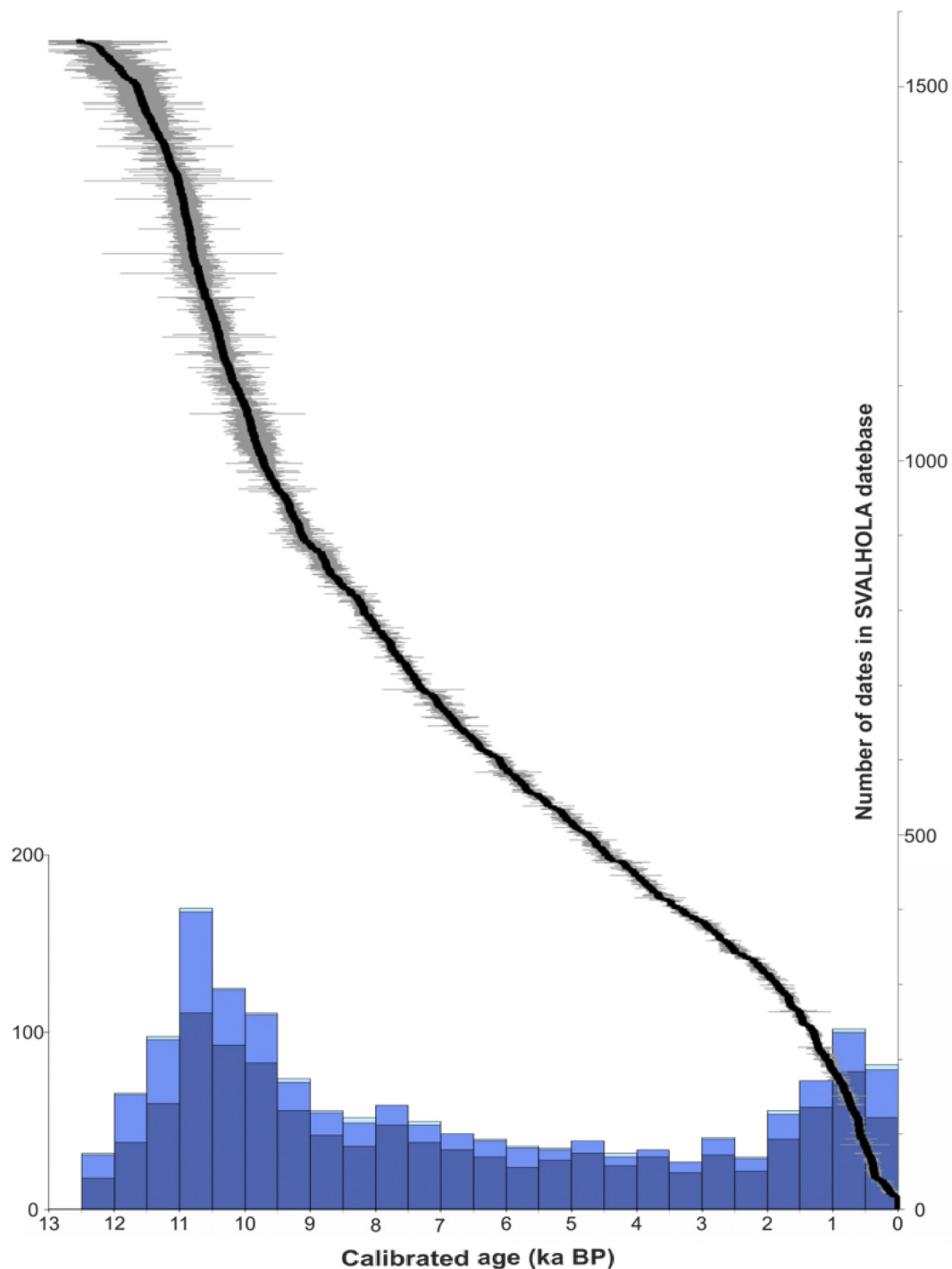
Fig. 5. Histogram of radiocarbon ages contained within the SVALHOLA database with dates presented with a 500-year bin size modified from 1000-year bin size presented by Hughes et al. (2016). Dates colored according to quality rating 1 (dark blue), 2 (blue) and 3 (light blue). The plot displays the same 1667 SVALHOLA dates with the centers for the age distributions stacked chronologically (black dots) and associated error bars (grey). Ages extend over 12.0 ka BP as the database includes all ages in which error margins fall within the Holocene (Table S1). (For interpretation of the references to color in this figure legend, the reader is referred to the web version of this article.)

chronologies. Unlike lake records, crypto-tephra has not been utilized chronologically within Svalbard fjord records. Generally, Svalbard's Holocene marine records, exhibit lower chronological resolution than lake records. Composite Holocene fjord records average 4.9 m in length and average 1.8 ages per meter (Fig. 10).

3.2.4. Late Holocene glacier expansion

Starting *c.* 4.0 ka BP lake and fjord records across Svalbard begin to see increased sedimentation rates generally characterized by enhanced mineragenic input into lake basins and increasing IRD within fjord records (Figs. 9 & 10). Enhanced sediment transport from catchments to basins (between 4 – 0.5 ka BP) is associated with widespread Late Holocene glacier expansion, referred to as the Neoglacial (Werner, 1993).

Late Holocene glacier expansion is also reflected by glacial landforms associated with glacier growth and re-advance. Landforms and
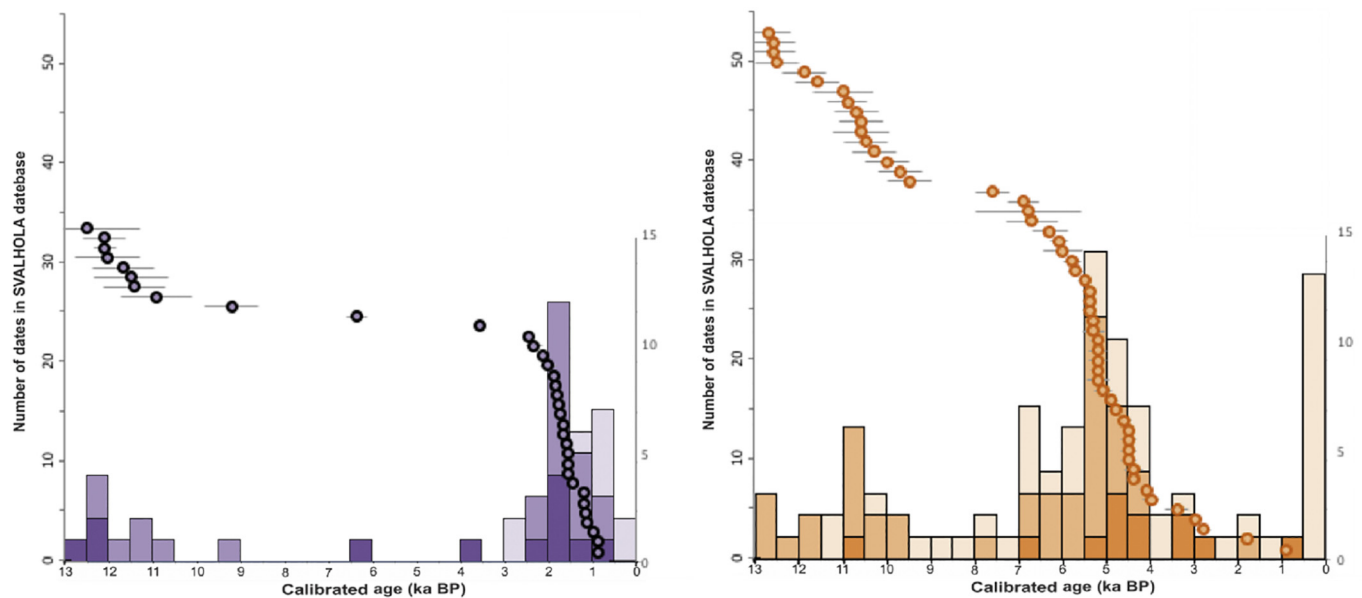
Fig. 6. Histogram of cosmogenic nuclide (purple) and luminescence (orange) ages contained within the SVALHOLA database with dates presented with a 500-year bin size modified from 1000-year bin size presented by Hughes et al. (2016). Dates colored according to quality rating 1 (dark purple/orange), 2 (purple/orange) and 3 (light purple/orange). The plot displays the same ages from the SVALHOLA database with the centers for the age distributions stacked chronologically (colored circles) and associated error bars (grey) excluding the likely unreliable quality 3 ages. Ages extend over 12.0 ka BP as the database includes all ages in which error margins fall within the Holocene (For interpretation of the references to color in this figure legend, the reader is referred to the web version of this article.)

sediment have been constrained in time where molluscs, whalebones or vegetation have been radiocarbon dated or TCN dating has been conducted on glacier-deposited boulders. Despite no geochronological constrains on glacial deposits dating to the Middle Holocene (8.2 – 4.2 ka), there are abundant exposure ages as well as molluscs found within re-sedimented or overlain by glacial deposits of Late Holocene age (since 4.2 ka; Fig. 11). Roughly half of Late Holocene glacier re-advances are constrained by re-worked molluscs found within glacial deposits (Punning et al., 1976; Werner, 1993; Sharin et al., 2014; Farnsworth et al., 2017; Lovell et al., 2018).

Nearly half of the ages constraining Late Holocene glacier advances (in addition to the mollusc shells) are from over-ridden (*in situ*) vegetation (Baranowski and Karlén, 1976; Dzieriek et al., 1990; Furrer 1991; Humlum et al., 2005). Ages become more frequent in the last 2 millennia (Fig. 11). In addition to material that has been reworked or overridden by glaciers, plants that have been entombed in passive ice (cold-based, perennial snow patches and firn) have also been sampled and dated (Fig. 11). Over 40 samples of moss and vegetation preserved under cold-based ice have been collected from retreating modern ice margins in central Spitsbergen (Miller et al., 2017). While the oldest ages range back to nearly 4 ka BP, *c.* 80% of the samples are younger than 2.0 ka BP (Fig. 11).

3.3. Holocene sea level and environment

Not all ages within the SVALHOLA database directly reflect glacier activity. However, many of these ages have been used to enhance our understanding of Svalbard's Holocene glacier history by providing chronological envelopes for environmental conditions that relate to the behavior of the glacier systems.

3.3.1. Variability in Svalbard's glacioisostatic rebound

The dominant fingerprint of Holocene coastal geomorphology on Svalbard is flights of raised beaches and marine sediments. These raised beaches indicate previous shorelines that have subsequently been uplifted relative to local sea level as a result of glacioisostatic rebound (Forman et al., 1987; Bondevik et al., 1995). For the last 60 years, postglacial relative sea level curves have been constructed for regions

all over Svalbard (Feyling-Hanssen, 1955; Birks, 1991, Blake, 1962; Forman et al., 2004; Schomacker et al., 2019; Fig. 12). The variability in uplift exhibited in Svalbard's relative sea level curves is a result of glacial history and behavior. Svalbard's relative sea level history is a product of ice-cover thickness, duration, timing of deglaciation and in some cases, subsequent ice expansion (Ingólfsson and Landvik, 2013; Fjeldskaar et al., 2018). Elevations of postglacial marine limits (where curves have been developed) range from slightly under 20 m a.s.l. in Southern Spitsbergen to greater than 100 m a.s.l. on Kong Karls Land in Eastern Svalbard (Fig. 12).

Holocene uplift rates have been derived from radiocarbon dated whalebones, driftwood and shells found on or in raised beaches (Salvigsen, 1981; Häggblom, 1982; Forman et al., 2004). While there is large amount of variability, the Early Holocene exhibits the greatest rates of isostatic uplift recorded in the last 11.7 ka BP. For some locations, minimum uplift rates derived from raised marine shorelines suggest 10 – 25 meters of uplift per 1.0 ka during the Early Holocene on Svalbard (Salvigsen, 1981; Salvigsen and Österholm, 1982; Forman et al., 2004). The ages of raised marine shorelines suggest glacioisostatic uplift rates decline throughout the Middle Holocene and equate to *c.* 5 m per 1.0 ka (Bondevik et al., 1995; Forman et al., 2004). In several locations on the northern and western coasts of Svalbard, regression ceased and Middle Holocene transgressions occurred, as interpreted through a combination of shoreline morphology and geochronology (Forman, 1990; Forman and Ingólfsson, 2000). Through the Late Holocene, dated raised marine shorelines indicate a further decrease in relative uplift rates (Forman et al., 2004). Generally, it is believed Late Holocene relative sea level was regressive around Svalbard (Bondevik et al., 1995; Forman et al., 2004; Sessford et al., 2015). It is unknown to what extent Neoglacial glacier expansion influenced relative sea level in Svalbard during the Late Holocene as eustatic sea level is suggested to have out-paced relative land uplift along Spitsbergen's western coast (Forman et al., 2004; Fjeldskaar et al., 2018).

3.3.2. Holocene driftwood

Radiocarbon ages of driftwood make up roughly 10 % of the SVALHOLA database and 35 % of the terrestrial ages. The occurrence of driftwood found on Arctic shorelines has been used as a proxy for semi-
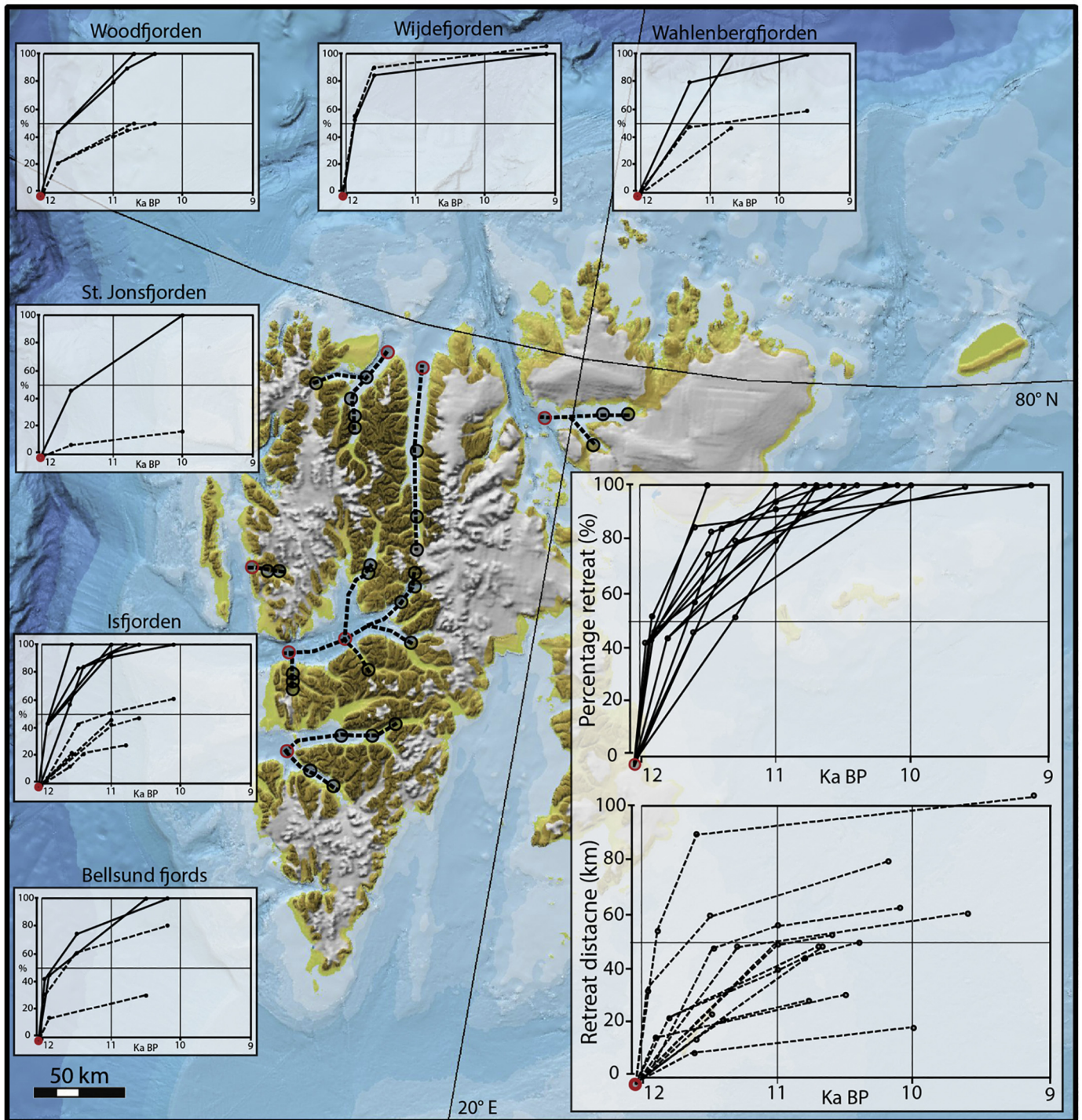
Fig. 7. Transects highlight Early Holocene ice retreat within fjord systems; Bellsund, Isfjorden, St. Jonsfjorden, Woodfjorden, Wijdefjorden and Wahlenbergfjorden. Plots present retreat length (km) and percentage retreat (%) over time separately for each fjord system and comparatively for all fjord systems. Fjord length calculations are based on the distance between database ages rather than modern fjord dimensions. Thus, fjord lengths are in some cases underrepresented as ages do not reach modern fjord heads while other fjord lengths are overrepresented as ages are found in fjord valleys, presently located kilometers inland.

permanent sea-ice extent (Häggblom, 1982; Funder et al., 2011; Nixon et al., 2016; Hole and Macias-Fauria, 2017). Where sea-ice cover is too low no driftwood arrives, while with multiyear sea ice, driftwood is shielded from the shorelines (Funder et al., 2011). The frequency of radiocarbon dated driftwood from Svalbard's raised marine shorelines exhibits an increasing rate of arrival between 12.0 – 10.5 ka BP which is followed by a stepped and variable decline in occurrence to 9.0 ka (Fig. 13). Peak driftwood arrival occurs between 11.0 and 10.5 ka BP

(Fig. 13). The presence of driftwood on raised Middle Holocene shorelines remains lower than the peak occurrence from the Early Holocene, yet suggests consistent arrival of material from roughly 9.0 to 6.5 ka BP. This interval is followed by a steady but variable arrival of driftwood from 6.5 to 4.2 ka BP (Fig. 13). During the first half of the Late Holocene driftwood occurrence remains low (Fig. 13). The period between 2.5 – 2.0 ka BP marks the Holocene minimum in driftwood arrival and matches the occurrence rate seen during the end of the Younger Dryas
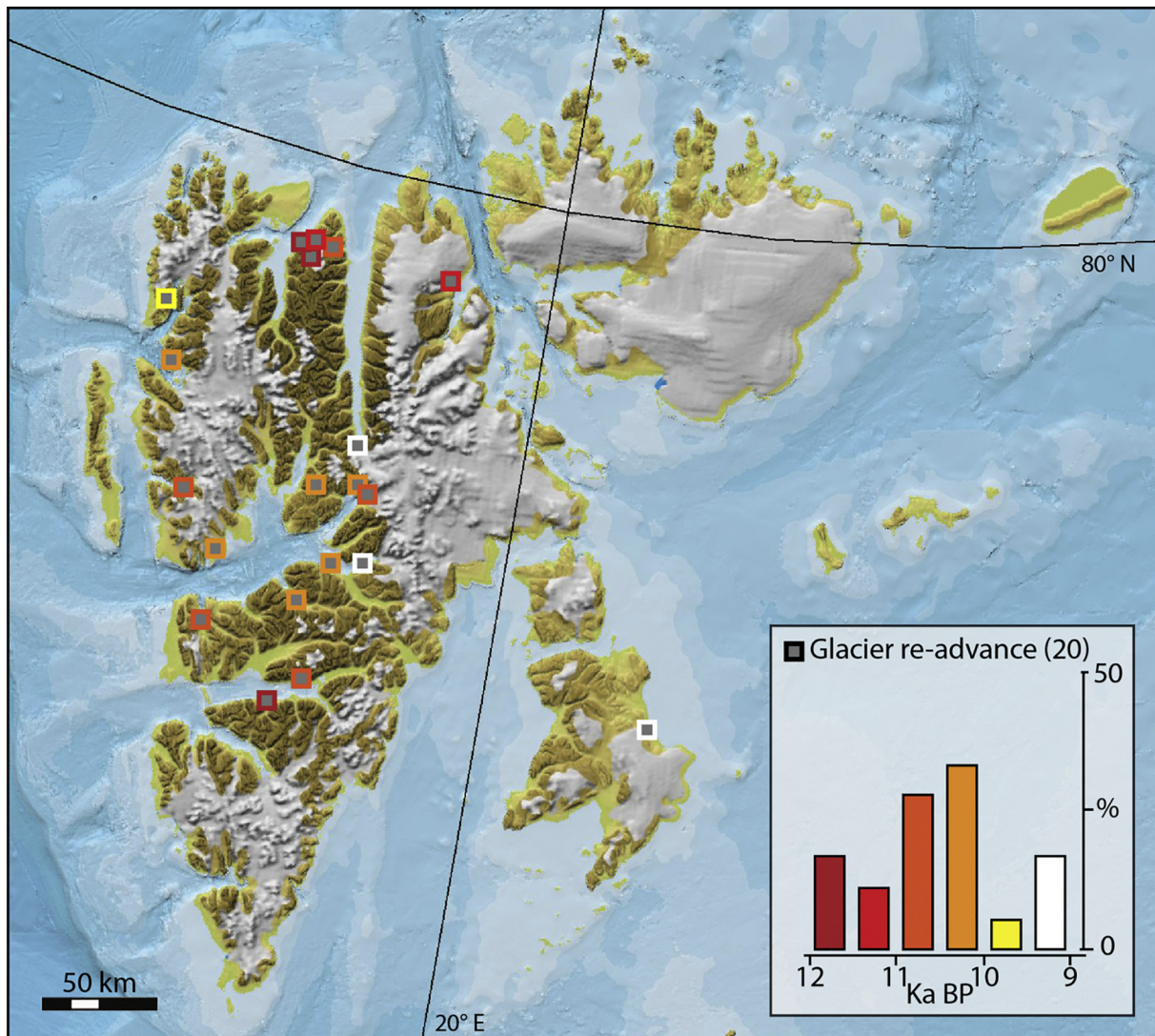
Fig. 8. Distribution of Early Holocene glacier re-advances identified around Svalbard. Re-advances occur from 12 – 9 ka BP with greater than half of the glacier re-advances happening between 11 – 10 ka BP. Dates were compiled from references presented in Tables S1-S3 and at the end of this manuscript (full references are included in the supporting information; Data S1).

period (12.0 – 11.5 ka BP; Fig. 13). A sharp increase in the number of dated driftwood is exhibited during the last two millennia. The driftwood count from the most recent 500 years (bin 0.5 ka BP to modern) has been excluded given the general lack of studies targeting radiocarbon dated driftwood accumulated at or slightly above the modern shorelines. Furthermore, the occurrence of Holocene driftwood on raised marine shorelines is influenced by preservation, and therefore may as well be influenced by Middle and Late Holocene transgressions.

3.3.3. Thermophilous marine species

Several species of molluscs are suggested to indicate "warm regional waters" around Svalbard at different time intervals in the Holocene based on their modern habitats (Feyling-Hanssen, 1955; Salvigsen et al., 1992). These thermophilous molluscs that once inhabited Svalbard can be found preserved in raised marine sediments of Early-Middle Holocene age (Fig. 13; Feyling-Hanssen, 1955; Salvigsen et al., 1992; Hjort et al., 1995; Salvigsen, 2002; Blake, 2006; Hansen et al., 2011; Farnsworth et al., 2017; Mangerud and Svendsen, 2017). The earliest radiocarbon ages of the warm water species *Mytilus edulis* date slightly before 11.0 ka BP and suggest the sea temperatures around Svalbard were roughly 2 °C warmer than present (Fig. 13; Mangerud and Svendsen, 2017). Additionally, the occurrence of *Zirfaea crispata* and

Arctica islandica around Svalbard has been used to suggest shallow ocean temperatures peak between 10.0 – 9.2 ka BP and were at least 6 °C warmer than present, framing the marine Holocene thermal maximum (HTM; Mangerud and Svendsen, 2017 and references therein). Thermophilous molluscs persist in Svalbard waters throughout the Middle Holocene. A slight decline in the occurrence of thermophiles suggests a short-lived cooling following the marine HTM between 9 and 8.2 ka BP. However, ocean temperatures still remained roughly 2 °C warmer than present based on the persistence of *Mytilus edulis* (Mangerud and Svendsen, 2017). Both *Mytilus edulis* and *Modiolus modiolus* remained in Svalbard waters into the Middle Holocene suggesting ocean temperatures were *c.* 4 °C warmer than present 8.0 – 6.5 ka BP (Salvigsen et al., 1992; Salvigsen, 2002; Blake *et al.* 2006; Mangerud and Svendsen, 2017). The occurrence of thermophilous molluscs decreases through the Middle Holocene and tapers off entirely at the start of the Late Holocene, when reconstructed ocean temperatures reach those comparable to modern (Fig. 13; Mangerud and Svendsen, 2017). In addition to the two *Mytilus edulis* dating *c.* 3.7 ka BP, it appears the species may have returned to inner Isfjorden based on a single young sample dating 0.9 ka BP (Fig. 13; Samtleben, 1985; Mangerud and Svendsen, 2017).

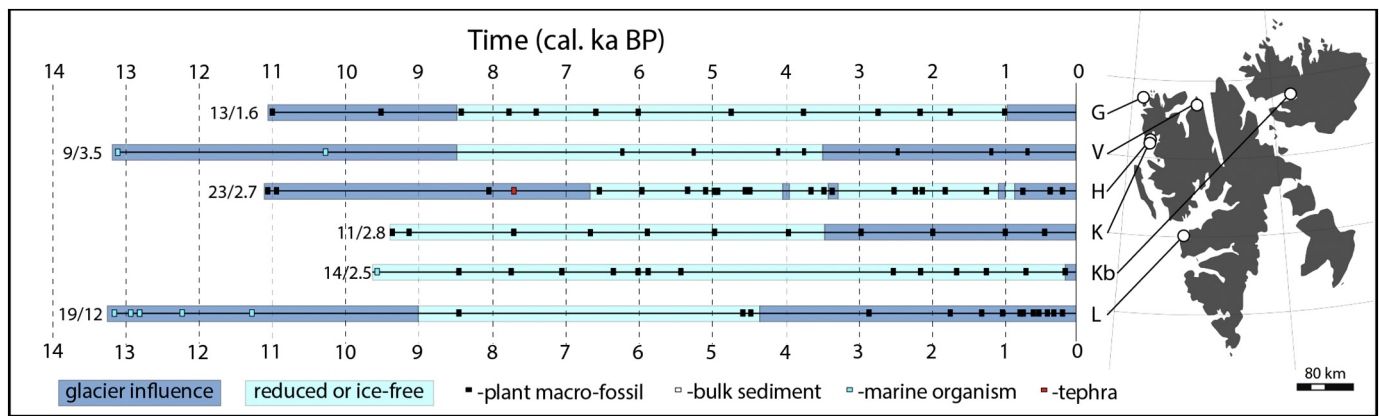Warm waters are not just reconstructed from the shallow inner

Fig. 9. Diagram highlighting the chronology and distribution of glacial lake records on Svalbard used to reconstruct Holocene glacier activity. Blue bars indicate high (dark blue) and low/reduced (light blue) minerogentic input within the lake records. Minerogentic input has be used to suggest the presence or absence of an active glacier within the lake catchment. Terrestrial plant macrofossils (black boxes), crypto-tephra (red boxes), marine mollusc shells and foraminifera (blue boxes) and bulk sediment ages (white boxes) are used to constrain core chronologies. Values to the left of the chronologies indicate the number of dates and the composite core length of each record. Inset map shows the location of the different records: G = Gjøavatnet (de Wet et al., 2018), V = Vårfluesjøen (Mäusbacher et al., 2002; Røthe et al., 2018), H = Hajeren (van der Bilt et al., 2016), K = Kløsa (Røthe et al., 2015), Kb = Kløverbladvatnet (Schomacker et al., 2019) and L = Linnévatnet (Svendsen and Mangerud, 1997; Svendsen and Mangerud, 1997; Snyder et al., 2000). (For interpretation of the references to color in this figure legend, the reader is referred to the web version of this article.)
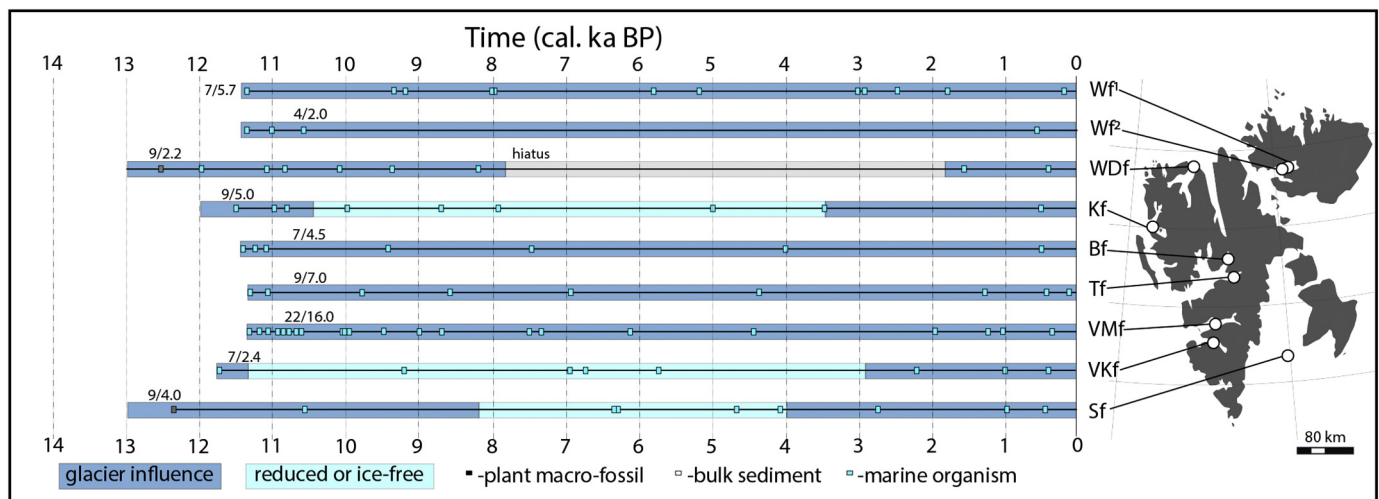

Fig. 10. Diagram highlighting the age and distribution of investigated glacial influenced fjord systems used to reconstruct Holocene glacier activity. Blue bars indicate high (dark blue) and low/reduced (light blue) ice rafted debris within the marine records. Ice-rafted debris concentrations have been used to suggest the presence or absence of a glacier calving margin within the fjord system. Terrestrial plant macrofossils (black boxes), marine mollusc shells and foraminifera (blue boxes) are used to constrain core chronologies. Values at left above chronologies indicate the number of dates and the composite core length of each record. Inset map shows the location of the different records. Fjords: Wf = Wahlenbergfjorden ([1]Flink et al., 2017; [2]Bartels et al., 2018), Wdf = Woodfjorden (Bartels et al., 2017), Kf = Kongsfjorden (Skirbekk et al., 2010), Bf = Billefjorden (Baeten et al., 2010), Tf = Tempelfjorden (Forwick et al., 2010), VMf = Van Mijenfjorden (Hald et al., 2004), VKf = Van Kuelenfjorden (Kempf et al., 2013), Sf = Storfjorden (Nielsen and Rasmussen, 2018). (For interpretation of the references to color in this figure legend, the reader is referred to the web version of this article.)

fjords-systems of Svalbard. Marine micropaleontology records from outer fjords and regional waters, also suggest warm conditions prior to the onset and throughout the Early Holocene (Hald et al., 2004; Ślubowska-Woldengen et al., 2007; Skirbekk et al., 2010; Rasmussen et al., 2012; Łącka et al., 2015; Allaart et al., 2020). Warm Atlantic water is associated with the dominance of *N. labradorica* and relative decline in *N. pachyderma* (sinistral) found within the Early Holocene fjord systems (Rasmussen et al., 2012).

4. Discussion

We begin by refining our understanding of ice cover during the transitions from Late Pleistocene to Early Holocene in comparison to previous reconstructions (Mangerud and Landvik, 2007; Hormes et al.,

2013; Hughes et al., 2016; Hogan et al., 2017). We then discuss evidence of Holocene glacier activity from the marine, terrestrial and lacustrine archives for each stage: Early (11.7 – 8.2 ka BP), Middle (8.2 – 4.2 ka BP) and Late (4.2 ka BP to present) Holocene. Following each Holocene stage, we discuss reconstructed environmental conditions which likely influenced glacier behavior. We complete our discussion by considering the key drivers of Holocene glaciers on Svalbard and how ice margins behaved during cooling events and warming events. Despite certain micro-climatic variability, we choose not to subgroup data geographically, but generally discuss ages for the entire Svalbard region. In some cases, we refer to more detailed locations e.g. the mouth of a fjord, relative to the tributary or head of the fjord system.
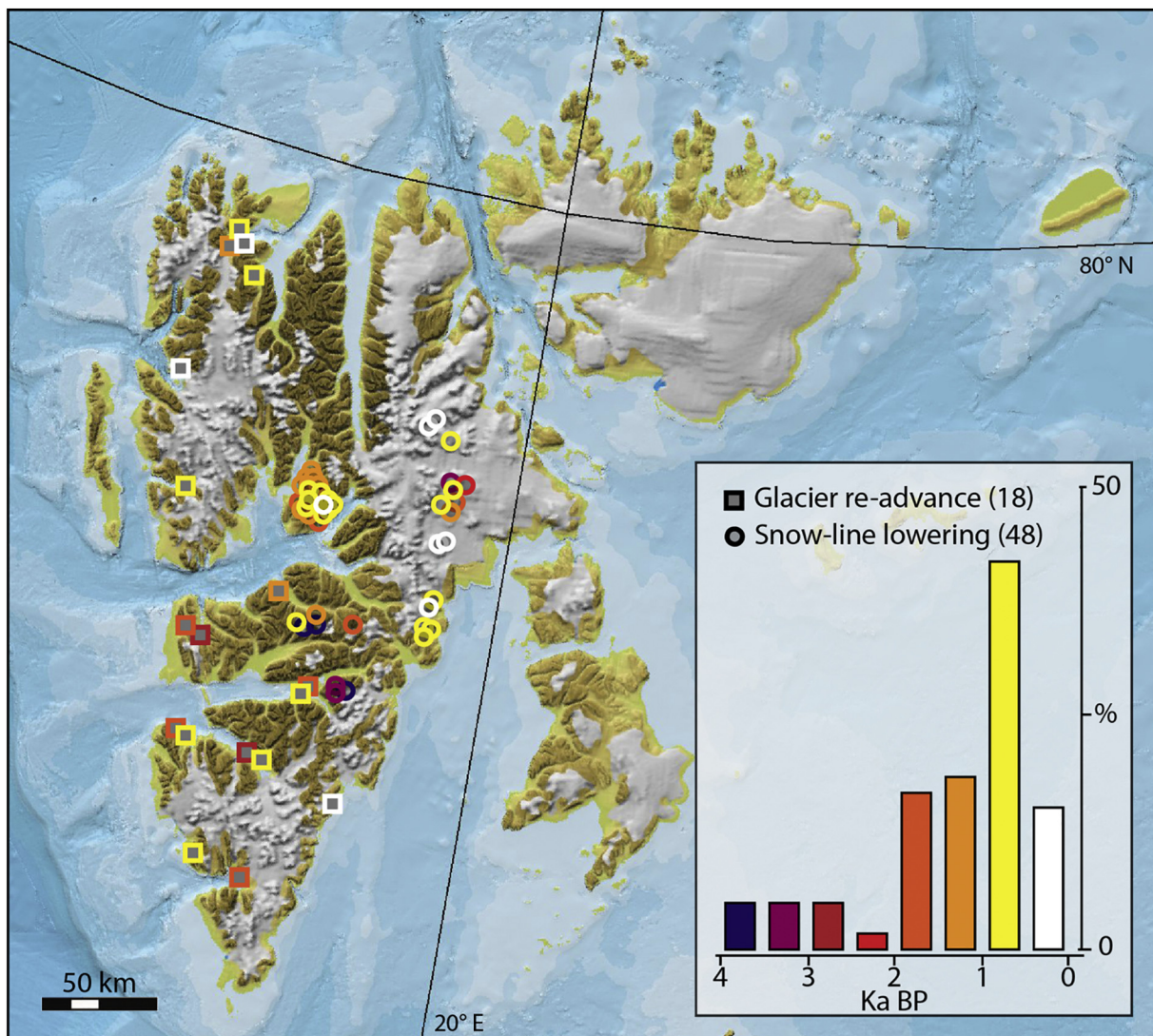
Fig. 11. Distribution of Late Holocene glacier re-advances associated with glacial landforms or deposits (marked by colored squares). Late Holocene snow-line-lowering (marked by colored circles) indicates where dead vegetation identified at passive ice margins has been radiocarbon dated. Constraining ages occur from 4 – 0 ka BP with nearly 50% of Late Holocene glacier re-advances dating to between 1 – 0.5 ka BP. Dates were compiled from references presented in Tables S1-S3 and at the end of this manuscript (full references are included in the supporting information; Data S1). (For interpretation of the references to color in this figure legend, the reader is referred to the web version of this article.)

4.1. Late Pleistocene – Holocene transition

We recognize the importance of constraining the extent of glacier cover during the transition from Late Pleistocene to the Holocene. While timeslices give an approximate distribution of glacier cover over a region during a window in time, they often over simplify critical information (e.g., ice thickness and dynamics) and extrapolate between sparse data. Our dataset generally indicates the lack of ice (e.g., deglaciation or ice free conditions), rather than the actual distribution (e.g., ice marginal positions). However, where ample geochronological data is tied with morphology or stratigraphy it is possible to develop a map representing glacier cover, if spatial scale allows. We feel any attempt to map glacier distribution at regional scale for Svalbard, limited by constraining data (geochronology and morphology) is likely an over-representation of limited knowledge. We choose to limit our timeslices reconstructions to only target the maximum and minimum range of ice cover during the Holocene on Svalbard (Fig. 14A).

Maximum ice cover since 12.0 ka BP was likely around 12.0 ka BP, as residual SBSIS still covered the majority of Svalbard (Fig. 14). The exact ice extent is not well understood given the limited number of ice marginal positions and sparse data throughout the region. Additionally, it is unknown how tightly the deglaciation ages from marine sediment cores and raised marine sediments constrain the actual deglaciation as these ages are minimum constraining values and could potentially reflect conditions centuries after the actual deglaciation (Hald et al., 2004; Larsen et al., 2018). Reconstructions of ice margins during the transition from Late Glacial to Early Holocene are challenged by potential deglaciation ice-shelves that may have limited the formation of ice-marginal landforms (Furze et al., 2018; Farnsworth, 2018). Based on ages found in the SVALHOLA database we suggest the most-credible ice cover timeslice from DATED-1 likely over-estimates glacier cover on Svalbard at the transition from Late Pleistocene to Early Holocene (Fig. 14A; Hughes et al., 2016).

The same is true for comparisons to the regional reviews by Hormes et al. (2013) and Hogan et al. (2017). While there is minimal evidence of ice loss between 12.0 – 11.7 ka BP (Fig. 14A), by 11.0 ka BP it seems the bulk of fjords and land submerged under postglacial relative sea level are likely ice free (Fig. 14B).
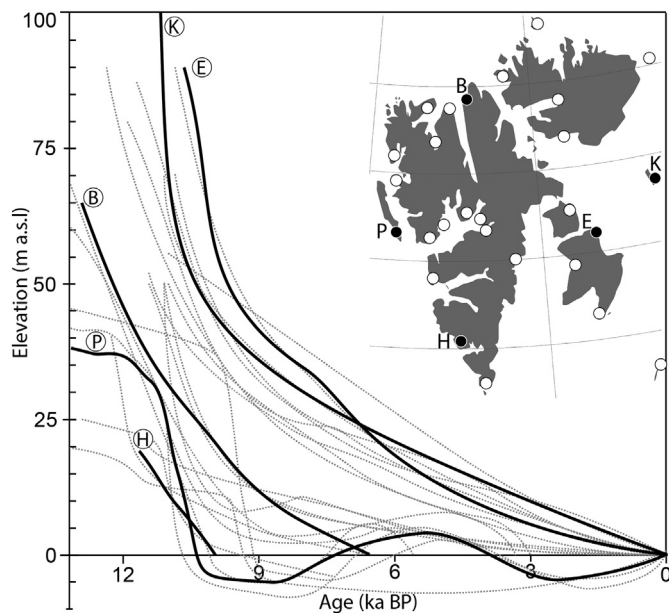
Fig. 12. Plot exhibits variability in postglacial relative sea level from around Svalbard. Map indicates the distribution of sea level curves according to (Forman et al., 2004 and references therein; Sessford et al., 2015; Schomacker et al., 2019). Five relative sea level curves have been highlighted in bold, selected from different key sites around Svalbard, exhibiting unique variability in postglacial sea level; P = Prins Karls Forland, H = Hornsund, B = Bangenhuk, E = Edgeøya (Humla) and K = Kong Karls Land. Curves constructed from data present in Table S1 with full references located in Data S1).

4.2. Early Holocene (11.7 - 8.2 ka BP)

4.2.1. Early Holocene glaciers

Early Holocene glaciers on Svalbard undergo extensive ice-mass-loss (Fig. 7 & 14). Conceptually, deglaciation continued in a time-transgressive manner, characterized by initial retreat through the fjords and subsequently in the fjord-valleys and terrestrial realms (Ingólfsson and Landvik, 2013; Gilbert et al., 2018). Deglaciation is observed across marine, terrestrial and lacustrine records (Fig. 9, 10, 12 & 14). Fjords, lake basins and shorelines become ice-free allowing for the deposition of datable material (Fig. 13). Marine sediment cores from fjords in western and northern Svalbard exhibit high, yet diminishing sedimentation rates with persistent outsized particles interpreted as IRD from retreating marine ice margins (Hald et al., 2004; Forwick and Vorren, 2009; Flink et al., 2017; Bartels et al., 2017, 2018; Allaart et al., 2020). Similarly, lacustrine records from Svalbard often exhibit a high minerogenic fraction with sedimentation rates that taper off through the Early Holocene (Snyder et al., 1994; Svendsen and Mangerud, 1997; Røthe et al., 2015; van der Bilt et al., 2016; de Wet et al., 2018; Røthe et al., 2018; Schomacker et al., 2019). Records have been interpreted to indicate most marine-terminating glaciers retreated onto land, while cirque glaciers greatly diminished in size and in some cases disappeared completely (Svendsen and Mangerud, 1997; Snyder et al., 2000; Forwick and Vorren, 2009; de Wet et al., 2018). On northeastern Nordaustlandet, shells sampled from within a thrusted debris band located 6 km inside the modern ice margin of a major outlet glacier date to 10.3 ± 0.49 ka BP and suggest that the fjord system had retreated to at least this position early in the Holocene (Blake, 1989). Thus, by 10 ka BP most tidewater glacier margins are located well inside of their late Holocene extents.

However, glacier activity during the Early Holocene is complex and does not solely indicate consistent ice-marginal retreat. Despite the progressive deglaciation, evidence from glaciers of varying size found across Svalbard suggests asynchronous ice margin re-advance(s) (Fig. 8 & 13; Salvigsen et al., 1990; Mangerud et al., 1992; Ronnert and

Landvik, 1993; Brückner *et al.* 2002; Eitel et al., 2002; Lønne, 2005; Forwick et al., 2010; Farnsworth et al., 2017, 2018; Larsen et al., 2018). Although the exact magnitudes of the re-advances are unknown, ice margin extent is often several kilometers distal to Late Holocene glacier maxima (Lønne, 2005; Farnsworth et al., 2018). Generally, the timing of the re-advances seems to follow the time transgressive deglaciation (Landvik et al., 2014; Farnsworth et al., 2018). The earliest re-advances have been identified near the mouths of the fjords while younger Early Holocene re-advances are found in the inner tributaries and heads of fjord systems (Larsen et al., 2018). The ultimate glacier re-advance (*c.* 9.1 ± 0.19 ka BP) identified in the Early Holocene redeposited shells up to 180 m a.s.l. in inner Wijdefjorden (*c.* 6.5 km inside and *c.* 100 m above of the present glacier margin; Marks & Wysokinski 1986; Klysz et al., 1988; Table S1). Although the extent of the re-advance interpreted from these deposits is unknown, the data suggests not only had the palaeo-outlet glacier undergone significant Early Holocene retreat, it re-advanced to a marginal position unmatched at any point in the Late Holocene. There are still numerous pre-Middle Holocene moraines that have been identified in marine and terrestrial environments, that remain poorly dated (Salvigsen and Österholm, 1982; Forwick et al., 2010; Henriksen et al., 2014; Røthe et al., 2015; Flink et al., 2017; Farnsworth et al., 2018; Flink and Noormets, 2018; Dowdeswell et al., 2020).

4.2.2. Early Holocene environment

Environmental reconstructions from marine archives suggest early and marked warm regional conditions driven by the incursion of Atlantic waters around Svalbard prior to 11 ka BP (Hald et al., 2004; Forwick and Vorren, 2009; Rasmussen et al., 2012; Mangerud and Svendsen, 2017). Evidence from marine microfossils suggests warm regional conditions prior to the onset and throughout the Early Holocene (Hald et al., 2004, 2007; Ślubowska-Woldengen et al., 2007; Skirbekk et al., 2010; Łącka et al., 2015). Reconstructions of sea-ice extent based on the sea-ice biomarker IP$_{25}$ (Müller and Stein, 2014; Bartels et al., 2018; Allaart et al., 2020) and IRD flux (Hald et al., 2004; Forwick and Vorren, 2009), suggest a decline in sea-ice extent around the onset of the Early Holocene *c.* 12-11 ka BP. Additionally, there is a high and variable accumulation of driftwood during the Early Holocene (Fig. 13). The initial peak in Early Holocene driftwood could be related to sea-ice cover transitioning from permanent to semi-permanent at the onset of the Holocene as well as the increased availability of deglaciated shorelines as catchment for driftwood (Fig. 13 & 14; Häggblom, 1982).

The records of raised marine mollusc shells identified in Early Holocene sediments across the coastal regions of Svalbard corroborates with the environmental reconstructions from fjord records. Reviews of thermophilous marine molluscs found around Svalbard also indicate early and exceptionally warm conditions within fjords (Salvigsen et al., 1992; Salvigsen, 2002; Blake, 2006; Mangerud and Svendsen, 2017). The occurrences of *Zirfaea crispata* and *Arctica islandica* in the Svalbard raised marine record only between 10.0 – 9.2 ka BP suggests that the maximum ocean temperatures occurred soon after the onset of the Holocene and prior to peak summer insolation (Mangerud and Svendsen, 2017).

Recent Early Holocene studies targeting ice-free terrestrial and lacustrine archives suggest the terrestrial environment is in phase with marine temperature reconstructions. Alkenone and hydrogen isotope records from low-altitude coastal lakes suggest early warm and moist conditions with peak Holocene temperatures reaching 7 °C warmer than today, *c.* 10 ka BP (Balascio et al., 2018; Gjerde et al., 2017; van der Bilt et al., 2018, 2019). Warm conditions have also been documented from *seda*DNA targeting vascular plants within lake sediment records (Alsos et al., 2015; Voldstad et al., 2020). Occurrence and diversity of thermophilous plant species like *Empetrum nigrum*, *Arnica angustifolia* and *Arabis alpine* indicate that during the Early Holocene, the ice-free terrestrial realm on Svalbard was warmer than present. Although the majority of the terrestrial landscape is presumed to still be evacuating
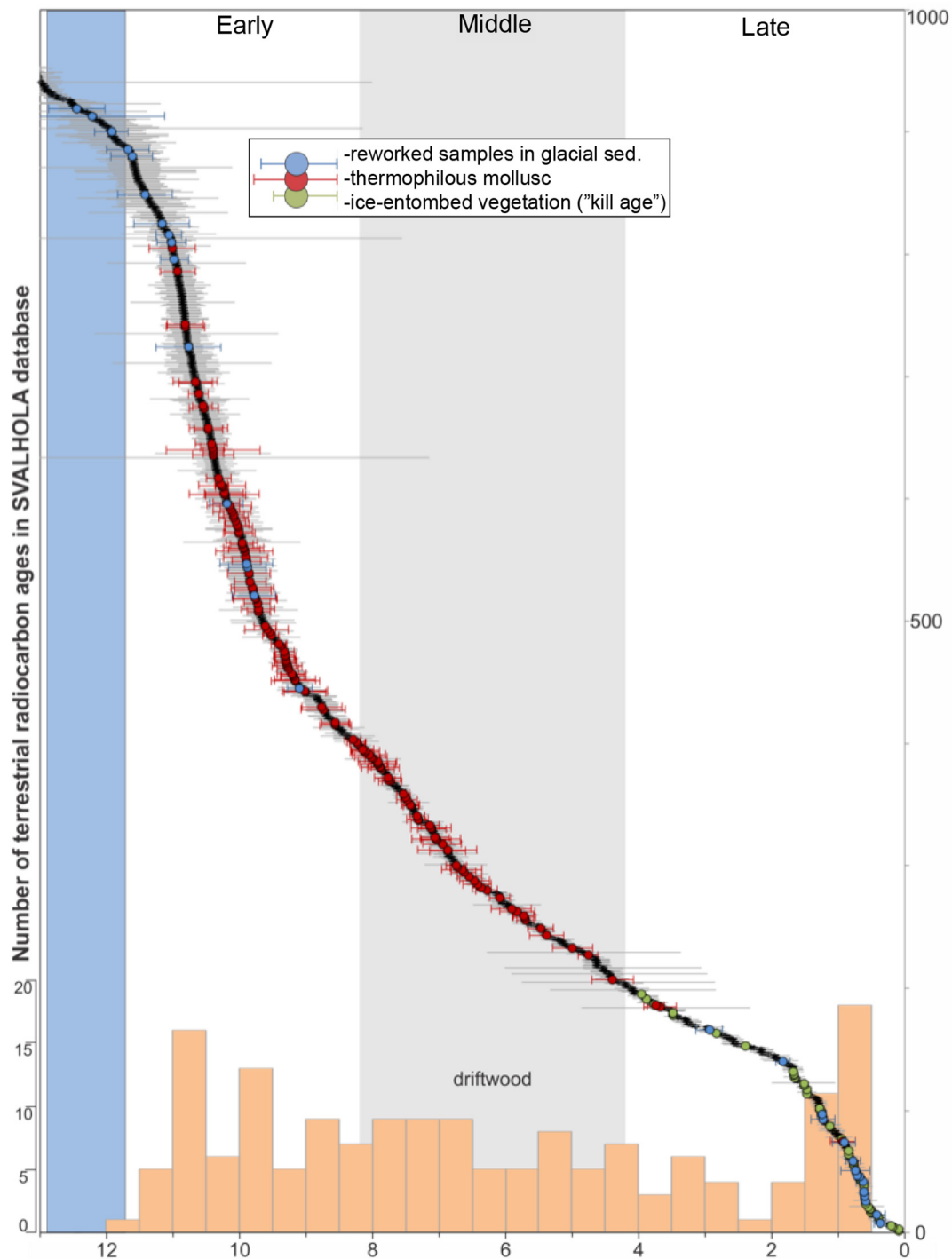
Fig. 13. Plot of the 930 radiocarbon ages (excluding lake and marine records) from the SVALHOLA database with the centers for the age distributions stacked chronologically (black dots) and associated error bars (grey) modified from Fig. 5. The Younger Dryas period is marked with a blue column while the Early and Late Holocene is divided by a grey column delimiting the Middle Holocene (Cohen et al., 2018). Specific radiocarbon ages from the database have been highlighted based on palaeoglaciological or environmental associations. Dateable material reworked in glacial sediments (blue); thermophilous marine molluscs (red) and ice-en-tombed moss (green) are represented by enlarged colored circles with error whiskers. Histogram plot at base indicates the number (total n = 170) of radiocarbon dated driftwood samples from Svalbard within a 500-year bin size (modified from Dyke et al., 1997). The youngest bin (modern – 0.5 ka BP) has been excluded due to lack of studies focusing on driftwood from modern shorelines. Data available in Tables S1-S3. (For interpretation of the references to color in this figure legend, the reader is referred to the web version of this article.)

SBSIS-ice in the Early Holocene, records of terrestrial plant diversity and lake temperatures suggest that ice-free terrain also exhibited early and exceptional warmth.

4.3. Middle Holocene (8.2 – 4.2 ka BP)

4.3.1. Middle Holocene glaciers

We have no exact spatial constraint on any Svalbard ice margins during the Middle Holocene. It is assumed that if glaciers survived the
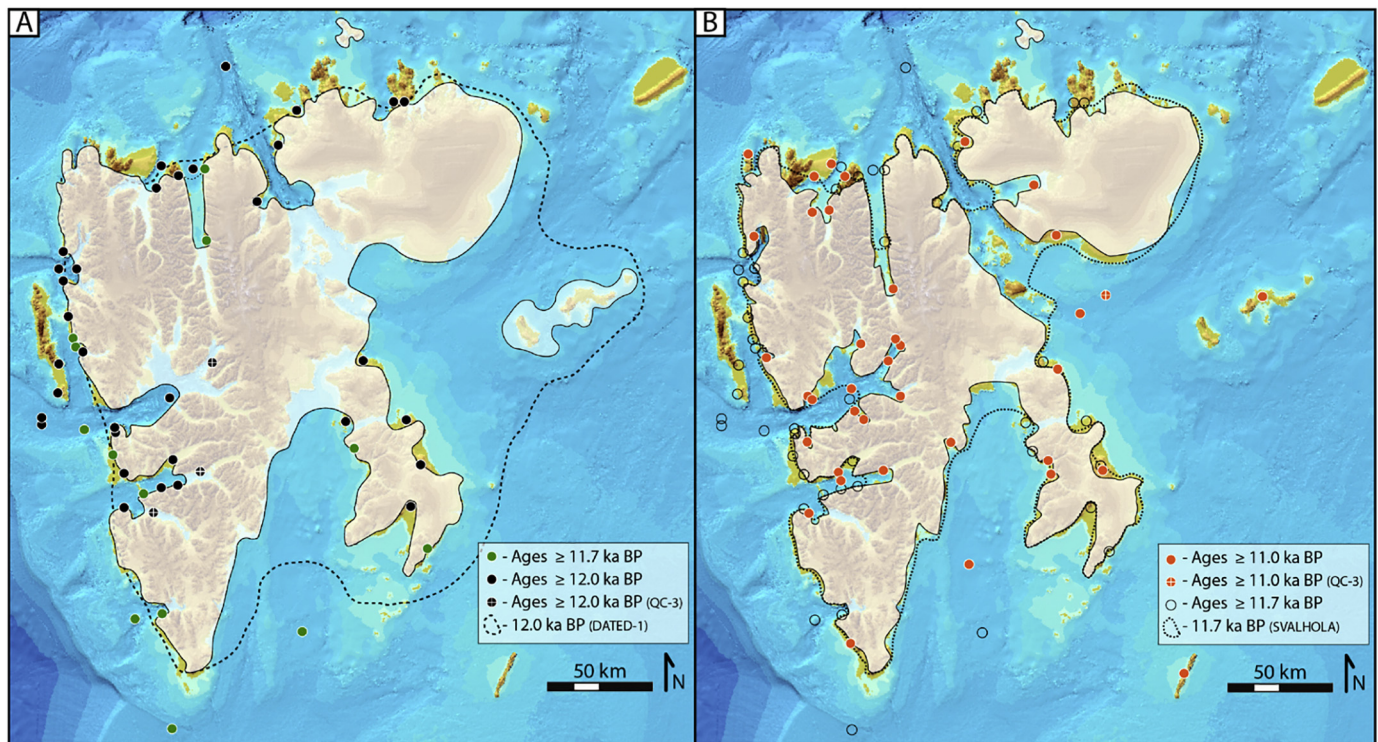
Fig. 14. IBCAO map of Svalbard with polygons reflecting ice cover during the transition from Late Glacial into the Early Holocene based on constraining deglacial ages from the SVALHOLA database. A) displays regional ice cover at around 12.0 ka BP and at 11.7 ka BP compared to the most-credible DATED-1 12.0 ka BP timeslice (Jakobsson et al., 2012; Hughes et al., 2016). B) indicates reconstructed ice marginal retreat between 11.7 and 11.0 ka BP. Northernmost ice cover polygon over the Seven Islands reflects reconstructed ice cover that existed until the Early Holocene (but lacks from other reconstructions due to resolution). Timeslice footprints represent the approximate extent of ice-cover during a period in time, yet take no account for glacier behavior or ice thickness (Hormes et al., 2013).

Middle Holocene, they were more reduced than any Late Holocene glacier extent on Svalbard (Mangerud and Landvik, 2007; Baeten et al., 2010). To our knowledge, there is no geomorphological evidence (e.g., end moraines) identifying any glacier margins, stand-stills or re-advances during this period (Fig. 13). At the mouth of Hornsund, terrestrial vegetation thrusted up into tidewater glacier ice suggests the marine terminus was terrestrial grounded prior to 8.0 ka BP (Oerlemans et al., 2011).

At present, there are over 850 km of marine-terminating glacier margins in Svalbard (Blaszczyk et al., 2009). However, it has been speculated if tidewater glaciers survived the Middle Holocene. There are two marine stratigraphical studies that have suggested Middle Holocene glacier activity at the mouth of Isfjorden and a bay on western Nordaustlandet based on fluctuating rates of minerogenic sedimentation (Forwick and Vorren, 2007; Kubishcta et al., 2011). However, it remains inconclusive if fluctuations in marine sedimentation from these sites relates to actual glacier re-advances or rather enhanced runoff from proximal glacier systems, submarine mass failures, or enhanced sea ice rafting. Most marine sediment cores reveal a decline in sedimentation rates, and IRD dissipates in many of Svalbard's fjord systems (Forwick and Vorren, 2009; Skirbekk et al., 2010; Kempf et al., 2013; Nielsen and Rasmussen, 2018). However, ice-rafted debris has been observed through the entire Holocene in sediment cores from several Svalbard fjords, including Van Mijenfjorden, Billefjorden, Tempelfjorden and Wahlenbergfjorden (Hald et al., 2004; Forwick and Vorren, 2009, 2010; Baeten et al., 2010; Flink et al., 2017; Bartels et al., 2018). Ice-rafted debris is a strong indicator of marine terminating glaciers within a fjord but has also been associated with sea ice, serving both as a raft for beach sediments as well as a (semi-) permanent restraint limiting ice rafting by icebergs (Forwick and Vorren, 2009; Joo et al., 2019). Assuming that Holocene IRD within Svalbard fjords relate to tidewater glacier systems, the IRD records indicate that Svalbard

glaciers not only survived the entire Holocene interglacial, but several Svalbard glaciers remained at their fjord-heads through the Holocene. Using IRD as a proxy for tidewater glaciers maybe less accurate within some shallow, inner Svalbard fjords (e.g., Dicksonfjorden) where sea ice appears to play a larger role in the rafting of outsized clasts to the marine archive (Joo et al., 2019).

Based on glacial lake sediment records, we presume that Svalbard glaciers retreated back to their Holocene minimum during the beginning of the Middle Holocene (Fig. 9). Records from (modern) proglacial lakes located on the northern and western coast of Svalbard suggest there was no glacigenic input from their corresponding glaciers during the Middle Holocene (Fig. 9 & 15; Linnévatnet, Svendsen and Mangerud, 1997; Linnévatnet, Snyder et al., 2000; Kløsa & Vårfluesjøen, Røthe et al., 2015, 2018; Hajeren, van der Bilt et al., 2016; Gjøavatnet, de Wet et al., 2018; Kløverbladvatnet, Schomacker et al., 2019).

These records are characterized by organic-rich strata with minimal minerogenic accumulation (Svendsen and Mangerud, 1997; Snyder et al., 2000; Røthe et al., 2015, 2018; van der Bilt et al., 2016; de Wet et al., 2018; Schomacker et al., 2019). None-glacial lake sediment records spanning the Middle Holocene also suggest high productivity and reduced sedimentation rates (Birks, 1991; Alsos et al., 2015; Gjerde et al., 2017).

It remains difficult to determine the Holocene minimum ice extent, and we can only speculate when glaciers on Svalbard reached a Holocene minimum (Fig. 15). While some lake sediment studies targeting cirque glaciers suggest that catchments were ice-free through the Middle Holocene, lake studies have yet to target larger lake basins corresponding to large glacier systems. Presumably, the Holocene glacial minimum occurred in the Middle Holocene, sometime between 8.0 – 6.0 ka BP. The glacial minimum certainly occurred after the marine thermal maximum (10.0 – 9.2 ka BP), potentially lagging the peak in
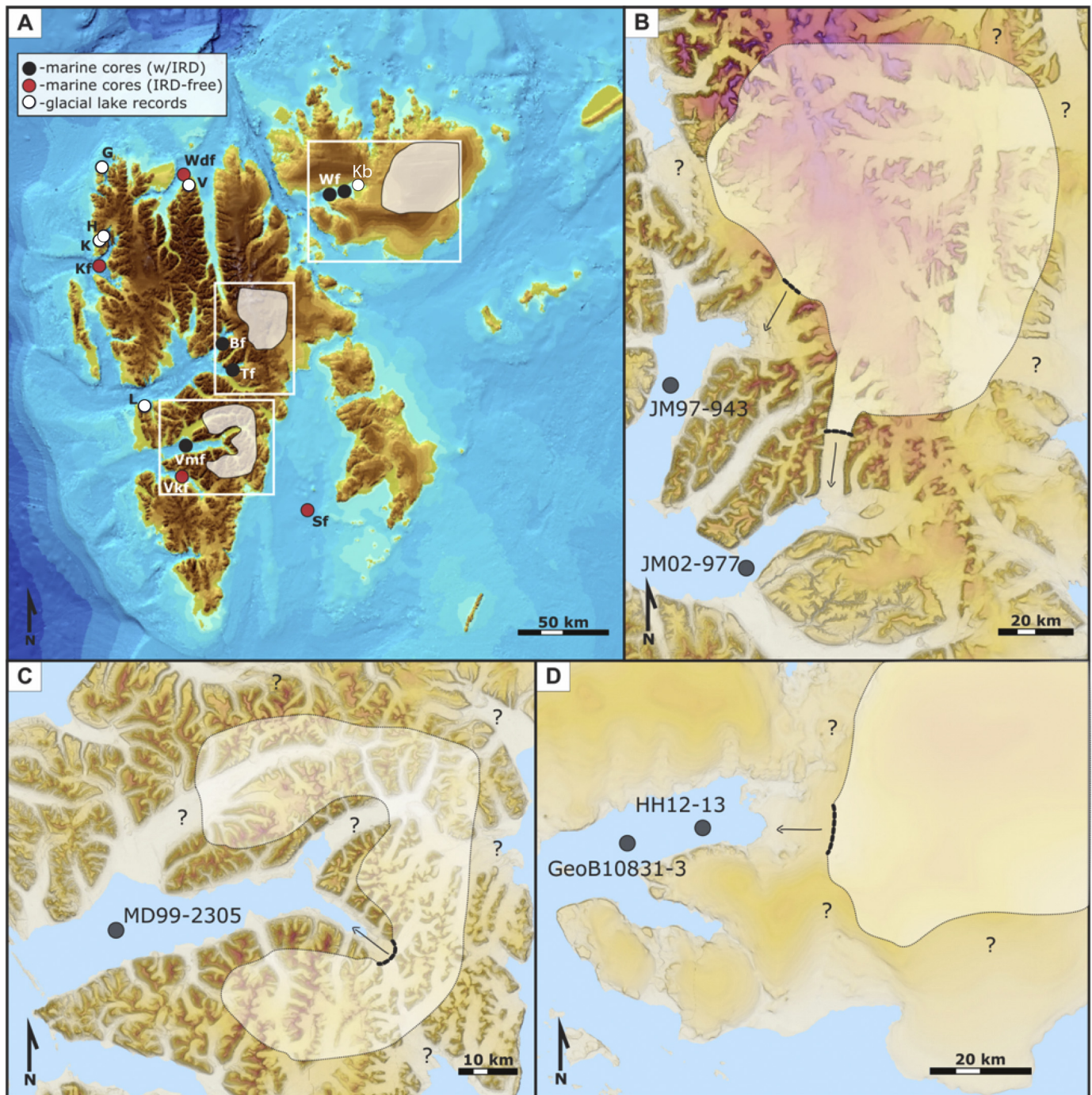
Fig. 15. Maps of provisional ice extent during the Holocene glacial minimum on Svalbard c. 8-6 ka BP. A) Glacial-lake records from Gjøavatnet (G), Hajeren (H), Kløsa (K) Vårfluesjøen (V) and Linnévatnet (L), suggest ice-free or greatly reduced glaciers in catchments during the Middle Holocene (Svendsen and Mangerud, 1997; Snyder et al., 2000; Røthe et al., 2015; van der Bilt et al., 2016; Røthe et al., 2018; de Wet et al., 2018; Schomacker et al., 2019). Reduced ice rafted debris in marine sediment cores from Kongsfjorden (Kf), Van Keulenfjorden (Vk), Woodfjorden (Wf) and Storfjorden (Sf) suggests tidewater glaciers have retreated back onshore to terrestrial margins (Skirbekk et al., 2010; Kempf et al., 2013; Bartels et al., 2017; Nielsen and Rasmussen, 2018). B) Ice-rafted debris in marine sediment records suggest tidewater glacier termini persistent in Billefjorden (JM97-943; Baeten et al., 2010), Tempelfjorden (JM02-977; Forwick et al., 2010), C) Van Mijenfjorden (MD99-2305; Hald et al., 2004), and D) Wahlenbergfjorden HH12-13; Flink et al., 2017 & GeoB10831-3; Bartels et al., 2018) throughout the Holocene. Maps modified from TopoSvalbard and IBCAO from (Jacobsson et al. 2012).

ocean temperatures and summer insolation on a millennial time scale.

A recent modeling study based on Holocene relative sea level concludes that some Svalbard glaciers survived the HTM and suggests Nordaustlandet and eastern Spitsbergen were the main regions that hosted Middle Holocene ice (Fjeldskaar et al., 2018). At present, these regions are characterized by cooler climate, based on elevation and distance from the West Spitsbergen Current (Fig. 1; Førland et al., 2011;

Østby et al., 2017). Although the Van Mijenfjorden region in SW Svalbard has summits reaching over 1000 m a.s.l., it generally does not reflect these same cool climatic characteristics (Østby et al., 2017). Similar to modern conditions, Forwick and Vorren (2009) suggest a strong E-W temperature gradient across Spitsbergen existed through the Holocene. While Paulabreen in southeastern Van Mijenfjorden is the primary source of IRD in the fjord at present, it was not necessarily the

dominant or the only source of IRD during the Early and Middle Holocene (Fig. 15). Based on the size of the Reindalen and Kjellströmdalen valleys, they seem to have held larger glacier systems in their catchments and may have more efficiently preserved their residual SBSIS ice.

4.3.2. Middle Holocene environment

Data from the marine archive suggests a general decline in ocean temperatures during the Middle Holocene. Cooling of regional waters during this period is indicated by marine microfossils (Hald et al., 2004, 2007; Ślubowska-Woldengen et al., 2007; Skirbekk et al., 2010; Łącka et al., 2015). Reconstructions of sea-ice extent derived from IP$_{25}$ bio-marker records spanning the Middle Holocene suggest a progressive increase in sea-ice cover starting around 8.0 ka BP (Müller and Stein, 2014).

Raised Middle Holocene marine sediments and the persistence of *Mytilus edulis* and *Modiolus modiolus* therein suggest Atlantic water continued to reach Svalbard, and ocean temperatures were *c.* 4 °C warmer than present between 8.0 – 6.5 ka BP (Salvigsen et al., 1992; Salvigsen, 2002; Blake, 2006; Mangerud and Svendsen, 2017). This period of stable warm ocean conditions is followed by a gradual decrease in temperatures until the end of the Middle Holocene, when sea surface temperature reached those comparable to modern (Hald et al., 2004; Mangerud and Svendsen, 2017).

The gentle decline of dated driftwood through the Middle Holocene (Fig. 7) follows the trend of declining ocean temperatures reconstructed from molluscs and marine microfossils as well as inversely correlates with the IP$_{25}$ derived sea-ice reconstructions (Hald et al., 2004, 2007; Ślubowska-Woldengen et al., 2007; Skirbekk et al., 2010; Müller and Stein, 2014; Rasmussen et al., 2012).

Evidence from terrestrial and lacustrine archives suggests the Middle Holocene environment on Svalbard was warmer than present, yet conditions had cooled since the peak in temperatures reconstructed from the Early Holocene. The Middle Holocene is characterized by a gradual, step-wise cooling, with dry conditions and summer lake temperatures 2 – 4°C warmer than present (Bakke et al., 2018; Røthe et al., 2018). Vascular plant reconstructions from *seda*DNA within lake sediment records present similar conditions, exhibiting cooling during the later Middle Holocene (Alsos et al., 2015; Voldstad et al., 2020).

4.4. Late Holocene (4.2 ka BP – present)

4.4.1. Late Holocene glaciers

The standard perspective that the (Late) Holocene glacial maximum marked the culmination of the LIA around the turn of the 20th Century AD (Svendsen and Mangerud, 1997; Snyder et al., 2000) is increasingly being challenged. Svalbard glaciers re-advanced throughout the Late Holocene, during the Neoglacial (Furrer et al., 1991; Werner, 1993; Reusche et al., 2014; Sharin et al., 2014; Røthe et al., 2015; van der Bilt et al., 2016; Philipps et al., 2017) and during the LIA (Baranowski and Karlén, 1976; Dzieriek et al., 1990; Svendsen and Mangerud, 1997; Snyder et al., 2000; Humlum et al., 2005; de Wet et al., 2018). Where Neoglacial ice margins have been identified, they are often on the order of tens of meters outboard LIA margins (Werner, 1993; Sharin et al., 2014). Observations of glaciers during the early 1900s describe Svalbard glaciers proximal to their Late Holocene maximum extents (Isachsen, 1915). However, this does not suggest anything about the timing of glacier advance, but rather that the glaciers had started to retreat.

The majority of Holocene glacier re-advances are constrained by radiocarbon dates from material re-deposited in or overlain by glacial deposits during the Late Holocene (Fig. 11 & 16). Most Late Holocene glacier re-advances (dated by overridden vegetation or mollusc shells) date to the early (between 1.0 - 0.5 ka BP), not the late LIA (Fig. 11). Dates constrain the maximum age of glacier re-advance during the Neoglacial or early LIA when glaciers grew to their Late Holocene maximum extent (Baranowski and Karlén, 1976; Dzieriek et al., 1990;

Furrer et al., 1991; Humlum et al., 2005). Several additional studies indicate Late Holocene glacier maxima occurred even earlier in the Neoglacial (Werner, 1993; Sharin et al., 2014; Lovell et al., 2018).

Despite criticism of the method (e.g. Osborn et al., 2015), lichenometry studies suggest glaciers across Svalbard have experienced several phases of glacier advance, followed by moraine stabilization during the last 2.0 ka BP (Fig. 11; Werner, 1993). Cosmogenic exposure dating of moraine ridges has been conducted on several Late Holocene glacier forelands as a means of testing whether the LIA was the most extensive glacial event of the Late Holocene (Fig. 11; Reusche et al., 2014; Philipps et al., 2017). The TCN studies have effectively supported earlier works, corroborating there have been numerous phases of glacial re-advance during the Late Holocene and conclude that the LIA is not the largest glacial event in most locations.

Further evidence of episodic glacier expansion during the Late Holocene is derived from the technique of radiocarbon dating ice-entombed plants over a range of elevations to reconstruct snow-line-lowering throughout a region (Miller et al., 2017). Results from a study presenting over 40 radiocarbon ages from central Spitsbergen suggest that there were at least four phases of widespread ice cover expansion resulting in a general snow line lowering between 2.0 ka BP and 0.5 ka BP prior to the LIA-ice expansion (Miller et al., 2017). They further demonstrate that ice expansion occurred as early as 4.0 ka BP (Fig. 11; Miller et al., 2017). Findings align with results from active ice margins however, this work has closely relied on the assumption that Arctic glaciers are solely controlled by summer temperature, overlooking the potential role of precipitation, shifts in storm-track or wind (Humlum et al., 2005; Wickström et al., 2020).

The record of ice entombed plants places ice-core stratigraphy studies in perspective (Isaksson et al., 2005; Divine et al., 2011; Miller et al., 2017). Previous ice core sample locations have targeted sites with continuous, undisturbed snow accumulation, which have extended back approximately 1 ka BP (Isaksson et al., 2003, 2005; Grinsted et al., 2009; Divine et al., 2011). However, ice-entombed vegetation ages suggest glacier cover nearly as old as the Middle Holocene, albeit lacking record continuity. Fragmented, albeit old records of precipitation may exist in Svalbard's cryostratigraphy, but have yet to be targeted or identified. Given the potentials of (crypto-)tephra records on Svalbard, older ice core chronologies may be possible despite lacking annual layer counts from the modern surface (Isaksson et al., 2005; Kekonen et al., 2005; Wastegård and Davies, 2009). Furthermore, the identification, mapping and investigation of old Holocene ice may provide information about the glacial minimum, shifts in precipitation patterns as well as processes related to glacier expansion.

Late Holocene glacier expansion is also interpreted from fjord and lacustrine sedimentary archives. Sedimentation rates in Svalbard fjords increase through the Late Holocene (Fig. 10; Hald et al., 2004; Forwick and Vorren, 2009; Baeten et al., 2010; Kempf et al., 2013; Łącka et al., 2015; Streuff et al., 2017; Flink et al., 2017; Bartels et al., 2018), interpreted to mean increased glacial activity in their catchments. Also, Late Holocene proglacial lake records generally suggest increasing glacial influence, characterized by rising rates of sedimentation and transitions from organic-rich to minerogenic strata (Fig. 9 &16). Some lake sediment records suggest episodic increases in glacial activity within catchments starting as early as *c.* 4 ka BP (Hajeren; van der Bilt et al., 2016) and prior to 3.0 ka BP (Kløsa and Linnévatnet; Røthe et al., 2015; Svendsen and Mangerud, 1997). In Gjøavatnet (1 m a.s.l.), located in northwestern Svalbard, the transition from organic-rich to glacial sedimentation does not occur until *c.* 1 ka BP. All glacial lake records show enhanced glacial influence during the last millennium (Fig. 11). A regional glacier equilibrium line altitude (ELA) has been reconstructed from the Kløsa lake sediment record in northwestern Svalbard suggesting variable but declining ELA over the last 4 ka BP (Røthe et al., 2015).

Several glacier re-advances constrained to the Neoglacial – LIA have been characterized as surges based on size, landsystem, extent of glacial
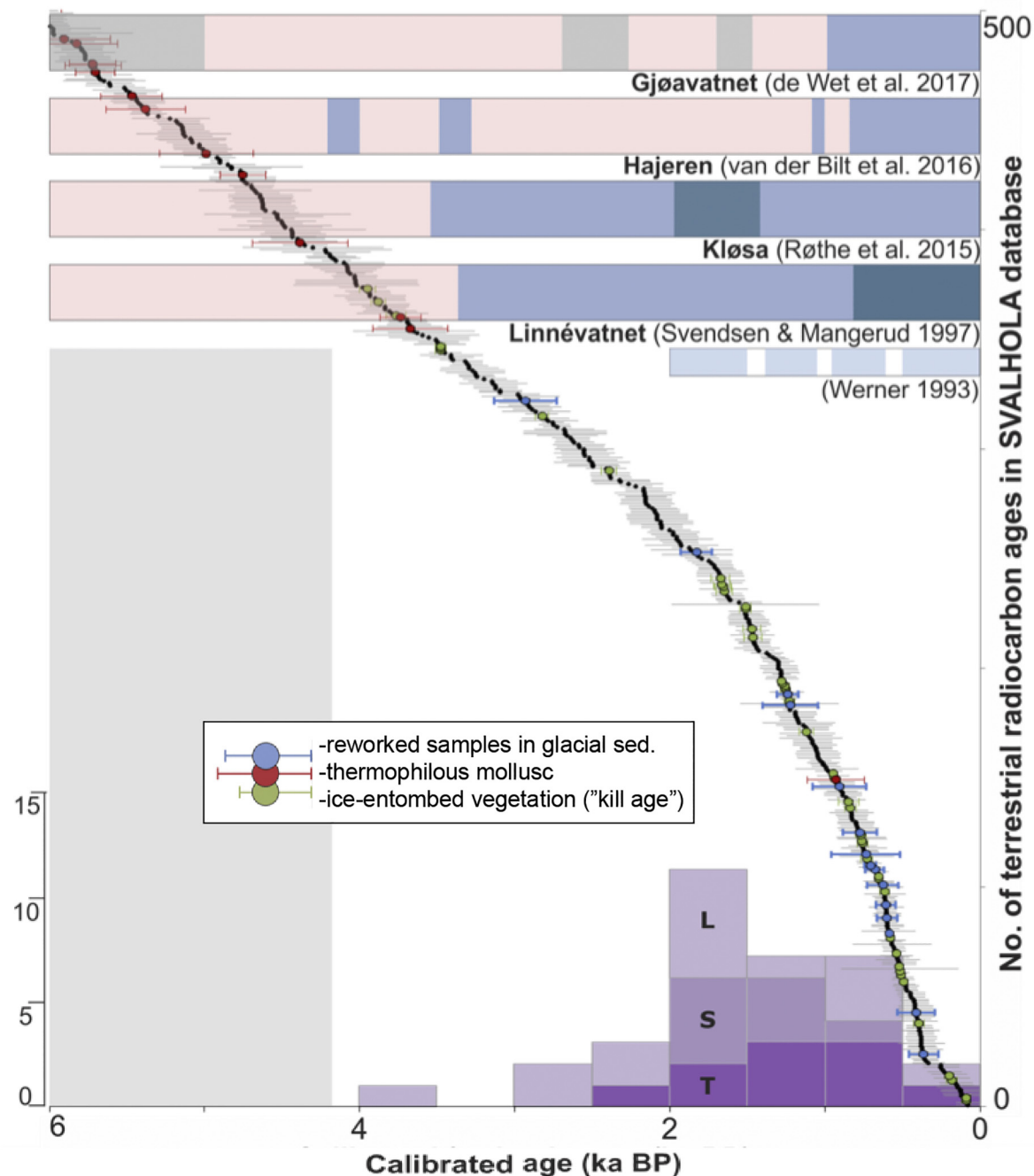
Fig. 16. Plot of 497 terrestrial radiocarbon ages and raised marine from the SVALHOLA database from the last 6 ka BP. Grey column delimits the end of the Middle Holocene (4.2 ka). Specific radiocarbon ages from the database have been highlighted as colored circles with error bars based on palaeoglaciological and climatological associations. Histogram at base indicates TCN exposure age distribution within 500 year bins for moraine ridge boulders for three sites, L = Linnébreen, S = Scottbreen and T = Treskelen (Reusche et al., 2014; Philipps et al., 2017). Shaded bars at top represent a schematic view of Late Holocene glacial activity reconstructed from lake sediments of four proglacial lakes from western Spitsbergen (Gjøavatnet, Hajeren, Kløsa and Linnévatnet). Blue boxes represent periods of glacial activity (dark blue suggest enhanced glacial activity), red boxes suggest no glacier was present in the catchment or glacial activity was greatly reduced; gray boxes indicate periods of reduced organic matter accumulation (Gjøavatnet; modified from de Wet et al., 2018). Light blue boxes indicate periods of glacier growth interrupted by moraine stabilization (white boxes) reconstructed with lichenometry (Werner, 1993). Data available in Tables S1 & S2. (For interpretation of the references to color in this figure legend, the reader is referred to the web version of this article.)

deformation and preservation of landforms (related to rapid ice advances) corresponding to associated ice-margins (Plassen et al., 2004; Ottesen et al., 2008; Kristensen et al., 2009; Kempf et al., 2013; Farnsworth et al., 2016, 2017; Flink et al., 2017; Lovell and Boston, 2017; Lyså et al., 2018; Lovell et al., 2018; Aradóttir et al., 2019). While the most extensive Late Holocene glacial deposits have been associated with surge-type behavior during, or at, the culmination of the LIA

(Schomacker and Kjær, 2008; Kristensen et al., 2009; Kempf et al., 2013; Flink et al., 2015; Lyså et al., 2018) an increasing number of studies have identified both complete and fragmented moraine ridges outboard of the LIA maxima (Werner, 1993; Sletten et al., 2001; Reusche et al., 2014; Sharin et al., 2014; Philipps et al., 2017; Larsen et al., 2018).

4.4.2. Late Holocene environment

The combination of decreasing summer insolation (Berger and Loutre, 1991; Laskar et al., 2004) and the progressive cooling of regional waters draws Svalbard into the Neoglacial period (Fig 13; (Skirbekk et al., 2010; Rasmussen et al., 2014; Łącka et al., 2015; Svendsen and Mangerud, 1997). The Neoglacial is characterized by gentle decline in temperatures initiated before the onset of the Late Holocene, *c.* 5.0 ka BP, superimposed by a series of episodic (multidecadal to multicentenial) steps in deteriorating climate throughout the North Atlantic (Bradley and Bakke, 2019).

Trends in marine microfossil fauna assemblages indicate Late Holocene ocean cooling around Svalbard (Hald et al., 2004; Rasmussen et al., 2012; Werner et al., 2013; Müller and Stein, 2014; Pawłowska et al., 2020). Regional waters exhibit an increasing flux of IRD suggesting enhanced tidewater glacier influence (Ślubowska-Woldengen et al., 2007; Rasmussen et al., 2014; Flink et al., 2017; Bartels et al., 2018). Reconstructions of sea-ice cover derived from IP$_{25}$ suggest a progressive increase in ice-cover through the Late Holocene (Müller and Stein, 2014; Bartels et al., 2018; Allaart et al., 2020). In inner fjords, a decrease in IRD flux has been related to more persistent sea ice suppressing iceberg rafting (Forwick and Vorren, 2009; Baeten et al., 2010; Forwick et al., 2010). The coldest oceanographic conditions around Svalbard in the Holocene is assumed to be the period from 4.0 – 2.0 ka BP (Rasmussen et al., 2012).

The period 2.5 – 2.0 ka BP marks the Holocene minimum in driftwood arrival and matches the occurrence rate seen during the end of the Pleistocene (Fig. 7). It is unclear how well driftwood arrival through the Late Holocene reflects sea-ice cover around Svalbard (Fig. 7). However, it is possible the Holocene minimum in driftwood arrival relates to persistent or semi-permanent land-fast ice, minimizing the transport of and catchment for driftwood accumulation (Funder et al., 2011). The increase in driftwood arrival exhibited through the last 2 ka of the Holocene record resembles the increase seen in the first half of the Early Holocene (Fig. 7). IP$_{25}$ derived sea-ice reconstructions suggest variability in sea-ice cover during the Late Holocene associated with sporadic warm sea surface temperatures (Müller et al., 2012; Sarnthein et al., 2003; Jernas et al., 2013; Pawłowska et al., 2020). Brine formation is believed to reflect sea-ice cover above basins and a Late Holocene record from Storfjorden suggests episodic periods of intense brine production separated by periods of reduced brine formation (Rasmussen and Thomsen, 2014).

The re-occurrence of *Mytilus edulis* at 0.9 ka BP (in Dicksonfjorden) coincides with the "Medieval Warm Period" and may suggest warm Atlantic waters were more widespread around Svalbard (Fig. 16; Lamb, 1965; Mann et al., 2009). The mapped distribution of these warm water molluscs around Svalbard from Mangerud and Svendsen (2017) suggests the species thrive in the inner shallow branches of fjord systems with nominal glacial influence (e.g., Dicksonfjorden Woodfjorden and outer Billefjorden; Salvigsen et al., 1992; Salvigsen, 2002; Blake, 2006; Mangerud and Svendsen, 2017). Thermophilous molluscs seem to generally reflect surface water conditions around Svalbard, however, may not necessarily represent the large-scale oceanographic condition that existed on the continental shelf or towards the east of Spitsbergen.

Lacustrine records from non-glacial lakes (Hakluytvatnet, Skardstjørna and Jodavatnet) suggest decreasing productivity, declining plant species diversity as well as increased Late Holocene minerogenic input due to increased runoff (Alsos et al., 2015; Gjerde et al., 2017; Voldstad et al., 2020). Additionally, a 1.8 ka alkenone based (summer) temperature record from Kongressvatnet, located in central western Spitsbergen, suggests the LIA was relatively mild in the region, implying precipitation may-be the key driver behind glacier expansion (D'Andrea et al., 2012). While it is important to highlight our limited knowledge of past precipitation, there is ample evidence suggesting that air and ocean temperatures were relatively cool and favored glaciers during the late Neoglacial and LIA (Divine et al., 2011; Bartels et al., 2017; Røthe et al., 2018; van der Bilt et al., 2018; Balascio et al.,

2018; Luoto et al., 2018). The Kongressvatnet record however, does highlight that the LIA was not the main event of the Late Holocene rather a late phase of a generally cool Neoglacial period.

As previously noted, sea-ice conditions during the Neoglacial and LIA are characterized by increasing but variable sea-ice extent around Svalbard (Fig. 12; Müller et al., 2012; Jernas et al., 2013; Müller and Stein, 2014Bartels et al., 2017; Allaart et al., 2020). Although increasing sea-ice cover reconstructed through most of the Late Holocene is presumed to favor glacier growth (suppressing summer temperatures, minimizing the number of positive degree days and decreasing frontal ablation) it is unclear how much this restricts precipitation.

Another indicator for Holocene environmental conditions on Svalbard is the formation of permafrost landforms and ground ice (Humlum et al., 2003; Humlum, 2005). A sedimentological investigation detailing the formation of permafrost in lowland terrain from central Spitsbergen highlights the inter-connection of relative sea level and permafrost aggradation during the Late Holocene (Gilbert et al., 2018). This work compliments earlier studies which present maximum constraining ages from the last 4.0 ka BP of various permafrost landforms and periglacial deposits, including pingos (Yoshikawa and Nakamura, 1996), ice-wedge polygons (Jeppesen, 2001) and aeolian loess deposits (Oliva et al., 2014). Generally, lowland permafrost landforms display a close correlation with uplift emergence patterns and Neoglacial cooling (Yoshikawa and Nakamura, 1996; Gilbert et al., 2018). Ground ice however, is also identified above the post-glacial marine limit, and potentially formed earlier in the Holocene (or in some cases earlier in the Quaternary) although ice-bodies generally lack the same detail of chronological constraint as investigated lowland ground ice (Humlum, 2005; Humlum et al., 2007; Siewert et al., 2012; Eckerstorfer et al., 2013).

4.5. Drivers of Holocene glacier activity on Svalbard

4.5.1. Glacier response to Holocene cooling events

Holocene "cooling events" on Svalbard associated with meltwater pulses or cold episodes within the North Atlantic (Bond et al., 2001; Jennings et al., 2015) have been proposed by various proxies from lake and fjord records, suggesting distinct events e.g. 11.3 ka BP (Tian et al., 2020), 9.3 ka BP (van der Bilt et al., 2019), 8.2 ka BP (Hald and Korsum, 2008) and 4.2 ka BP (van der Bilt et al., 2016). Despite proxy records promoting distinct environmental shifts during these periods in the Holocene, no glacial landform on Svalbard has been constrained to any of these events. In comparison, ice-marginal reconstructions from both sides of Baffin Bay seem well behaved, exhibiting synchronous breaths of Early – Middle Holocene punctuated decline (Lesnek and Briner, 2018; Young et al., 2020). However, there are no indications of a similar synchronous glacier response in Svalbard. Consequently, these cooling events, although some cases influential in Svalbard's Holocene environmental reconstructions, were not effective drivers of Svalbard-wide Holocene glacier activity. This may indicate that the extent of glacier mass loss experienced during the Early – Middle Holocene forced cooling-event-ice-margins inside of what would later become the Late Holocene maximum extent. Furthermore, although periods of reduced summer temperatures may halt ablation, they do not (necessarily) recharge Svalbard's glacier catchments. Subsequently, the interconnection between cool and dry versus warm and wet may-be critical with respect to the slow glacier turn-over characteristic of Svalbard's High Arctic glaciers (Wanner et al., 2001; Østby et al., 2017).

In comparison to these relatively short cooling events, the extended and episodic phase of Late Holocene cooling forced by declining high latitude summer insolation and explosive volcanism (Laskar et al., 2004; Miller et al., 2017; Bradley and Bakke, 2019), effectively revitalized Svalbard's modern glaciers (Bakke et al., 2018). Late Holocene glacier re-advances have been identified in terrestrial and marine archives as well as constrained from glacial lake and fjord sedimentary records (Fig. 17). Throughout the Late Holocene the percentage of
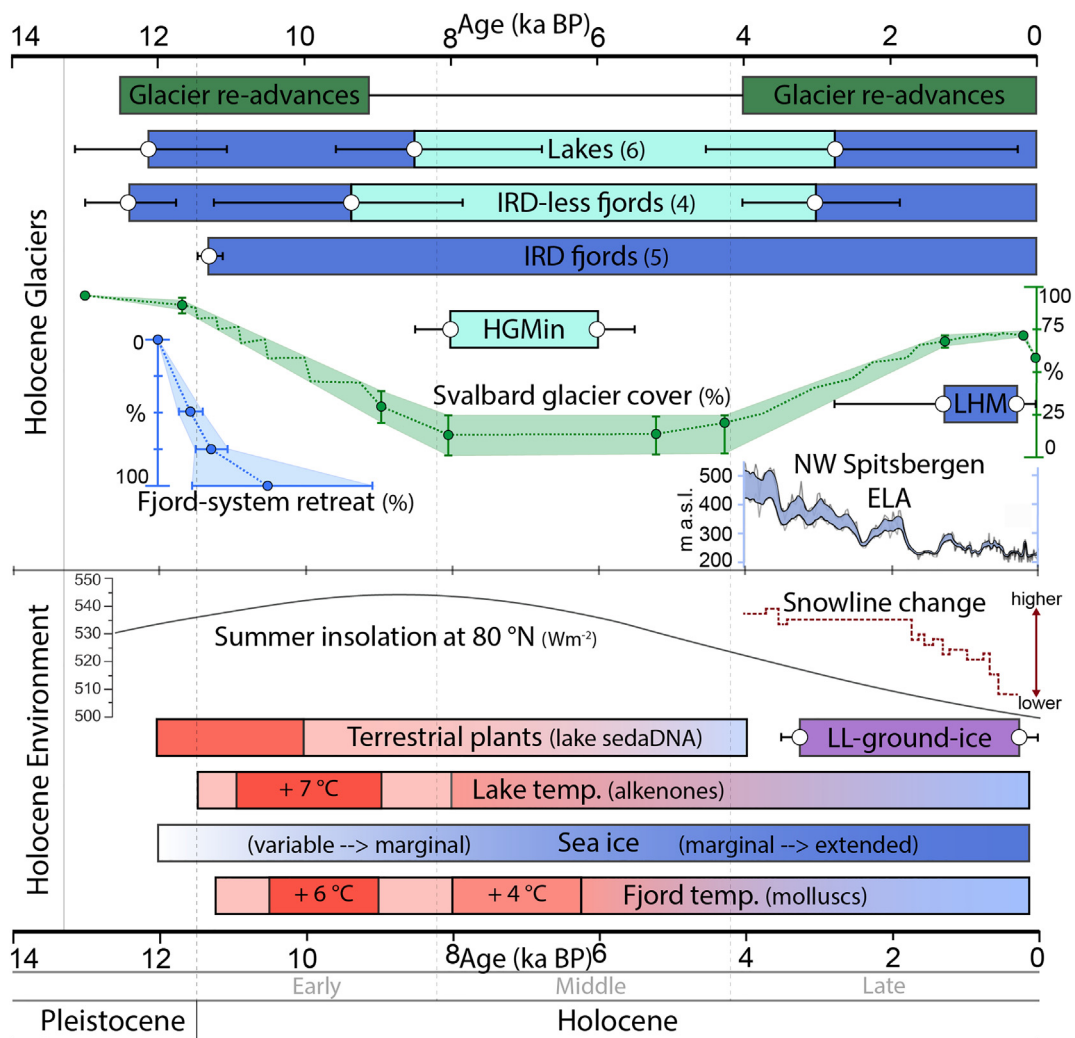
Fig. 17. Timeline of glacier and environmental history through the Late Pleistocene and Holocene with divisions of the Holocene indicated (Cohen et al., 2018). From top to bottom: Holocene glacier activity (this study), glacial lake records (Svendsen and Mangerud, 1997; Svendsen and Mangerud, 1997; Snyder et al., 2000; Mäusbacher et al., 2002; Røthe et al., 2015; van der Bilt et al., 2016; Røthe et al., 2018; de Wet et al., 2018; Schomacker et al., 2019), fjord records (IRD-fjords; Hald et al., 2004; Baeten et al., 2010; Forwick et al., 2010; Flink et al., 2017; Bartels et al., 2018; IRD-less fjords; Skirbekk et al., 2010; Kempf et al., 2013; Bartels et al., 2017; Nielsen and Rasmussen, 2018) estimated percentage of glacier cover across Svalbard (modified from Fjeldskaar et al., 2018), fjord system retreat (this study), change in equilibrium line altitude (ELA) from NW Spitsbergen (Røthe et al., 2015), inferred change in snowline (Miller et al., 2017), Late Holocene maximum (LHM; this study) and Holocene glacier minimum (HGMin; this study). Holocene environmental reconstructions from top to bottom: Mean monthly summer (June 21st – July 20th) insolation at 80 °N (Wm^{-2}; Laskar et al., 2004), low-land ground ice formation (LL-ground-ice; Gilbert et al., 2018 and others therein). terrestrial plant reconstructions (lake sediment sedaDNA; Alsos et al., 2015; Voldstad et al., 2020), lake temperature (alkenones; D'Andrea et al., 2012; van der Bilt et al., 2018, 2019), sea ice (Müller et al., 2012; Bartels et al., 2018; Allaart et al., 2020) and fjord temperatures (Svendsen and Mangerud, 1997 and others therein).

inferred ice-cover on Svalbard may have ranged from as low ~25 %, up to nearly 75 % during the Late Holocene glacier maximum (LHM), while regional snowline lowered and reconstructed equilibrium line altitude (ELA) dropped ~250 m (Fig.17; Røthe et al., 2015; Miller et al., 2017).

Environmental reconstructions of lakes and terrestrial conditions (e.g. vegetation and permafrost ground-ice) suggest temperatures progressively cooled over the last 5 ka (Fig. 17). Marine records also suggest fjord temperatures episodically declined in step with sea-ice cover transitioning from marginal to extended (Fig. 17). Ice-margins extend in episodic fashion through the Late Holocene, culminating in a period with peak ice-cover and extended glacier-systems (Fig. 17; Werner, 1993; Svendsen and Mangerud, 1997; Miller et al., 2017; Philipps et al., 2017). While the Neoglacial exhibited no marked event signaling its initiation, persistent climatic deterioration through the second half of the Holocene re-invigorated Svalbard's glaciers (Bradley and Bakke, 2019).

4.5.2. Glacier response to Holocene warming events

Early Holocene warmth forces Svalbard into the Middle Holocene glacial minimum (HGMin; Fig. 17). However, the response of glaciers on Svalbard to warming conditions is sometimes more complex than simple; enhanced ablation resulting in ice marginal retreat (Dunse et al., 2015; Østby et al., 2017; Sevestre et al., 2018). While increased ablation was a dominant forcing on Early Holocene glacier-systems, effectively driving glacier retreat in the fjords (Fig. 7, 14 & 17), additional factors must have also influenced glacier behavior during this time (Farnsworth et al., 2017, 2018). Early Holocene warming resulted in several other key processes that likely had an indirect, yet substantial impact on glaciers including (but not limited to), shifts in precipitation patterns, glacier thermal regime, surface-profile and hydrologic system (Ingólfsson and Landvik, 2013; Landvik et al., 2013; Balascio et al., 2018). Furthermore, Early Holocene warming driving regional ice-mass-loss directly resulted in glacial isostatic adjustment which in some regions has influenced glacier dynamics (Norðdahl and Ingólfsson,

2015).

While Early Holocene glacier re-advances may not draw much attention, being mere interruptions in deglaciation, the process understanding has the potential to improve projections of ongoing and future ice loss. Whether Early Holocene glacier re-advances were driven by internal dynamics or mass-balance, they were short-lived and unsustainable glacier fluctuations. By kinematicly passing long accumulated ice mass below an ELA and spreading it within an ablation zone, the (dynamic) rate of ice loss will exceed non-dynamic ablation (Willis et al., 2018). Thus, a glacier advancing into a warming climate will undergo greater mass loss than a glacier-system at equilibrium in the same climate.

Early Holocene glacier re-advances undoubtedly increased a small percentage of ice cover on Svalbard at various points, yet (unlike the Neoglacial) were not necessarily a result of positive glacier mass balance (Fig. 8, 13 & 17). Reconstructed Early Holocene warmth derived from fjord, lake and terrestrial records suggests climate conditions were not entirely favorable for glacier mass accumulation (Fig. 17). Consequently, the key driver of Early Holocene glacier activity is unknown. Constraints on the amount Early Holocene precipitation are need to evaluate if regions experienced periods of positive mass balance, effectively outweighing glacier retreat (Thomas et al., 2018). Additionally, enhanced precipitation may have been factored by the severity of Early Holocene isostatic uplift resulting in an environment where glaciers traveled up through their ELAs (Norðdahl and Ingólfsson, 2015). Conceptually, glacier ablation area would have decreased while accumulation zones extended (Farnsworth, 2018). These processes may have driven Early Holocene glacier fluctuations, yet remain to be tested and modeled.

Observations during 20th century warming has led to developments in process understanding which may serve as analogues to Early Holocene conditions. For example, modern enhanced precipitation has been correlated to warming conditions and decreasing sea-ice (Nowak and Hodson, 2013; Bintanja and Selten, 2014), yet glacier accumulation on Svalbard has not outpaced ablation (Østby et al., 2017). However, still some glacier-systems has continued to exhibit ice-marginal advances (Dunse et al., 2015; Lovell et al., 2018; Sevestre et al., 2018). Ice dynamics have played an important role in 20th century glacier fluctuations (Flink et al., 2015; Sevestre and Benn, 2015; Farnsworth et al., 2016; Lovell et al., 2018), yet the extent of ice dynamics driving ice-marginal fluctuations at different periods (either warm or cold) in the Holocene in unknown.

In the surge-type glacier enthalpy model introduced by Sevestre and Benn (2015), a theoretical climatic envelope is constructed around a global inventory of glaciers, suggesting an ideal environment for glacier surge behavior. Given shifting climatic conditions, it is possible to have a glacier-system move from outside to inside this theoretical climatic envelope. The enthalpy model aligns with a conceptual model used to explain the deposition of transitional landforms during the Late Glacial deglaciation on the West coast of Svalbard (Landvik et al., 2013, 2014). The conceptual model suggests a shift in glacier basal conditions was a likely contributor to ice marginal re-advances during the deglaciation (Landvik et al., 2013). Interestingly, recent developments in process understanding of modern surge behavior on Svalbard suggests that warming environmental conditions has effected glacier thermal regime, hydrologic system and dynamics which has had a direct effect on glacier basal conditions and ice-marginal extent (Dunse et al., 2015; Sevestre et al., 2018). While these surge events have increased the percentage of ice-cover on Svalbard, they have not been fostered from phases of positive mass balance. The change in percentage ice-cover has been a result of a shift in basal conditions driving the kinematic redistribution of mass and a dynamic advance as the profile of the glacier-system flattens (Hagen, 1987; Sevestre et al., 2018; Willis et al., 2018).

While we have developed a general understanding of shifts in Svalbard's ice cover throughout the Holocene, our understanding of shifts in glacier basal conditions remain limited, yet may play a critical role in Holocene glacier marginal fluctuations. The Early Holocene deglaciation was punctuated by glacier re-advances during what is reconstructed to be an exceptionally warm environment. These re-advances appear to relate to the time-transgressive nature of deglaciation rather than a glacier event driven by a short period of cooling or an interval of enhanced precipitation yet this remains to be tested. Regardless of driving factor, glacier re-advances during a warm event reflect the complex style and efficient dynamic mass loss of glaciers in a changing climate.

5. Summary and perspective

Throughout the Holocene, Svalbard glaciers have responded to a varying combination of climatic, environmental and dynamic driving factors which influence both the extent and behavior of ice margins. Holocene glacier history, dynamics and processes provide key insights into glacier response to shifting climate and environment. Our understanding of Svalbard's ice-marginal fluctuations and glacier behavior through the Holocene allows us to refine our projections of future glacier conditions.

- Ice cover on Svalbard during the transition from Late Glacial to Early Holocene was likely less extensive than previously reconstructed (e.g. DATED-1). However, the region was still more extensively glaciated than any other period during the interglacial. Future investigations focusing on this transition should strive to further define ice-margins and test whether deglacial ice-shelves had an effect on ice-marginal landform development or glacier dynamics.

- Svalbard fjord systems deglaciated rapidly, in a time-transgressive fashion, during the first half of the Early Holocene (12.0 – 10.5 ka BP) which environmental reconstructions suggest exhibited exceptional regional warmth. While fjord system retreat-percentage provides a perspective on the timing of deglaciation, retreat rates provide a simplistic range of potential scenarios of ice loss.

- Early Holocene ice retreat on Svalbard was punctuated by widespread glacier re-advances, presumably dynamic and unsustainable (i.e., not driven by positive mass balance). Glacier behavior served as an efficient mechanism of deglaciation and reflects the complex style of ice-mass-loss during a changing climate. Modelling environmental conditions capable of driving Early Holocene glacier fluctuations may elucidate key driving factor(s) behind this ice-marginal behavior.

- The Holocene glacial minimum on Svalbard occurred during the beginning of the Middle Holocene (between 8.0 – 6.0 ka BP). However, a small portion of Svalbard glaciers (~25 % land-cover) located in the north and east of Svalbard presumably survived the minimum with some fjord systems hosting calving margins throughout the entire interglacial. In order to test these findings, evidence should be sought from other archives (lacustrine or ice core records) which indicate glaciers persistent through the glacial minimum.

- No glacial landforms have been identified corresponding to glacier re-advances or still-stands (9.0 – 4.5 ka BP) during the Middle Holocene. Consequently, relatively little is known about the extent of Svalbard glaciers during the Middle Holocene other than lake and some fjord records suggesting catchments hosted severely reduced ice cover. Better understanding glacial minimum conditions would improve (glacier, climate and isostatic adjustment) model domains and provide a potential perspective of Svalbard's future glaciers.

- Late Holocene glacier re-advances and corresponding deposits have been attributed to episodic Neoglacial cooling and the LIA. Glacier re-advances have predominantly been dated to between 4.0 – 0.5 ka BP with the highest frequency constrained between 1.0 – 0.5 ka BP. Much like Early Holocene glacier activity, the role of precipitation and seasonality versus summer temperatures remains poorly

defined. Past precipitation patterns likely exhibited significant variability and impact on Holocene glaciers. Any development will enhance a critical (yet poorly constrained) component of the mass balance of Svalbard's glaciers.

- Despite post-LIA glaciers on Svalbard exhibiting widespread negative mass balance, ice marginal retreat, and glacier thinning, some Svalbard glaciers have continued to exhibit surge-type re-advances. Dynamic glacier behavior has been linked to shifts in thermal regime, hydrologic system and surface profile, likely reflecting a similar pattern as the dynamic deglaciation during the Early Holocene. Ultimately, an enhanced understanding of Holocene glaciers and their driving factors will foster better projections of glaciers in response to changing climate.

- Syntheses of existing geochronological data are useful for identifying gaps in data and knowledge. While Svalbard currently exhibits relatively widespread geochronological constraint of glaciers and environment through the Holocene, holistic multidisciplinary investigations could be developed to target known-unknowns related to glaciers, geochronology and environment. One venue that has the potential to enhanced geochronology constraint in all (and in between) records, is further detailing the distal deposition of tephra on Svalbard. Defining a Holocene chronostratigraphic tephra framework for Svalbard, based on pan-Arctic volcanism, would strengthen high-Arctic lacustrine terrestrial and marine chronologies. Additionally, a framework of (crypto-)tephra horizons would allow for time-synchronous comparison between archives with the potential to further resolve leads and lags between terrestrial, lacustrine and marine systems.

REFERENCES within the SVALHOLA Database (see Data S1)

Aagaard-Sørensen *et al.* (2014), Adrielsson *et al.* (1992), Alexanderson *et al.* (2013), Allaart *et al.* (2020), Alsos *et al.* (2015), Andersen *et al.* (1996), Andersson *et al.* (1999, 2000), Baeten *et al.* (2010), Bakke *et al.* (2017), Balascio *et al.* (2018), Baranowski & Karlén (1976), Bartels *et al.* (2017, 2018), Beierlein *et al.* (2015), Berben *et al.* (2014) Bernardová & Kosnar (2012), Berge *et al.* (2005), van der Bilt *et al.* (2015, 2017a, 2017b), Birkenmajer & Olsson (1970), Birks (1991), Blake (1961a, 1961b, 1962, 1989, 2006), Blake *et al.* (1965), Bondevik *et al.* (1995), Boulton (1979), Boulton *et al.* (1999), Bratlie, (1994), Brückner & Halfar (1994), Brückner (1996), Brückner *et al.* (2002), Brückner & Schellmann (2003), Bunin (2015), Bøyum & Kjensmo (1980), Cable *et al.* (2018), Cameron *et al.* (1999), Chauhan *et al.* (2014, 2016), Corbel (1966), Cyposa *et al.* (1982), D'Andrea *et al.* (2012), Divine *et al.* (2011), Dinely (1953), Dokken (1995), Dokken & Hald (1996), Dylmer *et al.* (2013), Dzieriek *et al.* (1990), Ebbesen *et al.* (2007), Eitel *et al.* (2002), Elgersma & Helliksen (1986), Elverhøi & Solheim (1983), Elverhøi *et al.* (1995a, 1995b, 1998), Evans & Rea (2005), Farnsworth *et al.* (2017, 2018) Feyling-Hanssen (1955), Feyling-Hanssen & Jørstad (1950), Feyling-Hanssen & Olsson (1960), Fjeldskaar *et al.* (2018), Flink *et al.* (2017a, 2017b), Flink & Noormets (2018), Forman (1989, 1990a,1990b, 1999), Forman *et al.* (1987, 2004), Forman & Miller (1984), Forman & Ingólfsson (2000), Forwick & Vorren (2007, 2009), Forwick *et al.* (2010), Fransner *et al.* (2017, 2018), Furrer *et al.* (1991), Gilbert *et al.* (2018), Gjerde *et al.* (2017), Gjermundsen *et al.* (2015), Goslar & Pazdur (1985), Guilizzoni *et al.* (2006), Gottlich & Hornburg (1982), Haga (1978), Hald & Korsum (2008), Hald *et al.* (2001a, 2001b, 2004, 2007), Hansen & Knudsen (1995), Hansen *et al.* (2011), Hebbeln & Wefer (1997), Heiri *et al.* (2011), Henriksen *et al.* (2014), Hjort *et al.* (1995), Hogan *et al.* (2010a, 2010b, 2017), Hole & Macias-Fauria (2017), Holm *et al.* (2011), Holmgren *et al.* (2010), Hoppe (1972), Hoppe *et al.* (1969), Hormes *et al.* (2011, 2013), Houmark-Nielsen & Funder (1999), Humlum *et al.* (2005), Hughes *et al.* (2016), Hyvärinen (1970), Haggblom (1982), Isakssonv *et al.* (2005), Jankovská (1994), Jeppesen (2001), Jernas *et al.* (2013), Jessen *et al.* (2010), Jonsson (1983), Joo *et al.* (2019), Kaakinen *et al.* (2009), Karlén (1987), Kempf *et al.* (2013), Klysz *et al.* (1988), van der Knaap, W.O. (1985, 1988a, 1988b, 1989), Knape (1971), Koç *et al.* (2002), Kristensen *et al.* (2009, 2013), Kubishcta *et al.* (2011), Łącka *et al.* (2015), Landvik *et al.* (1987, 1992a, 1992b, 1995, 1998, 2003, 2005, 2013, 2014), Larsen *et al.* (2018), Lehman (1989), Lehman & Forman (1992,1987), Lindner *et al.* (1991), Lloyd *et al.* (1996), Long *et al.* (2012), Lovell *et al.* (2018), Lucchi *et al.* (2013, 2015), Luoto *et al.* (2011, 2018), Lyså *et al.* (2018), Lønne & Fuglei (1997), Lønne & Mangerud (1991), Lønne & Nemec (2004), Lønne (2005), Majewski *et al.* (2009), Mangerud & Gulliksen (1975), Mangerud & Svendsen (1990a, 1990b, 1992, 2017), Mangerud *et al.* (1992, 1998, 2006), Mäusbucher *et al.* (2002), Miller (1982), Miller *et al.* (2017), Möller *et al.* (1995), Müller *et al.* (2012), Müller & Stein (2014), Nagy (1984), Nevalainen *et al.* (2012), Nielsen & Rasmussen (2018), Oerlemans *et al.* (2011), Ojala *et al.* (2014, 2016), Oliva *et al.* (2014), Olsson (1959, 1960), Olsson & Piyanui (1965), Panieri *et al.* (2014), Péwé *et al.* (1982), Philipps *et al.* (2017), Plassen *et al.* (2004), Punning *et al.* (1976, 1977, 1978, 1980, 1982), Rasmussen & Thomsen (2009, 201a, b, 2015), Rasmussen *et al.* (2007, 2014), Reusche *et al.* (2014), Ronnert & Landvik (1993), Rowanm *et al.* (1982), Rozema *et al.* (2006), Rüther *et al.* (2012), Røthe *et al.* (2015, 2018), Salvigsen, O. (1977, 1978, 1979, 1981, 1984, 2002), Salvigsen & Elgersma (1993), Salvigsen & Høgvard (2005), Salvigsen & Mangerud (1991), Salvigsen & Österholm (1982), Salvigsen *et al.* (1990, 1991, 1992), Samtleben (1985), Sarnthein *et al.* (2003), Schomacker *et al.* (2019), Sessford *et al.* (2015), Sharin & Arslanov (2011), Sharin & Derzhavin (2012), Sharin *et al.* (2007, 2011, 2014), Singh *et al.* (2011), Skirbekk *et al.* (2010), Ślubowska-Woldengen *et al.* (2005, 2007, 2008), Snyder *et al.* (1994, 2000), Solheim *et al.* (1991), Solheim & Forsberg (1996), Stuiver & Polach (1977), Stankowski *et al.* (1989), Sternal *et al.* (2014), Streuff *et al.* (2017a, 2017b), Svendsen & Mangerud (1997), Svendsen *et al.* (1989, 1992, 1996), Svensson (1970),Szczucinski *et al.* (2009), Troitsky *et al.* (1979), Voldstad *et al.* (2020), Werner (1988, 1990, 1993), Werner *et al.* (2013), de Wet, *et al.* (2018), Winkelmann & Knies (2005), Wójcik, A., Zala, W. (1993), Yang *et al.* (2018), Yuan *et al.* (2009, 2011), Yoshikawa & Nakamura (1996), Young *et al.* (2018), Zale & Brydsten (1993), Zelikson (1971), Ziaja & Salvigsen (1995), Österholm (1986, 1990).

Data availability

Datasets related to this article and the SVALHOLA database have been uploaded to the open access online data repository, PANGEA (https://www.pangaea.de/submit/) with reference ID: PDI-24556. Upon PANGAE publication, shapefiles can be found at https://www.dropbox.com/sh/blacsl4gwwa2mo5/AABj_atdbtPfqfudUwnznG-Oa?dl=0.https://www.pangaea.de/submit/

Author Contributions

Ó.I., W.R.F., A.S., and M.R. conceived this work. W.R.F., L.A., and H.A., developed the database. All authors contributed with literature compilation, data interpretation and the discussion of results. W.R.F. wrote the paper with contributions from all co-authors.

Declaration of Competing Interest

The authors declare that they have no known competing financial interests or personal relationships that could have appeared to influence the work reported in this paper.

Acknowledgements

Appendix A. Supplementary data

Supplementary data to this article can be found online at https://doi.org/10.1016/j.earscirev.2020.103249.

References[1]

Aagaard, K., Foldvik, A., Hillman, S., 1987. The West Spitsbergen Current: disposition and water mass transformation. J. Geophys. Res. Oceans 92, 3778–3784.

Alexanderson, H., Murray, A.S., 2012a. Luminescence signals from modern sediments in a glaciated bay, NW Svalbard. Quat. Geochronol. 10, 250–256.

Alexanderson, H., Murray, A.S., 2012b. Problems and potential of OSL dating Weichselian and Holocene sediments in Sweden. Quat. Sci. Rev. 44, 37–50.

Alexanderson, H., Ingólfsson, Ó., Murray, A.S., Dudek, J., 2013. An interglacial polar bear and an earlyWeichselian glaciation at Poolepynten, western Svalbard. Boreas 42, 532–543.

Allaart, L., Müller, J., Schomacker, A., Rydningen, T.A., Håkansson, L., Kjellman, S.E., Mollenhauer, G., Forwick, M., 2020. Late Quaternary glacier and sea-ice history of northern Wijdefjorden, Svalbard. Boreas. https://doi.org/10.1111/bor.12435. ISSN 0300-9483.

Alsos, I.G., Sjögren, P., Edwards, M.E., Landvik, J.Y., Gielly, L., Forwick, M., Coissac, E., Brown, A.G., Jakobsen, L.V., Føreid, M.K., Pedersen, M.W., 2015. Sedimentary ancient DNA from Lake Skartjørna, Svalbard: assessing the resilience of arctic flora to Holocene climate change. The Holocene 26, 627–642.

Aradóttir, N., Ingólfsson, Ó., Noormets, R., Benediktsson, Í.Ö., Ben-Yehoshua, D., Håkansson, L., Schomacker, A., 2019. Glacial geomorphology of Trygghamna, western Svalbard - Integrating terrestrial and submarine archives for a better understanding of past glacial dynamics. Geomorphology 344, 75–89.

Arlov, T.B., 2005. The Discovery and Early Exploitation of Svalbard. Some Historiographical Notes. Acta Borealia 22, 3–19.

Baeten, N.L., Forwick, M., Vogt, C., Vorren, T.O., 2010. Late Weichselian and Holocene sedimentary environments and ice rafting in Isfjorden, Spitsbergen. Geol. Soc. Lond. Spec. Publ. 344, 207–223.

Bakke, J., Balascio, N., van der Bilt, W., Bradley, R., D'Andrea, W., Gjerde, M., Ólafsdóttir, S., Røthe, T., de Wet, G., 2018. The Island of Amsterdamøya: a key site for studying past climate in the Arctic Archipelago of Svalbard. Quat. Sci. Rev. 183, 157–163.

Balascio, N.L., D'Andrea, W.J., Gjerde, M., Bakke, J., 2018. Hydroclimate variability of High Arctic Svalbard during the Holocene inferred from hydrogen isotopes of leaf waxes. Quat. Sci. Rev. 183, 177–187. https://doi.org/10.1016/j.quascirev.2016.11.036.

Balco, G., Stone, J.O., Lifton, N.A., Dunai, T.J., 2008. A complete and easily accessible means of calculating surface exposure ages or erosion rates from ^{10}Be and ^{26}Al measurements. Quaternary Geochronology 3, 174–195.

Baranowski, S., Karlén, W., 1976. Remnants of Viking Age tundra in Spitsbergen and northern Scandinavia. Geografiska Annaler Series A 58, 35–39. https://doi.org/10.2307/520741.

Bartels, M., Titschack, J., Fahl, K., Stein, R., Seidenkrantz, M.S., Hillaire-Marcel, C., Hebbeln, D., 2017. Atlantic water advection vs. glacier dynamics in northern Spitsbergen since early deglaciation. Clim. Past 13, 1717–1749. https://doi.org/10.5194/cp-13-1717-2017.

Bartels, M., Titschack, J., Fahl, K., Stein, R., Hebbeln, D., 2018. Wahlenbergfjord, eastern Svalbard: a glacier-surrounded fjord reflecting regional hydrographic variability during the Holocene? Boreas 48, 1003–1021. https://doi.org/10.1111/bor.12325. ISSN 0300–9483.

Berger, A., Loutre, M.F., 1991. Insolation values for the climate of the last 10 million years. Quat. Sci. Rev. 10, 297–317.

Bertrand, A., 1852. Voyages de la Commission scientifique du Nord en Scandinavie. 1, Danemark, Norvège, Spitzberg: Atlas historique et pittoresque, lithographié d'aprés les dessins de MM. Mayer, Lauvergne et Giraud.

Bintanja, R., Selten, F., 2014. Future increases in Arctic precipitation linked to local evaporation and sea-ice retreat. Nature 509 (7501), 479–482.

Birks, H., 1991. Holocene vegetational history and climatic change in west Spitsbergen – Plant macrofossils from Skardtjørna, an Arctic lake. The Holocene 1, 209–218.

Blake, W.J., 1962. Geomorphology and Glacial Geology in Nordaustlandet, Spitsbergen. Unpublished PhD thesis. Department of Geology, Ohio State University, Columbus, pp. 477.

Blake, W.J., 1989. Radiocarbon dating by accelerator mass spectrometry: A contribution to the chronology of Holocene events in Nordaustlandet, Svalbard. Geografiska Annaler, Series A 71, 59–74.

Blake, W.J., 2006. Occurrence of the Mytilus edulis complex on Nordaustlandet, Svalbard: Radiocarbon ages and climatic implications. Polar Res. 25, 123–137.

Blaszczyk, M., Jania, J.A., Hagen, J.O., 2009. Tidewater glaciers of Svalbard: Recent changes and estimates of calving fluxes. Polish Polar Research 30, 85–142.

Bond, G., Kromer, B., Beer, J., Muscheler, R., Evans, M.N., Showers, W., Hoffmann, S., Lotti-Bond, R., Hajdas, I., Bonani, G., 2001. Persistent solar influence on north Atlantic climate during the Holocene. Science 294, 2130–2136.

Bondevik, S., Mangerud, J., Ronnert, L., Salvigsen, O., 1995. Postglacial sea-level history of Edgeoya and Barentsoya, eastern Svalbard. Polar Res. 14, 153–180.

Boulton, G.S., 1979. Glacial history of the Spitsbergen archipelago and the problem of a Barents Shelf ice sheet. Boreas 8, 31–57.

Bradley, R.S., Bakke, J., 2019. Is there evidence for a 4.2 ka BP event in the northern North Atlantic region? Clim. Past 15, 1665–1676.

Bradley, R.S., Mackay, A., Battarbee, R., Birks, J., Oldfield, F., 2003. Climate forcing during the Holocene. In: Global change in the Holocene. UK Hodder Arnold, London, pp. 10–19.

Briner, J.P., McKay, N.P., Axford, Y., Bennike, O., Bradley, R.S., de Vernal, A., Fisher, D., Francus, P., Fréchette, B., Gajewski, K., Jennings, A., Kaufman, D.S., Miller, G., Rouston, C., Wagner, B., 2016. Holocene climate change in Arctic Canada and Greenland. Quat. Sci. Rev. 147, 340–364.

Christiansen, H.H., Etzelmüller, B., Isaksen, K., Juliussen, H., Farbrot, H., Humlum, O., Johansson, M., Ingeman-Nielsen, T., Kristensen, L., Hjort, J., Holmlund, P., Sannel, A.B.K., Sigsgaard, C., Åkerman, H.J., Foged, N., Blikra, L.H., Pernosky, M.A., Ødegård, R.S., 2010. The thermal state of permafrost in the nordic area during the international polar year 2007–2009. Permafr. Periglac. Process. 21, 156–181.

Claesz, N., 1598. Het Nieuwe Land (Dutch for "the New Land") Map of Arctic exploration.

Cohen, K.M., Finney, S.C., Gibbard, P.L., Fan, J.X., 2018. The ICS international chronostratigraphic chart (2018/07). International Commission on Stratigraphy, IUGS. Episodes 36, 199–204.

D'Andrea, W.J., Vaillencourt, D.A., Balascio, N.L., Werner, A., Roof, S.R., Retelle, M., Bradley, R.S., 2012. Mild little ice age and unprecedented recent warmth in an 1800-year lake sediment record from Svalbard. Geology 40, 1007–1010. https://doi.org/10.1130/G33365.1.

Dansgaard, W., Johnsen, S.J., Clausen, H.B., Dahl-Jensen, D., Gundestrup, N.S., Hammer, C.U., Hvidberg, C.S., Steffensen, J.P., Sveinbjörnsdottir, A.E., Jouzel, J., Bond, G., 1993. Evidence for general instability of past climate from a 250-kyr ice-core record. Nature 364, 218–220.

De Geer, G., 1908. The Spitsbergen expedition of 1908 and the geological excursion to Spitsbergen 1910. Exkursionen till Spetsbergen 1908 och expeditionen till Spetsbergen 1910 (Gerard De Geer). Ymer 28, 341–344.

de Wet, G.A., Balascio, N.L., D'Andrea, W.J., Bakke, J., Bradley, R.S., Perren, B., 2018. Holocene glacier activity reconstructed from proglacial lake Gjøavatnet on Amsterdamøya, NW Svalbard. Quat. Sci. Rev. 183, 188–203. https://doi.org/10.1016/j.quascirev.2017.03.018.

Dickson, R.R., Osborn, T.J., Hurrell, J.W., Meincke, J., Blindheim, J., Adlandsvik, B., Vinje, T., Alekseev, G., Maslowski, W., 2000. The Arctic Ocean response to the North Atlantic Oscillation. J. Clim. 13, 2671–2696.

Divine, D., Isaksson, E., Martma, T., Meijer, H.A.J., Moore, J., Pohjola, V., van de Wal, R.S.W., Godtliebsen, F., 2011. Thousand years of winter surface air temperature variations in Svalbard and northern Norway reconstructed from ice-core data. Polar Res. 30, 7379.

Dowdeswell, J.A., Ottesen, D., Bellec, V.K., 2020. The changing extent of marine-terminating glaciers and ice caps in northeastern Svalbard since the 'Little Ice Age' from marine-geophysical records. The Holocene 30 (3), 389–401.

Drange, H., Dokken, T., Furevik, T., Gerdes, R., Berger, W., Nesje, A., Orvik, K.A., Skagseth, Ø., Skjelvan, I., Østerhus, S., 2005. The Nordic Seas: an overview. In: Drange, H., Dokken, T., Furevik, T. (Eds.), The Nordic seas: an integrated perspective. American Geophysical Union, Washington, DC, pp. 1–10.

Duller, G.A.T., 2006. Single grain optical dating of glacigenic deposits. Quat. Geochronol. 1, 296–304.

Duller, G.A.T., 2008. Single-grain optical dating of Quaternary sediments: why aliquot size matters in luminescence dating. Boreas 37, 589–612.

Dunse, T., Schellenberger, T., Hagen, J., Kääb, A., Schuler, T., Reijmer, C., 2015. Glacier-surge mechanisms promoted by a hydro-thermodynamic feedback to summer melt. Cryosphere 9, 197–215.

Dyke S, A, England, J, Reimnitz, E, Jette, H, et al., 1997. Changes in driftwood delivery to the Canadian Arctic Archipelago: the hypothesis of postglacial oscillations of the transpolar drift. Arctic 50, 1–16.

Dzieriek, J., Nitychoruk, J., Rzetkowska, A., 1990. Geological-geomorphological analysis and ^{14}C dating of submoraine organogenic deposits within the Renardhreen outer margin, Wedel-Jarlsberg Land, Spitsbergen. Polar Res. 8, 215–281.

Eckerstorfer, M., Christiansen, H.H., 2011. The "High Arctic Maritime Snow Climate" in Central Svalbard. Arct. Antarct. Alp. Res. 43, 11–21.

Eckerstorfer, M., Christiansen, H.H., Rubensdotter, L., Vogel, S., 2013. The geomorphological effect of cornice fall avalanches in the Longyeardalen valley, Svalbard. Cryosphere 7 (5), 1361–1374.

Eitel, B., van der Borg, K., Eberle, J., Megies, H., 2002. Late Pleistocene/Early Holocene glacial history of northern Andreeland (northern Spitsbergen/Svalbard Archipelago): evidence from glacial and fluvio-glacial deposits. Zeitschrift Fur Geomorphologie 46, 337–364.

Ekholm, N.G., 1887. Observations Faites au Cap Thorsden, Spitzberg par l'Expédition Suédoise. L'Academie Royale des Sciences de Suede Vol. 1, 218 pp.; Vol. 2, 207 pp.

England, J., Dyke, A.S., Coulthard, R.D., McNeely, R., Aitken, A., 2013. The exaggerated

---

[1] Note this list only includes citations from the main text of the paper. Database references are listed in Data S1.

radiocarbon age of deposit-feeding molluscs in calcareous environments. Boreas 42, 362–373.

Farnsworth, W.R., 2018. Holocene glacier history of Svalbard: Retracing the style of (de) glaciation. Doctoral thesis. Department of Geosciences, UiT The Arctic University of Norway, Tromsø, pp. 228.

Farnsworth, W.R., Ingólfsson, Ó., Retelle, M., Schomacker, A., 2016. Over 400 previously undocumented Svalbard surge-type glaciers identified. Geomorphology 264, 52–60.

Farnsworth, W.R., Ingólfsson, Ó., Noormets, R., Allaart, L., Alexanderson, H., Henriksen, M., Schomacker, A., 2017. Dynamic Holocene glacial history of St. Jonsfjorden, Svalbard. Boreas 46, 585–603.

Farnsworth, W.R., Ingólfsson, Ó., Retelle, M., Allaart, L., Håkansson, L., Schomacker, A., 2018. Svalbard glaciers re-advanced during the Pleistocene-Holocene transition. Boreas 47, 1022–1032.

Feyling-Hanssen, R.W., 1955. Stratigraphy of the marine Late- Pleistocene of Billefjorden, Vestspitsbergen. Nor. Polarinst. Skr. 107, 1–226.

Fjeldskaar, W., Bondevik, S., Amantov, A., 2018. Glaciers on Svalbard survived the Holocene thermal optimum. Quat. Sci. Rev. 199, 18–29.

Flink, A.E., Noormets, R., 2018. Submarine glacial landforms and sedimentary environments in Vaigattbogen, northeastern Spitsbergen. Mar. Geol. 402, 244–263.

Flink, A.E., Noormets, R., Kirchner, N., Benn, D.I., Luckman, A., Lovell, H., 2015. The evolution of a submarine landform record following recent and multiple surges of Tunabreen glacier, Svalbard. Quatern. Sci. Rev. 108, 37–50.

Flink, A.E., Noormets, R., Fransner, O., Hogan, K.A., O'Regan, M., Jakobsson, M., 2017. Past ice flow in Wahlenbergfjorden and its implications for late Quaternary ice sheet dynamics in northeastern Svalbard. Quat. Sci. Rev. 163, 162–179.

Førland, E.J., Hanssen-Bauer, I., Nordli, P.Ø., 1997. Climate statistics and longterm series of temperature and precipitation at Svalbard and Jan Mayen. Rapport 21/97 – Report Series of the Norwegian Meteorological Institute, pp. 92.

Førland, E.J., Benestad, R., Hanssen-Bauer, I., 2011. Temperature and precipitation development at Svalbard 1900–2100. Adv. Meteorol. 2011, 1–14 893790.

Forman, S.L., 1990. Post-glacial relative sea-level history of northwestern Spitsbergen, Svalbard. Geol. Soc. Am. Bull. 102, 1580–1590.

Forman, S.L., 1999. Infrared and red stimulated luminescence dating of Late Quaternary near-shore sediments from Spitsbergen, Svalbard. Arct. Antarct. Alp. Res. 31, 34–49.

Forman, S.L., Ingólfsson, Ó., 2000. Late Weichselian glacial history and postglacial emergence of Phippsøya, Sjuøyane, northern Svalbard: a comparison of modelled and empirical estimates of a glacial-rebound hinge line. Boreas 29, 16–25.

Forman, S.L., Mann, D.H., Miller, G.H., 1987. Late Weichselian and Holocene relative sea-level history of Bröggerhalvöya, Spitsbergen. Quat. Res. 27, 41–50.

Forman, S.L., Lubinski, D.J., Ingólfsson, Ó., Zeeberg, J.J., Snyder, J.A., Siegert, M.J., Matishov, G.G., 2004. A review of postglacial emergence on Svalbard, Franz Josef Land and Novaya Zemlya, northern Eurasia. Quat. Sci. Rev. 23, 1391–1434.

Forwick, M., Vorren, T., 2007. Holocene mass-transport activity and climate in outer Isfjorden, Spitsbergen: marine and subsurface evidence. The Holocene 17, 707–716.

Forwick, M., Vorren, T.O., 2009. Late Weichselian and Holocene sedimentary environments and ice rafting in Isfjorden, Spitsbergen. Palaeogeogr. Palaeoclimatol. Palaeoecol. 280, 258–274.

Forwick, M., Vorren, T.O., Hald, M., Korsun, S., Roh, Y., Vogt, C., Yoo, K.-C., 2010. Spatial and temporal influence of glaciers and rivers on the sedimentary environment in Sassenfjorden and Tempelfjorden, Spitsbergen. Geol. Soc. Lond., Spec. Publ. 344, 163–193.

French, M.H., 2007. The Periglacial Environment, Third edition. John Wiley & Sons, Chichester, U.K. and Hoboken, New Jersey, pp. 458.

Fuchs, M., Owen, L.A., 2008. Luminescence dating of glacial and associated sediments: review, recommendations and future directions. Boreas 37, 636–659.

Funder, S., Goosse, H., Jepsen, H., Kaas, E., Kjær, K.H., Korsgaard, N.J., Larsen, N.K., Linderson, H., Lyså, A., Möller, P., Olsen, J., Willerslev, E., 2011. A 10,000-Year Record of Arctic Ocean Sea-Ice Variability—View from the Beach. Science 333, 747–750.

Furrer, G., Stapfer, A., Glaser, U., 1991. Zur nacheiszeitlichen Gletschergeschichte des Liefdefjords (Spitzbergen) Ergebnisse der Geowissenschaftlichen Spitzbergenexpedition 1990. Geographica Helvetica 147–155.

Furze, M.F.A., Pieńkowski, A.J., McNeely, M.A., Bennett, R., Cage, A.G., 2018. Deglaciation and ice shelf development at the northeast margin of the Laurentide Ice Sheet during the Younger Dryas chronozone. Boreas 47, 271–296.

Geirsdóttir, Á., Miller, G.H., Axford, Y., Ólafsdóttir, S., 2009. Holocene and latest Pleistocene climate and glacier fluctuations in Iceland. Quat. Sci. Rev. 28, 2107–2118.

Gilbert, G.L., O'Neill, H.B., Nemec, W., Thiel, C., Christiansen, H.H., Buylaert, J.-P., 2018. Late Quaternary sedimentation and permafrost development in a Svalbard fjord-valley, Norwegian high Arctic. Sedimentology 65. https://doi.org/10.1111/sed. 12476.

Gjerde, M., Bakke, J., D'Andrea, W.J., Balascio, N.L., Bradley, R.S., Vasskog, K., Ólafsdóttir, S., Røthe, T.O., Perren, B.B., Hormes, A., 2017. Holocene multi-proxy environmental reconstruction from lake Hakluytvatnet, Amsterdamøya Island, Svalbard (79.5°N). Quat. Sci. Rev. 183, 164–176.

Gjermundsen, E.F., Briner, J.P., Akçar, N., Salvigsen, O., Kubik, P., Gantert, N., Hormes, A., 2013. Late Weichselian local ice dome configuration and chronology in Northwestern Svalbard: early thinning, late retreat. Quat. Sci. Rev. 72, 112–127.

Grinsted, A., Moore, J.C., Jevrejeva, S., 2009. Reconstructing sea level from paleo and projected temperatures 200 to 2100AD. Clim. Dyn. 34, 461–472.

Gudmundsson, H.J., 1997. A review of the Holocene environmental history of Iceland. Quat. Sci. Rev. 16, 81–92.

Hacquebord, L., 1995. In search of Het-Behouden-Huys A survey of the remains of the house of Barentsz, Willem on Novaya-Zemlya. Arctic 48, 248–256.

Hagen, J.O., 1987. Glacier surge at Usherbreen, Svalbard. Polar Res. 5, 239–252.

Häggblom, A., 1982. Driftwood in Svalbard as an indicator of sea ice conditions. Geografiska Annaler Series A 64, 81–94.

Hald, M., Korsum, S., 2008. The 8200-cal. yr. BP reflected in the Arctic fjord, Van Mijenfjorden. The Holocene 18, 981–990.

Hald, M., Ebbesen, H., Forwick, M., Godtliebsen, F., Khomenko, L., Korsun, S., Ringstad Olsen, L., Vorren, T.O., 2004. Holocene paleoceanography and glacial history of the West Spitsbergen area, Euro-Arctic margin. Quat. Sci. Rev. 23, 2075–2088.

Hald, M., Andersson, C., Ebbesen, H., Jansen, E., Klitgaard-Kristensen, D., Risebrobakken, B., Salomonsen, G.R., Sarnthein, M., Sejrup, H.P., Telford, R.J., 2007. Variations in temperature and extent of Atlantic Water in the northern North Atlantic during the Holocene. Quat. Sci. Rev. 26, 3423–3440.

Hansen, J., Hanken, N.-M., Nielsen, J.K., Thomsen, E., 2011. Late Pleistocene and Holocene distribution of Mytilus edulis in the Barents Sea region and its palaeoclimatic implications. J. Biogeogr. 38, 1197–1212.

Hanssen-Bauer, I., Kristensen Solås, M., Steffensen, E.L., 1990. The climate of Spitsbergen. Norwegian Meteorological Institute Report 39/90, pp. 40.

Henriksen, M., Alexanderson, H., Landvik, J.Y., Linge, H., Peterson, G., 2014. Dynamics and retreat of the Late Weichselian Kongsfjorden ice stream, NW Svalbard. Quat. Sci. Rev. 92, 235–245.

Heyman, J., Stroeven, A.P., Harbor, J.M., Caffee, M.W., 2011. Too young or too old: evaluating cosmogenic exposure dating based on an analysis of compiled boulder exposure ages. Earth Planet. Sci. Lett. 302, 71–80.

Hjort, C., Mangerud, J., Adrielsson, L., Bondevik, S., Landvik, J.Y., Salvigsen, O., 1995. Radiocarbon dated common mussels Mytilus edulis from eastern Svalbard and the Holocene marine climatic optimum. Polar Res. 14, 239–243.

Hogan, K.A., Dowdeswell, J.A., Hillenbrand, C.-D., Ehrmann, W., Noormets, R., Wacker, L., 2017. Subglacial sediment pathways and deglacial chronology of the northern Barents Sea Ice Sheet. Boreas 46, 750–771.

Hole, G.M., Macias-Fauria, M., 2017. Out of the woods: Driftwood insights into Holocene pan-Arctic sea ice dynamics. J. Geophys. Res. Oceans 122, 7612–7629.

Holmström, L.P., 1865. Märken efter istiden, iagttagna i Skåne. Cronholmska boktryckeriet, Malmö.

Hormes, A., Akçar, N., Kubik, P.W., 2011. Cosmogenic radionuclide dating indicates ice-sheet configuration during MIS 2 on Nordaustlandet, Svalbard. Boreas 40, 636–649.

Hormes, A., Gjermundsen, E.F., Rasmussen, T.L., 2013. From mountain top to the deep sea—deglaciation in 4D of the northwestern Barents Sea ice sheet. Quat. Sci. Rev. 75, 78–99.

Hughes, A.L.C., Gyllencreutz, R., Lohne, Ø.S., Mangerud, J., Svendsen, J.I., 2016. The last Eurasian ice sheets—a chronological database and time-slice reconstruction, DATED-1. Boreas 45, 1–45.

Humlum, O., 2005. Holocene permafrost aggradation in Svalbard. In: Harris, C., Murton, J.B. (Eds.), Cryospheric Systems: Glaciers and Permafrost. Geological Society, London, pp. 119–130 Special Publication 242.

Humlum, O., Instanes, A., Sollid, J.L., 2003. Permafrost in Svalbard: a review of research history, climatic background and engineering challenges. Polar Res. 22, 191–215.

Humlum, O., Elberling, B., Hormes, A., Fjordheim, K., Hansen, O.H., Heinemeier, J., 2005. Late-Holocene glacier growth in Svalbard, documented by subglacial relict vegetation and living soil microbes. The Holocene 1, 396–407.

Humlum, O., Christiansen, H.H., Juliussen, H., 2007. Avalanche-derived rock glaciers in Svalbard. Permafr. Periglac. Process. 18, 75–88.

Hyvärinen, H., 1970. Flandrian pollen diagrams from Svalbard. Geografiska Annaler Series A 52, 213–222.

Ingólfsson, Ó., 2011. Fingerprints of Quaternary glaciations on Svalbard. Geol. Soc. Lond., Spec. Publ. 354, 15–31.

Ingólfsson, Ó., Landvik, J.Y., 2013. The Svalbard-Barents Sea ice sheet– Historical, current and future perspectives. Quat. Sci. Rev. 64, 33–60.

Isachsen, G., 1915. Green Harbour, Spitsbergen. Scott. Geogr. Mag. 31 (1), 1–22.

Isaksson, E., Hermanson, M., Hicks, S., Igarashi, M., Kamiyama, K., Moore, J., Motoyama, H., Muir, D., Pohjola, V., Vaikmäe, R., van de Wal, R.S.W., Watanabe, O., 2003. Ice cores from Svalbard - useful archives of past climate and pollution history. Phys. Chem. Earth 28, 1217–1228.

Isaksson, E., Divine, D., Kohler, J., Martma, T., Pohjola, V., Motoyama, H., Watanabe, O., 2005. Climate oscillations as recorded in Svalbard ice core delta[18]O records between AD 1200 and 1997. Geografiska Annaler Series A 87, 203–214.

Ivy-Ochs, S., Briner, J.P., 2014. Dating disappearing ice with cosmogenic nuclides. Elements 10, 351–356.

Ivy-Ochs, S., Kerschner, H., Maisch, M., Christl, M., Kubik, P.W., Schlüchter, C., 2009. Latest Pleistocene and Holocene glacier variations in the European Alps. Quat. Sci. Rev. 28, 2137–2149.

Jakobsson, M., Mayer, L.A., Coakley, B., Dowdeswell, J.A., Forbes, S., Fridman, B., Hodnesdal, H., Noormets, R., Pedersen, R., Rebesco, M., 2012. The international bathymetric chart of the Arctic Ocean (IBCAO) version 3.0. Geophys. Res. Lett. 39, L12609. https://doi.org/10.1029/2012GL052219.

Jennings, A., Andrews, J., Pearce, C., Wilson, L., Ólfasdóttir, S., 2015. Detrital carbonate peaks on the Labrador shelf, a 13–7ka template for freshwater forcing from the Hudson Strait outlet of the Laurentide Ice Sheet into the subpolar gyre. Quat. Sci. Rev. 107, 62–80.

Jeppesen, J.W., 2001. Ice wedges and host sediments as palaeoclimatic indicators in central Spitsbergen, Svalbard (in Danish). M.S. thesis. University of Copenhagen, Denmark, pp. 101.

Jernas, P., Klitgaard Kristensen, D., Husum, K., Wilson, L., Koç, N., 2013. Palaeoenvironmental changes of the last two millennia on the western and northern Svalbard shelf. Boreas 42, 236–255.

Joo, Y.J., Forwick, M., Park, K., Joe, Y., Son, Y.J., Nam, S.-I., 2019. Holocene environmental changes in Dicksonfjorden, west Spitsbergen, Svalbard. Polar Res. 38, 3426.

Kaakinen, A., Salonen, V.-P., Kubischta, F., Eskola, K.O., Oinonen, M., 2009. Weichselian

glacial stage in Murchinsonfjorden, Nordaustlandet, Svalbard. Boreas 38, 718–729.

Kekonen, T., Moore, J., Perämäki, P., Mulvaney, R., Isaksson, E., Pohjola, V., van de Wal, R.S.W., 2005. The 800 year long ion record from the Lomonosovfonna (Svalbard) ice core. J. Geophys. Res. 110, D07304.

Kelly, M.A., Lowell, T.V., 2009. Fluctuations of local glaciers in Greenland during latest Pleistocene and Holocene time. Quaternary Science Reviews 28, 2088–2106.

Kempf, P., Forwick, M., Laberg, J.S., Vorren, T.O., 2013. Late Weichselian and Holocene sedimentary palaeoenvironment and glacial activity in the high-arctic van Keulenfjorden, Spitsbergen. The Holocene 23, 1607–1618.

Klysz, P., Lindner, L., Makowska, A., Leszek, M., Wysokinski, L., 1988. Late Quaternary glacial episodes and sea level changes in the northeastern Billefjorden region, Central Spitsbergen. Acta Geol. Pol. 38, 107–123.

Kristensen, L., Benn, D.I., Hormes, A., Ottesen, D., 2009. Mud aprons in front of Svalbard surge moraines: evidence of subglacial deforming layers or proglacial glaciotectonics? Geomorphology 111, 206–221.

Kubishcta, F., Knudsen, K.L., Ojala, A.E.K., Salonen, V.−P., 2011. Holocene benthic foraminiferal record from a high−arctic fjord, Nordaustlandet, Svalbard. Geografiska Annaler Series A 93, 227–242.

Łącka, M., Zajączkowski, M., Forwick, M., Szczuciński, W., 2015. Late Weichselian and Holocene palaeoceanography of Storfjordrenna, southern Svalbard. Clim. Past 11, 587–603.

Lal, D., 1991. Cosmic ray labeling of erosion surfaces: in situ nuclide production rates and erosion models. Earth and Planetary Science Letters 104, 424–439.

Lamb, H.H., 1965. The early medieval warm epoch and its sequel. Palaeogeogr. Palaeoclimatol. Palaeoecol. 1, 13–37.

Landvik, J.Y., Mangerud, J., Salvigsen, O., 1987. The Late Weichselian and Holocene shoreline displacement on the west-central coast of Svalbard. Polar Res. 5, 29–44.

Landvik, J.Y., Bondevik, S., Elverhøi, A., Fjeldskaar, W., Mangerud, J., Salvigsen, O., Siegert, M.J., Svendsen, J.I., Vorren, T.O., 1998. The last glacial maximum of Svalbard and the Barents Sea area: ice sheet extent and configuration. Quat. Sci. Rev. 17, 43–75.

Landvik, J.Y., Brook, E.J., Gualtieri, L., Linge, H., Raisbeck, G., Salvigsen, O., Yiou, F., 2013. 10Be exposure age constraints on the LateWeichselian ice-sheet geometry and dynamics in inter-ice-stream areas, western Svalbard. Boreas 42, 43–56.

Landvik, J.Y., Alexanderson, H., Henriksen, M., Ingólfsson, Ó., 2014. Landscape imprints of changing glacial regimes during ice-sheet build-up and decay: a conceptual model from Svalbard. Quat. Sci. Rev. 92, 258–268.

Larsen, E.A., Lyså, A., Rubensdotter, L., Farnsworth, W.R., Jensen, M., Nadeau, M.J., Ottesen, D., 2018. Late-Glacial and Holocene glacier activity in the Van Mijenfjorden area, western Svalbard. Arktos 4, 9. https://doi.org/10.1007/s41063-018-0042-2.

Laskar, J., Robutel, P., Joutel, F., Gastineau, M., Correia, A., Levrard, B., 2004. A long-term numerical solution for the insolation quantities of the Earth. Astron. Astrophys. 428, 261–285.

Lesnek, A.J., Briner, J.P., 2018. Response of a land-terminating sector of the western Greenland Ice Sheet to early Holocene climate change: Evidence from 10Be dating in the Søndre Isortoq region. Quat. Sci. Rev. 180, 145–156.

Lønne, I., 2005. Faint traces of high Arctic glaciations: an early Holocene ice-front fluctuation in Bolterdalen, Svalbard. Boreas 34, 308–323.

Lottin, V., Bravais, A., Lilliehöök, C.B., 1842. Voyages de la commission scientifique du nord, en Scandinavie, en Laponie, au Spitzberg et aux Feröe, pendant les années 1838, 1839 et 1840, sur la corvette 'La Recherche'. Arthus Bertrand, Paris.

Lovell, H., Boston, C.M., 2017. Glacitectonic composite ridge systems and surge-type glaciers: an updated correlation based on Svalbard. Norway. arktos 3, 1–16.

Lovell, H., Benn, D.I., Lukas, S., Ottesen, D., Luckman, A., Hardiman, M., Barr, I.D., Boston, C.M., Sevestre, H., 2018. Multiple Late Holocene surges of High-Arctic tidewater glacier systems in Svalbard. Quat. Sci. Rev. 201, 162–186.

Luoto, T.P., Ojala, A.E.K., Arppe, L., Brooks, S.J., Kurki, E., Oksman, M., Wooller, M.J., Zajączkowski, M., 2018. Synchronized proxy-based temperature reconstructions reveal mid- to late Holocene climate oscillations in High Arctic Svalbard. J. Quat. Sci. 33, 93–99.

Lyså, A., Larsen, E., Høgaas, F., Jensen, M.A., Klug, M., Rubensdotter, L., Szczucinski, W., 2018. A temporary glacier-surge ice-dammed lake, Braganzavågen, Svalbard. Boreas 47, 837–854.

Mangerud, J., Landvik, J.Y., 2007. Younger Dryas cirque glaciers in western Spitsbergen: smaller than during the Little Ice Age. Boreas 36, 278–285.

Mangerud, J., Landvik, J.Y., 2007. Younger Dryas cirque glaciers in western Spitsbergen: smaller than during the Little Ice Age. Boreas 36, 278–285.

Mangerud, J., Svendsen, J.I., 1992. The last interglacial-glacial period on Spitsbergen, Svalbard. Quat. Sci. Rev. 11, 633–664.

Mangerud, J., Svendsen, J.I., 2017. The Holocene Thermal Maximum around Svalbard, Arctic North Atlantic; molluscs show early and exceptional warmth. The Holocene 28, 65–83.

Mangerud, J., Bolstad, M., Elgersma, A., Helliksen, D., Landvik, J.Y., Lønne, I., Lycke, A.K., Salvigsen, O., Sandahl, T., Svendsen, J.I., 1992. The last glacial maximum on Spitsbergen, Svalbard. Quat. Res. 38, 1–31.

Mangerud, J., Dokken, T., Hebbeln, D., Heggen, B., Ingólfsson, Ó., Landvik, J.Y., Mejdahl, V., Svendsen, J.I., Vorren, T.O., 1998. Fluctuations of the Svalbard Barents Sea Ice Sheet during the last 150 000 years. Quat. Sci. Rev. 17, 11–42.

Mangerud, J., Bondevik S., Gulliksen, S., Hufthammer, A., Høisæter, T., 2006. Marine 14C reservoir ages for 19th century whales and molluscs from the North Atlantic. Quat. Sci. Rev. 25, 3228–3245.

Mann, M.E., Bradley, R.S., Hughes, M.K., 2009. Northern hemisphere temperatures during the past millennium: inferences, uncertainties, and limitations. Geophys. Res. Lett. 26, 759–762.

Marks, L., Wysokinski, L., 1986. Early Holocene advance in the Austfjorden region, northern Spitsbergen. Bulletin of the Polish Academy of Sciences 34, 437–446.

Mäusbacher, R., Borgvan der Daug, K.G., Kroemer, E., Müller, J., Wallner, J., 2002. Late Pleistocene and Holocene environmental changes in NW Spitsbergen - Evidence from lake sediments. Zeitschrift für Geomorphologi 46, 417–439.

Mayewski, P.A., Rohling, E.E., Curt Stager, J., Karlen, W., Maasch, K.A., David Meeker, L., Meyerson, E.A., Gasse, F., van Kreveld, S., Holmgren, K., Lee-Thorp, J., Rosqvist, G., Rack, F., Staubwasser, M., Schneider, R.R., Steig, E.J., 2004. Holocene climate variability. Quat. Res. 62, 243–255.

McKay, N.P., Kaufman, D.S., 2014. An extended Arctic proxy temperature database for the past 2,000 years. Scientific Data 1, 140026. https://doi.org/10.1038/sdata/2014.26.

Miller, G.H., Landvik, J.Y., Lehman, S.J., Southon, J.R., 2017. Episodic Neoglacial snowline descent and glacier expansion on Svalbard reconstructed from the 14C ages of ice-entombed plants. Quat. Sci. Rev. 155, 67–78.

Müller, J., Stein, R., 2014. High-resolution record of late glacial and deglacial sea ice changes in Fram Strait corroborates ice–ocean interactions during abrupt climate shifts. Earth Planet. Sci. Lett. 403, 446–455.

Müller, J., Werner, K., Stein, R., Fahl, K., Moros, M., Jansen, E., 2012. Holocene cooling culminates in sea ice oscillations in Fram Strait. Quat. Sci. Rev. 47, 1–14.

Nielsen, T., Rasmussen, T.L., 2018. Reconstruction of ice sheet retreat after the Last Glacial maximum in Storfjorden, southern Svalbard. Mar. Geol. 402, 228–243.

Nixon, F.C., England, J.H., Lajeunesse, P., Hanson, M.A., 2016. An 11 000-year record of driftwood delivery to the western Queen Elizabeth Islands, Arctic Canada. Boreas 45, 494–507.

Norðdahl, H., Ingólfsson, Ó., 2015. Collapse of the Icelandic ice sheet controlled by sea-level rise? Arktos 1, 13. https://doi.org/10.1007/s41063-015-0220-x.

Nowak, A., Hodson, A., 2013. Hydrological response of a High-Arctic catchment to changing climate over the past 35 years: a case study of Bayelva watershed, Svalbard. Polar Res. 32 (1), 19691.

Nuth, C., Kohler, J., König, M., von Deschwanden, A., Hagen, J.O., Kääb, A., Moholdt, G., Pettersson, R., 2013. Decadal changes from a multitemporal glacier inventory of Svalbard. Cryosphere 7, 1603–1621.

O'Brien, S.R., Mayewski, P.A., Meeker, L.D., Meese, D.A., Twickler, M.S., Whitlow, S.I., 1995. Complexity of Holocene climate as reconstructedfrom a Greenland ice core. Science 270, 1962–1964.

Oerlemans, J., Jania, J., Kolondra, L., 2011. Application of a minimal glacier model to Hansbreen, Svalbard. Cryosphere 5, 1–11.

Oliva, M., Vieira, G., Pina, P., Pereira, P., Neves, M., Freitas, M.C., 2014. Sedimentological characteristics of ice-wedge polygon terrain in Adventdalen (Svalbard) – environmental and climatic implications for the late Holocene. Solid Earth 5, 901–914.

Østby, T.I., Schuler, T.V., Hagen, J.O., Hock, R., Kohler, J., Reijmer, C.H., 2017. Diagnosing the decline in climatic mass balance of glaciers in Svalbard over 1957–2014. Cryosphere 11, 191–215.

Österholm, H., 1990. The Late Weichselian Glaciation and Holocene Shore Displacement on Prins Oscars Land, Nordaustlandet, Svalbard. Geografiska Annaler Series A 72, 301–317.

Ottesen, D., Dowdeswell, J.A., Benn, D.I., Kristensen, L., Christiansen, H.H., Christensen, O., Hansen, L., Lebesbye, E., Forwick, M., Vorren, T.O., 2008. Submarine landforms characteristic of glacier surges in two Spitsbergen fjords. Quat. Sci. Rev. 27, 1583–1599.

Patton, H., Hubbard, A., Andreassen, K., Auriac, A., Whitehouse, P.L., Stroeven, A.P., Shackleton, C., Winsborrow, M.C.M., Heyman, J., Hall, A.M., 2017. Deglaciation of the Eurasian ice sheet complex. Quat. Sci. Rev. 169, 148–172.

Pawłowska, J., Łącka, M., Kucharska, M., Pawlowski, J., Zajaczkowski, M., 2020. Multiproxy evidence of the Neoglacial expansion of Atlantic Water to eastern Svalbard. Clim. Past 16, 487–501.

Philipps, W., Briner, J.P., Gislefoss, L., Linge, H., Koffman, T., Fabel, D., Xu, S., Hormes, A., 2017. Late Holocene glacier activity at inner Hornsund and Scottbreen, southern Svalbard. J. Quat. Sci. 32, 501–515.

Plassen, L., Vorren, T.O., Forwick, M., 2004. Integrated acoustic and coring investigation of glacigenic deposits in Spitsbergen fjords. Polar Res. 23, 89–110.

Punning, J.-M., Troitsky, L., Rajamäe, R., 1976. The genesis and age of the Quaternary deposits in the eastern part of Van Mijenfjorden, West Spitsbergen. Föreningens i Stockholm Förhandlingar 9, 343–347.

Rasmussen, T.L., Thomsen, E., 2014. Brine formation in relation to climate changes and ice retreat during the last 15,000 years in Storfjorden, Svalbard, 76–78°N. Paleoceanography 29, 911–929.

Rasmussen, T.L., Forwick, M., Mackensen, A., 2012. Reconstruction of inflow of Atlantic Water to Isfjorden, Svalbard during the Holocene: correlation to climate and seasonality. Mar. Micropaleontol. 94–95, 80–90.

Rasmussen, T.L., Thomsen, E., Skirbekk, K., Ślubowska-Woldengen, M., Klitgaard Kristensen, D., Koç, N., 2014. Spatial and temporal distribution of Holocene temperature maxima in the northern Nordic seas: interplay of Atlantic-, Arctic- and polar water masses. Quat. Sci. Rev. 92, 280–291.

Reimer, P.J., Bard, E., Bayliss, A., Beck, J.W., Blackwell, P.G., Bronk Ramsey, C., Buck, C.E., Cheng, H., Edwards, R.L., Friedrich, M., Grootes, P.M., Guilderson, T.P., Haflidason, H., Hajdas, I., Hatte, C., Heaton, T.J., Hoffmann, D.L., Hogg, A.G., Hughen, K.A., Kaiser, K.F., Kromer, B., Manning, S.W., Niu, M., Reimer, R.W., Richards, D.A., Scott, E.M., Southon, J.R., Staff, R.A., Turney, C.S.M., van der Plicht, J., 2013. IntCal13 and Marine13 Radiocarbon Age Calibration Curves 0–50,000 Years cal BP. Radiocarbon 55, 1869–1887.

Reusche, M., Winsor, K., Carlson, A.E., Marcott, S.A., Rood, D.H., Novak, A., Roof, S., Retelle, M., Werner, A., Caffee, M., Clark, P.U., 2014. 10Be surface exposure ages on the late-Pleistocene and Holocene history of Linnébreen on Svalbard. Quat. Sci. Rev. 89, 5–12.

Rockström, J., Steffen, W., Noone, K., Persson, A., Chapin, F.S., Lambin, E.F., Lenton, T.M., Scheffer, M., Folke, C., Schellnhuber, H.J., Nykvist, B., de Wit, C.A., Hughes, T., van der Leeuw, S., Rodhe, H., Sorlin, S., Snyder, P.K., Costanza, R., Svedin, U., Falkenmark, M., Karlberg, L., Corell, R.W., Fabry, V.J., Hansen, J., Walker, B., Liverman, D., Richardson, K., Crutzen, P., Foley, J.A., 2009. A safe operating space for humanity. Nature 461, 472–475.

Rogers, J.C., Yang, L., Li, L., 2005. The role of Fram Strait winter cyclones on sea ice flux and on Spitsbergen air temperatures. Geophys. Res. Lett. 32, L06709.

Ronnert, L., Landvik, J.Y., 1993. Holocene glacial advances and moraine formation at Albrechtbreen, Edgeøya, Svalbard. Polar Res. 12, 57–63.

Røthe, T.O., Bakke, J., Vasskog, K., Gjerde, M., D'Andrea, W.J., Bradley, R.S., 2015. Arctic Holocene glacier fluctuations reconstructed from lake sediments at Mitrahalvøya, Spitsbergen. Quat. Sci. Rev. 109, 111–125.

Røthe, T.O., Bakke, J., Støren, E.W.N., Bradley, R.S., 2018. Reconstructing Holocene Glacier and Climate Fluctuations from Lake Sediments in Vårfluesjøen, Northern Spitsbergen. Front. Earth Sci. 6, 1–20.

Salvigsen, O., 1981. Radiocarbon dated raised beaches in Kong Karls Land, Svalbard, and their consequences for the glacial history of the Barents Sea area. Geografiska Annaler Series A 63, 283–291.

Salvigsen, O., 2002. Radiocarbon-dated *Mytilus edulis* and *Modiolus modiolus* from northern Svalbard: Climatic implications. Nor. Geogr. Tidsskr. 56, 56–61.

Salvigsen, O., Österholm, H., 1982. Radiocarbon dated raised beaches and glacial history of the northern coast of Spitsbergen, Svalbard. Polar Res. 97–115.

Salvigsen, O., Elgersma, A., Hjort, C., Lagerlund, E., Liestøl, O., Svensson, N.-O., 1990. Glacial history and shoreline displacement on Erdmannflya and Bohemanflya, Spitsbergen, Svalbard. Polar Res. 8, 261–273.

Salvigsen, O., Forman, S.L., Miller, G.H., 1992. Thermophilous molluscs on Svalbard during the Holocene and their paleoclimatic implications. Polar Res. 11, 1–10.

Samtleben, C., 1985. Climatic influence on shell microstructure in *Mytilus edulis* from Spitsbergen. In: Paper presented at the 75. Jahrestagung der Geologischen Vereinung, Kiel.

Sarnthein, M., Van Kreveld, S., Erlenkeuser, H., Grootes, P.M., Kucera, M., Pflauman, U., Schulz, M., 2003. Centennial-to millennial-scale periodicities of Holocene climate and sediment injections off the western Barents shelf, 75°N. Boreas 32, 447–461.

Schomacker, A., Kjær, K.H., 2008. Quantification of dead-ice melting in ice-cored moraines at the high-Arctic glacier Holmströmbreen, Svalbard. Boreas 37, 211–225.

Schomacker, A., Farnsworth, W.R., Ingólfsson, Ó., Allaart, L., Håkansson, L., Retelle, M., Siggaard-Andersen, M.-L., Korsgaard, N.J., Rouillard, A., Kjellman, S.E., 2019. Postglacial relative sea level change and glacier activity in the early and late Holocene: Wahlenbergfjorden, Nordaustlandet, Svalbard. Sci. Rep. 9, 6799.

Sessford, E.G., Strzelecki, M.C., Hormes, A., 2015. Reconstruction of past patterns of change in a High Arctic coastal landscape, southern Sassenfjorden, Svalbard. Geomorphology 234, 98–107.

Sevestre, H., Benn, D.I., 2015. Climatic and geometric controls on the global distribution of surge-type glaciers: implications for a unifying model of surging. J. Glaciol. 61, 646–662.

Sevestre, H., Benn, D.I., Luckman, A., Nuth, C., Kohler, J., Lindbäck, K., Pettersson, R., 2018. Tidewater Glacier Surges Initiated at the Terminus. J. Geophys. Res. Earth Surf. 123, 1035–1051.

Sharin, V., Kokin, O., Gusev, E.A., Okunev, A.S., Arslanov, Kh.A., Maksimov, F.E., 2014. New geochronological data from Quaternary sediments of the Nordenskiöld Land area (the Spitsbergen Archipelago). Vestnik St. Petersburg State University, Series 7. Geol. Geogr. 1, 159–168 (in Russian with English abstract).

Siewert, M.B., Krautblatter, M., Christiansen, H.H., Eckerstorfer, M., 2012. Arctic rockwall retreat rates estimated using laboratory-calibrated ERT measurements of talus cones in Longyeardalen, Svalbard. Earth Surf. Process. Landf. 37, 1542–1555.

Skirbekk, K., Klitgaard-Kristensen, D., Rasmussen, T.L., Koç, N., Forwick, M., 2010. Holocene climate variations at the entrance to a warm Arctic fjord: evidence from Kongsfjorden trough, Svalbard. Geol. Soc. Lond., Spec. Publ. 344, 289–304.

Sletten, K., Lyså, A., Lønne, I., 2001. Formation and disintegration of a high-arctic ice-cored moraine complex, Scott Turnerbreen, Svalbard. Boreas 30, 272–284.

Ślubowska-Woldengen, M., Rasmussen, T.L., Koç, N., Klitgaard-Kristensen, D., Nilsen, F., Solheim, A., 2007. Advection of Atlantic Water to the western and northern Svalbard shelf since 17 500 cal yr BP. Quat. Sci. Rev. 26, 463–478.

Snyder, J.A., Miller, G.H., Werner, A., Jull, A.J.T., Stafford, J.T.W., 1994. AMS-radiocarbon dating of organic-poor lake sediment, an example from Linnévatnet, Spitsbergen, Svalbard. The Holocene 4, 413–421.

Snyder, J.A., Werner, A., Miller, G.H., 2000. Holocene cirque glacier activity in western Spitsbergen, Svalbard: sediment records from proglacial Linnévatnet. The Holocene 10, 555–563.

Solomina, O.N., Bradley, R.S., Hodgson, D.A., Ivy-Ochs, S., Jomelli, V., Mackintosh, A.N., Nesje, A., Owen, L.A., Wanner, H., Wiles, G.C., Young, N.E., 2015. Holocene glacier fluctuations. Quat. Sci. Rev. 111, 9–34.

Steffensen, J.P., Andersen, K.K., Bigler, M., Clausen, H.B., Dahl-Jensen, D., Fischer, H., Goto-Azuma, K., Hansson, M., Johnsen, S.J., Jouzel, J., Masson-Delmotte, V., Popp, T., Rasmussen, S.O., Röthlisberger, R., Ruth, U., Stauffer, B., Siggaard-Andersen, M.-L., Sveinbjörnsdóttir, A.E., Svensson, A., White, J.W.C., 2008. High resolution Greenland ice core data show abrupt climate change happens in few years. Science 321, 680–684.

Stone, J.O., 2000. Air pressure and cosmogenic isotope production. Journal of Geophysical Research: Solid Earth 105, 23753–23759.

Streuff, K., Cofaigh, Ó., Noormets, C., Lloyd, R., J.M., 2017. Submarine landforms and glacimarine sedimentary processes in Lomfjorden, East Spitsbergen. Mar. Geol. 390, 51–71.

Svendsen, J.I., Mangerud, J., 1997. Holocene glacial and climatic variations on Spitsbergen, Svalbard. The Holocene 7, 45–57.

Thomas, E.K., Castañeda, I.S., McKay, N.P., Briner, J.P., Salacup, J.M., Nguyen, K.Q., Schweinsberg, A.D., 2018. A wetter Arctic coincident with hemispheric warming 8,000 years ago. Geophys. Res. Lett. 45. https://doi.org/10.1029/2018GL079517.

Thrasher, I.M., Mauz, B., Chiverrell, R.C., Lang, A., Thomas, G.S.P., 2009. Testing an approach to OSL dating of Late Devensian glaciofluvial sediments of the British Isles. J. Quat. Sci. 24, 785–801.

Tian, S.Y., Moriaki Yasuhara, M., Yuanyuan Hong, Y., Huang, H.-H.M., Iwatani, H., Chiu, W.-T.R., Mamo, B., Okahashi, H., Rasmussen, T.L., 2020. Deglacial–Holocene Svalbard paleoceanography and evidence of meltwater pulse 1B. Quat. Sci. Rev. 233, 106237.

van der Bilt, W.G.M., Bakke, J., Vasskog, K., D'Andrea, W.J., Bradley, R.S., Olafsdóttir, S., 2016. Reconstruction of glacier variability from lake sediments reveals dynamic Holocene climate in Svalbard. Quat. Sci. Rev. 126, 201–218.

van der Bilt, W.G.M., Lane, C.S., Bakke, J., 2017. Ultra-distal Kamchatkan ash on Arctic Svalbard: Towards hemispheric cryptotephra correlation. Quat. Sci. Rev. 164, 230–235.

van der Bilt, W.G.M., D'Andrea, W.J., Bakke, J., Balascio, N.L., Werner, J.P., Gjerde, M., Bradley, R.S., 2018. Alkenone-based reconstructions reveal four-phase Holocene temperature evolution for High Arctic Svalbard. Quat. Sci. Rev. 183, 1–10.

van der Bilt, W.G.M., D'Andrea, W.J., Werner, J.P., Bakke, J., 2019. Early Holocene temperature oscillations exceed amplitude of observed and projected warming in Svalbard lakes. Geophys. Res. Lett. 46, 14,732–14,741.

Voldstad, L.H., Alsos, I.G., Farnsworth, W.R., Heintzman, P.D., Håkansson, L., Kjellman, S.E., Rouillard, A., Schomacker, A., Eidesen, P.B., 2020. A complete Holocene lake sediment ancient DNA record reveals long-standing high Arctic plant diversity hotspot in northern Svalbard. Quat. Sci. Rev. https://doi.org/10.1016/j.quascirev.2020.106207.

Wanner, H., Brönnimann, S., Casty, C., Gyalistras, D., Luterbacher, J., Schmutz, C., Stephenson, D.B., Xoplaki, E., 2001. North Atlantic Oscillation—Concepts and Studies. Surv. Geophys. 22, 321–381.

Walker, M.J.C., Berkelhammer, M., Björck, S., Cwynar, L.C., Fisher, D.A., Long, A.J., Lowe, J.J., Newnham, R.M., Rasmussen, S.O., Weiss, H., 2012. Formal subdivision of the Holocene series/epoch: a discussion paper by a working group of INTIMATE (integration of ice-core, marine and terrestrial records) and the subcommission on quaternary stratigraphy (international commission on stratigraphy). Journal of Quaternary Science 27, 649–659.

Wanner, H., Beer, J., Bütikofer, J., Crowley, T.J., Cubasch, U., Flückiger, J., Goosse, H., Grosjean, M., Joos, F., Kaplan, J.O., Küttel, M., Müller, S.A., Prentice, I.C., Solomina, O., Stocker, T.F., Tarasov, P., Wagner, M., Widmann, M., 2008. Mid- to Late Holocene climate change: an overview. Quat. Sci. Rev. 27, 1791–1828.

Wanner, H., Solomina, O., Grosjean, M., Ritz, S.P., Jetel, M., 2011. Structure and origin of Holocene cold events. Quat. Sci. Rev. 30, 3109–3123.

Wastegård, S., Davies, S.M., 2009. An overview of distal tephrochronology in northern Europe during the last 1000 years. J. Quat. Sci. 24, 500–512.

Werner, A., 1993. Holocene moraine chronology, Spitsbergen, Svalbard: lichenometric evidence for multiple Neoglacial advances in the Arctic. The Holocene 3, 128–137.

Werner, A., Spielhagen, R.F., Bauch, D., Hass, H.C., Kandiano, E., 2013. Atlantic water advection versus sea-ice advances in the eastern Fram Strait during the last 9 ka: multiproxy evidence for a two-phase Holocene. Paleoceanography 28, 283–295.

Wickström, S., Jonassen, M.O., Vihma, T., Uotila, P., 2020. Trends in cyclones in the high-latitude North Atlantic during 1979–2016. Quat. J. Roy. Meteorol. Soc. 146, 762–779.

Willis, M.J., Zheng, W., Durkin, W.J., Pritchard, M.E., Ramage, J.M., Dowdeswell, J.A., Benham, T.J., Bassford, R.P., Stearns, L.A., Glazovsky, A.F., Macheret, Y.Y., Porter, C.C., 2018. Massive Destabilization of an Arctic Ice Cap. Earth Planet. Sci. Lett. 502, 146–155.

Wintle, A.G., 2008. Fifty years of luminescence dating. Archaeometry 50, 276–312.

Wohlfarth, B., 2009. Ice-free conditions in Fennoscandia during Marine Oxygen Isotope Stage 3? Technical Report: TR-09-12. Swedish Nuclear Fuel and Waste Management Company, Stockholm.

Yoshikawa, K., Nakamura, T., 1996. Pingo growth ages in the delta area, Adventdalen, Spitsbergen. Polar Record 32, 347–352.

Young, N.E., Schaefer, J.M., Briner, J.P., Goehring, B.M., 2013. A [10]Be production-rate calibration for the Arctic. J. Quat. Sci. 28, 515–526.

Young, N.E., Lamp, J., Koffman, T., Briner, J.P., Schaefer, J., Gjermundsen, E.F., Linge, H., Zimmerman, S., Guilderson, T.P., Fabel, D., Hormes, A., 2018. Deglaciation of coastal south-western Spitsbergen dated with in situ cosmogenic [10]Be and ^{14}C measurements. J. Quat. Sci. 33, 763–776.

Young, N.E., Briner, J.P., Miller, G.H., Lesnek, A.J., Crump, S.E., Thomas, E.K., Pendleton, S.L., Cuzzone, J., Lamp, J., Zimmerman, S., Caffee, M., Schaefer, J.M., 2020. Deglaciation of the Greenland and Laurentide ice sheets interrupted by glacier advance during abrupt coolings. Quat. Sci. Rev. 229, 106091.